CXCR3 SIGNALING EFFECTS ON THE DEVELOPMENT AND IMMUNOREGULATION OF BASAL CELL CARCINOMA AND RELATED NEOPLASIAS

by

Blanche Ka Ki Lo

B.Sc., The University of British Columbia, 2005

A THESIS SUBMITTED IN PARTIAL FULFILLMENT OF
THE REQUIREMENTS FOR THE DEGREE OF

DOCTOR OF PHILOSOPHY

in

THE FACULTY OF GRADUATE STUDIES

(Experimental Medicine)

THE UNIVERSITY OF BRITISH COLUMBIA

(Vancouver)

March 2012

Abstract

Increasing evidence has revealed that the chemokines CXCL9, CXCL10, CXCL11, and their common receptor CXCR3, are associated with tumorigenesis. Basal cell carcinoma (BCC) is a type of non-melanoma skin cancer (NMSC) and is the most common malignancy encountered. In this thesis, I hypothesized that CXCR3 signaling provides a novel marker for the growth and putative immune privilege of BCC as well as for the development of other NMSCs, such as cutaneous squamous cell carcinoma (SCC).

Increased expression of chemokines CXCL10, 11 and CXCR3 was detected in cytokeratin 17 $(K17)^+$ BCC cells. CXCR3/CXCL11 signaling was found to support the proliferation and survival of primary $K17^+$ BCC cells derived from patient samples. Also, human BCC cells migrated in response to CXCL11 peptide in a dose-dependent manner. These findings suggest that CXCR3 signaling may be an important autocrine and/or paracrine mediator in BCC tumorigenesis. To further support the role of CXCR3 signaling in NMSC, expression of *CXCR3* and its ligands were found to be significantly upregulated in cutaneous SCC and its precancerous forms (greatest in SCC). Neutralization of CXCR3 bioactivity demonstrated that CXCR3/CXCL11 signaling supported the proliferation and survival of HaCaT neoplastic keratinocyte cell cultures. Moreover, HaCaT cells transmigrated in response to CXCL11 in a dose-dependent manner. Taken together, CXCR3/ligand signaling may be important for neoplastic keratinocyte proliferation and migration, especially in cutaneous SCCs.

Studies suggest BCCs exhibit immune privilege (IP), though the mechanisms have not been defined. Upregulation of a panel of IP-related genes, including *IDO1*, *IDO2*, *CD200* and *CD200R* was identified in BCC tissues with *IDO2* being expressed at the highest level.

Notably, the expression and enzymatic activity of indoleamine 2,3-dioxygenase (IDO) was increased in human $K17^+$ BCC cells *in vitro* with increased CXCR3/CXCL11 signaling. These results suggest that functional IDO is synthesized by human BCCs and may confer immunoprotection to the tumor cells, which may be enhanced by CXCR3 signaling.

This thesis has revealed novel roles of CXCR3 signaling as part of the mechanism of BCC and related neoplasia development. The data may improve our understanding of NMSC pathogenesis as well as enable invention and/or modification of treatment modalities.

Preface

- A version of chapter 3A has been published. [Lo, B.K.K.], Yu, M., Zloty, D., Cowan, B., Shapiro, J., and McElwee, K.J. CXCR3/ligands are significantly involved in the tumorigenesis of basal cell carcinomas. *Am J Pathol***.** 2010. 176:2435-2446
    - K.J.M. provided laboratory facilities and materials, and contributed to experimental designs and manuscript preparation. J.S. provided support in research facilities and manuscript revision. I designed and conducted most of the experiments, analyzed the data and composed the manuscript. M.Y. demonstrated experiments of RNA isolation, cDNA synthesis and quantitative real-time RT-PCR in Figure 3.1. D.Z. and B.C. provided patient samples in Figures 3.1 – 3.9.
- A version of chapter 4 has been published. [Lo, B.K.K.], Jalili, R.B., Zloty, D., Ghahary, A., Cowan, B., Dutz, J.P., Carr, N., Shapiro, J., and McElwee, K.J. CXCR3 ligands promote expression of functional indoleamine 2,3-dioxygenase (IDO) in basal cell carcinoma keratinocytes. *Br J Dermatol*. 2011.
    - K.J.M. provided laboratory facilities and materials, and contributed to experimental designs and manuscript preparation. J.S. provided support in research facilities and manuscript revision. I designed and conducted most of the experiments, analyzed the data and composed the manuscript. R.B.J. assisted in conducting Western blot and kynurenine assay in Figures 4.6 and 4.8 respectively. D.Z. provided patient samples for all experiments in Figures 4.3 – 4.9 and revised the manuscript. A.G. provided experimental materials of Western blot and kynurenine assay in Figures 4.6 and 4.8 respectively, and gave suggestion in project design. J.P.D. contributed in experimental design and manuscript revision.

B.C. and N.C. provided tissue samples in all experiments in Figures 4.3 – 4.9.

- A version of chapter 3B has been submitted for publication. [Lo, B.K.K.], Tai, N., Chen, L.H., Zhou, Y., Zloty, D., Cowan, B., Shapiro, J., and McElwee, K.J. Role of CXCR3 signaling in the survival and motility of non-melanoma skin cancer keratinocytes. 2011.
    - K.J.M. provided laboratory facilities and materials, and contributed to experimental designs and manuscript preparation. J.S. provided support in research facilities and manuscript revision. I designed and conducted most of the experiments, analyzed the data and composed the manuscript. N.T. and L.H.C. performed real-time RT-PCR in Figure 3.16. Y.Z. provided patient samples for real-time RT-PCR and immunohistochemistry in Figures 3.16 and 3.17 respectively as well as revised the manuscript draft. D.Z. and B.C. provided tissue samples for all experiments in Figures 3.16 – 3.20.
- List of publications:
    - Lo, B.K.K., Jalili, R.B., Zloty, D., Ghahary, A., Cowan, B., Dutz, J.P., Carr, N., Shapiro, J., and McElwee, K.J. CXCR3 ligands promote expression of functional indoleamine 2,3-dioxygenase (IDO) in basal cell carcinoma keratinocytes. *Br J Dermatol*. 2011. This work is located in chapter 4 with permission to reprint.
    - Lo, B.K.K., Yu, M., Zloty, D., Cowan, B., Shapiro, J., and McElwee, K.J. CXCR3/ligands are significantly involved in the tumorigenesis of basal cell carcinomas. *Am J Pathol***.** 2010. 176:2435-2446. This work is located in chapter 3A with permission to reprint.
    - Lo, B.K.K., Tai, N., Chen, L.H., Zhou, Y., Zloty, D., Cowan, B., Shapiro, J., and McElwee, K.J. Role of CXCR3 signaling in the survival and motility of non-

melanoma skin cancer keratinocytes. 2011. Submitted. This work is located in chapter 3B.

- Human tissue collection and usage in the thesis projects were approved by the University of British Columbia Clinical Research Ethics Board according to the Declaration of Helsinki Principles. The certificate number is C04-0600.

Table of contents

List of tables

List of figures

List of abbreviations

Abbreviation	Definition
1-MT	1-methyl-trytophan
ABC	Avidin:Biotinylated enzyme Complex
AK	Actinic keratosis
Akt	v-akt murine thymoma viral oncogene
ANOVA	Analysis of variance
ASIP	Agouti signaling protein
BCC	Basal cell carcinoma
BCNS	Basal cell nevus syndrome
BD	Bowen's disease
cAMP	Cyclic adenosine monophosphate
CD200	Cluster of differentiation 200
CD200R	Cluster of differentiation 200 receptor
CDK	Cyclin-dependent kinase
CTLA4	Cytotoxic T lymphocyte-associated antigen 4
DC	Dendritic cell
DCR3	Decoy receptor 3
DMEM	Dulbecco's Modified Eagle's Medium
ERK	Extracellular regulated MAP kinase
G protein	Guanine nucleotide-binding protein
GLI /Gli	Gliotactin

Abbreviation	Definition
GPCR	G protein-coupled receptor
hBCC cells	Primary human BCC cells
HF	Hair follicle
HH	Hedgehog
HPV	Human papillomavirus
IDO	Indoleamine 2,3-dixoygenase
IFN-α	Interferon-α
IHC	Immunohistochemistry
IKKα	Inhibitor of NFκB kinase-α
IL10	Interleukin 10
IL8	Interleukin 8
INK4	Cyclin-dependent kinase inhibitor 2A
IP	Immune privilege
K13	Cytokeratin 13
K17	Cytokeratin 17
KC	Keratinocyte
Kyn	L-kynurenine
MAPK	Mitogen-activated protein kinase
MC1R	Melanocortin 1 receptor
MHC	Major histocompatibility complex
MICA	MHC-I polypeptide related sequence A
MMP	Matrix metalloproteinase

Abbreviation	Definition
NFκB	Nuclear factor kappa B
NK cells	Natural killer cells
NKG2D	Natural killer group 2-receptor type D
NL	Non-lesional skin epithelium
NMSC	Non-melanoma skin cancer
NSCLC	Non-small cell lung carcinoma
P53	Protein 53
PBS	Phosphate-buffered saline
PTCH	Patched
qPCR	Quantitative real-time RT-PCR
SCC	Cutaneous squamous cell carcinoma
SCLC	Small cell lung cancer
SHH / Shh	Sonic hedgehog
shRNA	Small hairpin RNA
SMO / Smo	Smoothened
SUFU / Sufu	Suppressor of fused
TBS	Tris-buffered saline
TGFβ	Transforming growth factor β
Tregs	Regulatory T cells
TYR	Tyrosinase
UV	Ultraviolet
XP	Xeroderma pigmentosum

Abbreviation	Definition
α-MSH	α-melanocyte stimulating hormone
β_2M	beta-2 microglobulin

Acknowledgements

I would like to give my deepest gratitude to my supervisors, Dr. Kevin John McElwee and Dr. Jerry Shapiro, who provided me with the opportunity to have my graduate study in the Hair and Skin Cancer Research Laboratory team. Throughout my graduate training, Dr. McElwee and Dr. Shapiro have taught and helped me with experimental designs, given me insightful criticisms to improve my critical thinking and troubleshooting techniques, taught me both clinical and basic science research of skin cancers, and provided tremendous support during my dissertation preparation as well as my scholarship applications. The training and support they provided have made me become a better individual investigator.

It is a pleasure to thank my committee members, Drs Youwen Zhou and Jan Dutz as well as my mentor in the Canadian Institutes of Health Research-Skin Research Training Centre, Dr. Aziz Ghahary, for providing constructive advice for my projects and experimental problems as well as suggestions for my career development. Also, I would like to thank Drs David Zloty, Bryce Cowan and Nicholas Carr for providing tissue samples to me since I have started my research in the laboratory and teaching me clinical knowledge of various skin diseases.

I cannot thank my laboratory members enough for their support and help during my graduate study. Our research associate, Dr. Mei Yu, has taught me various experimental techniques and given me valuable advice for my research. Our Ph.D. student, Eddy Wang, has demonstrated to me several experimental protocols and helped me with revising my thesis. Our MSc student, Trisia Breitkopf, has given me suggestions and provided help for my experiments. Our laboratory technician, Gigi Leung, has assisted me by organizing

various laboratory duties and placing orders. Our graduated MSc student, Dr. Armin Barekatain, gave me advice on the graduate courses and my project experiments. Furthermore, I would like to thank all the summer students for making contributions to various parts of my thesis projects.

Also, I am greatly thankful to Dr. Harvey Lui, Karen Ng, Bay Gumboc and other staff of the Department of Dermatology and Skin Sciences as well as Dr. Vincent Duronio, Patrick Carew and Cornelia Reichelsdorfer from the program of Experimental Medicine for their encouragement and support throughout my graduate training.

Last but not least, I am honored to be the recipient of a Frederick Banting and Charles Best Canada Graduate Scholarship from the Canadian Institutes of Health Research, a Canadian Institutes of Health Research-Skin Research Training Award, a Pacific Century Graduate Scholarship, a UBC Four-Year Fellowship, a World Congress Fund Travel Fellowship of the International Investigative Dermatology Meeting and a UBC Graduate Student Travel Fund award. The research in this dissertation was funded by the Canadian Institutes of Health Research and the Canadian Dermatology Foundation.

Dedication

I dedicate this dissertation to my parents, my brother, Steve and my sister, Chloe, for their unconditional love, immense support and understanding during all these years. I extend my greatest appreciation to them.

Chapter 1. Introduction

1.1 Cancer

The disease of cancer has been reported since 1600 B.C., and was later named in 400 B.C. using a Greek word, karkinoma (means crab) by the Greek physician Hippocrates to describe cancer cells forming lobules of tumors that "claw" their way into tissues and organs (So, 2008). In 25 B.C., Aulus Cornelius Celsus, who was a Roman author and encyclopedia writer, translated "karkinoma" into the Latin term, cancer, which has been used since (So, 2008). Cancer can be defined in many ways. The consensus is that cancer is a disease with transformed cells that undergo proliferation without any restraints (Garrett, 2001), which is also known as unscheduled proliferation (Malumbres and Barbacid, 2009). Such uncontrolled proliferation results in clonal expansion of transformed cells that, together with genomic alterations, contributes to the destabilization of genomic and chromosomal integrity (Malumbres and Barbacid, 2009). At this stage, the transformed cells acquire aggressive abilities including initiation of vascularization and angiogenesis, invasion and metastasis, and insensitivity to apoptosis (Garrett, 2001; Malumbres and Barbacid, 2009). This whole process known as carcinogenesis may result in the death of the affected organism (Buzzell, 1996). These alterations are due to malfunction in the regulation of the normal cell cycle, which may involve both biochemical and genetic changes (Buzzell, 1996; Garrett, 2001; Malumbres and Barbacid, 2009)

1.1.1 Normal cell cycle

The normal cell cycle consists of two major components, the DNA replication stage (S phase) and mitosis (M phase) (Collins *et al.*, 1997; Garrett, 2001). There are two gap phases, G_1 and G_2 between the S and M phases. G_1 phase is after mitosis and exerts both positive and negative growth signals on the cell to prepare for DNA synthesis in S phase (Collins *et al.*, 1997; Garrett, 2001). In addition, G_1 can connect to a quiescent G_0 phase. Cells without appropriate growth signals reversibly enter the G_0 phase whereas cells that irreversibly enter G_0 are destined to undergo terminal differentiation or senescence (Garrett, 2001). G_2 follows S phase and allows the cell to prepare for mitosis (Garrett, 2001).

The initiation and progression from one phase to another during the cell cycle is mainly regulated by cyclin-dependent kinases (CDK), which are serine/threonine kinases, and checkpoint control (Collins *et al.*, 1997; Garrett, 2001; Malumbres and Barbacid, 2009). CDK requires association of a regulatory subunit, cyclin, which is expressed at a specific point during cell cycle and thus regulates CDK in a timely-manner (Collins *et al.*, 1997; Malumbres and Barbacid, 2009). There are many different subsets of CDKs and cyclins in humans; however, only certain CDK-cyclin complexes are involved in the cell cycle (Malumbres and Barbacid, 2009). For instance, CDK2, CDK4 and CDK6 are involved in the interphases G_1 and G_2, and CDK1 is a mitotic CDK. Also, there are four different classes of cyclins, A-, B-, D- and E-types, which contribute to 10 cyclins in total (Malumbres and Barbacid, 2009). In addition, the CDK-cyclin complex regulates the cell cycle in a cell-type specific manner. For example, D-type cyclins D1, D2 and D3 have high affinity to bind with CDK4 and CDK6 during the G_1 phase in pancreatic β-cells and erythroid lineage cells respectively; on the other hand, loss of function of CDK1 leads to cell cycle arrest and

inhibition of embryo development (Malumbres *et al.*, 2004; Rane *et al.*, 1999; Santamaria *et al.*, 2007). For checkpoint controls, each of the monitoring points is composed of three elements: a sensor mechanism to detect abnormality of cell cycle events, signal transduction to pass along signals from the sensor, and an effector mechanism to trigger cell cycle arrest after receiving the signals (Garrett, 2001). The major checkpoints are DNA damage checkpoints and are located at the G_1/S phase transition, S phase and G_2/M phase transition. If DNA repair is unsuccessful, the cells may undergo apoptosis or senescence to prevent accumulation of altered DNA and genomic instability (Garrett, 2001; Malumbres and Barbacid, 2009). After DNA replication, the cell cycle is monitored by a spindle assembly checkpoint, which is involved in mitosis, to ensure proper chromosomal segregation, and thus prevent chromosomal instability (Garrett, 2001; Malumbres and Barbacid, 2009). In addition, there is a restriction point between the mid and late stage of the G_1 phase. During this checkpoint, the cell needs to receive a sufficient growth signal to progress from G_1 to S phase; if the cell does not acquire appropriate signals, it enters the G_0 phase as mentioned earlier (Garrett, 2001).

Furthermore, CDK-cyclin complexes have been shown to be regulated by CDK inhibitors to ensure quiescence of different stem cell populations in adult human tissues (Malumbres and Barbacid, 2009). The inhibitors are divided into two families: cyclin-dependent kinase inhibitor 2A (also known as p16 or INK4), which includes INK4A, INK4B, INK4C and INK4D, and the Cip and Kip family, which includes p21, p27 and p57 (Malumbres and Barbacid, 2005). Proper cell growth and proliferation depends on the tight regulation of the CDK-cyclin complexes and checkpoint controls. Any defects or mutations of these two systems can result in uncontrollable cell proliferation and exacerbation of

genomic and chromosomal instability. As a result, quiescence of stem cell populations will be altered and/or probability of tumorigenesis will be increased (Figure 1.1) (Collins *et al.*, 1997; Malumbres, 2011).

For instance, sonic hedgehog (SHH) signaling pathway activation can induce tumorigenesis, particularly basal cell carcinoma (Epstein, 2008). SHH has been shown to upregulate the activity of CDK2 and CDK4 as well as inhibit the suppression effect of $p21^{Cip1}$ in human keratinocytes (Fan and Khavari, 1999). As such, continued proliferation of keratinocytes, inhibition of cell cycle arrest and tumor formation resulted (Fan and Khavari, 1999). Moreover, Rundhaug and colleagues demonstrated that the expression of cyclin D1 was associated with the progression of skin carcinogenesis (Rundhaug *et al.*, 1997). In the models of multistage mouse skin carcinogenesis, cyclin D1 expression was only found in the basal layer of the epidermis and one to two layers above in papillomas while such protein expression was detected in all skin layers of cutaneous squamous cell carcinomas; no cyclin D1 was detected in hyperplastic skin samples (Rundhaug *et al.*, 1997). As such, alteration of the homeostasis of cell cycle is essential in tumorigenesis including skin cancers.

Figure 1.1 Adult stem / progenitor cell function and its control by G_1 kinases

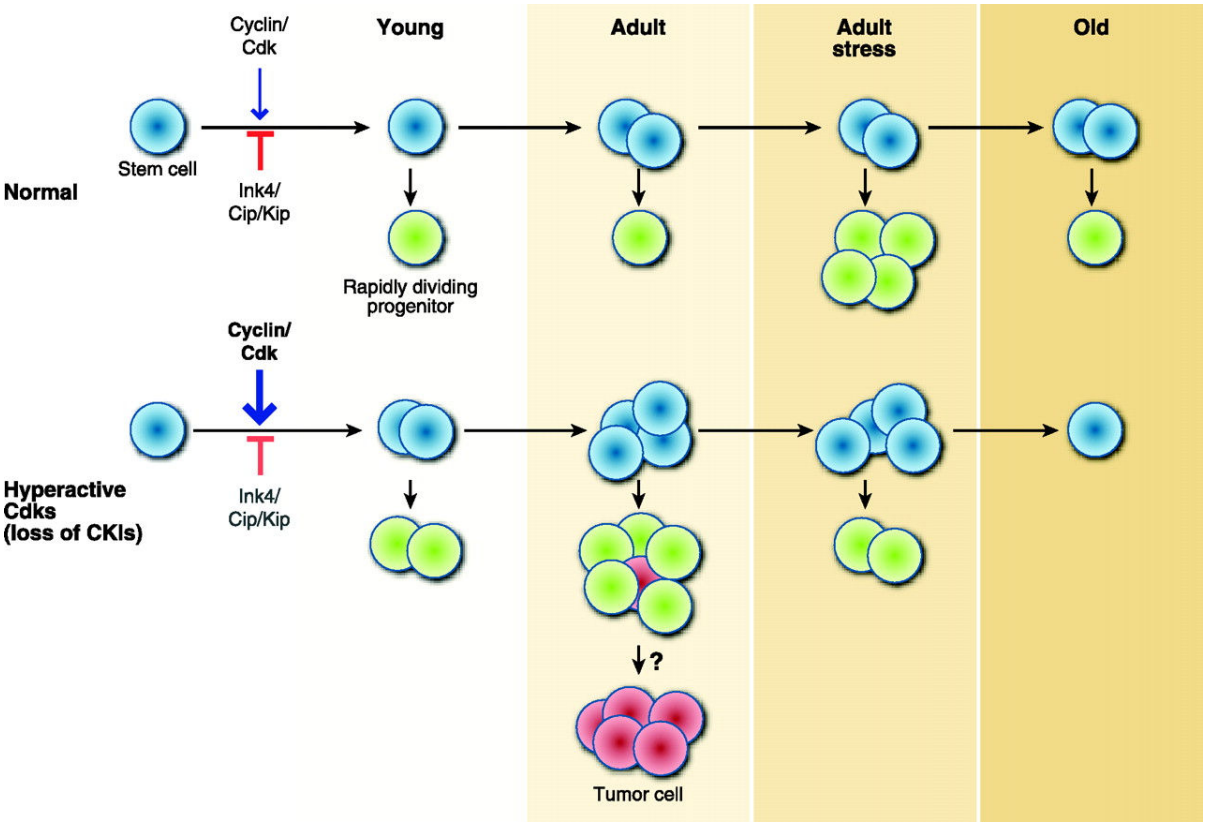

In normal tissues, stem cell self-renewal is tightly controlled to ensure proper tissue homeostasis and regeneration throughout life. Upon hyperactivation of G_1 CDKs (e.g. CDK2, CDK4 or CDK6) mediated by cyclin overexpression of loss of the corresponding inhibitors (INK4 or Cip / Kip families), proliferation of stem cells is increased possibly cooperating with tumor formation. Modified from Malumbres M. 2011 with permission to reprint.

1.1.2 Carcinogenesis

It has been well supported that a multistage model of carcinogenesis confers the development of malignancy (Armitage and Doll, 1954; Hanahan and Weinberg, 2011; So, 2008). The first stage is known as initiation, which involves one or more inherited or spontaneous mutations in the cell genome. Exogenous factors such as chemical or environmental agents can lead to initiation (Buzzell, 1996; Macdonald *et al.*, 2004). In order to progress to the subsequent stages, the initiated cell and its progeny need to proliferate and survive throughout the lifespan of the organism (Buzzell, 1996; Hanahan and Weinberg, 2011; Macdonald *et al.*, 2004). The second step is promotion, which allows selective clonal expansion of initiated cells and their progeny, and leads to larger populations of mutated cells for further genetic alterations and malignant conversion (Buzzell, 1996; Macdonald *et al.*, 2004). Activation of cell proliferation signaling pathways or inhibition of tumor suppressing signaling are involved in the promotion stage (Buzzell, 1996). This step requires exogenous and endogenous tumor promoters such as ultraviolet (UV) exposure, as an example of an exogenous agent, or mutation of the *p53* tumor-suppressor gene as an endogenous agent (Buzzell, 1996; Vargo, 2003). The last stage is progression, which comprises additional genomic mutations such as activation of proto-oncogenes or exposure to DNA damaging agents (Buzzell, 1996; Macdonald *et al.*, 2004). It results in enhancing genomic instability and transformation, which confers malignant and cancerous metastasis (Buzzell, 1996).

1.1.3 Types of cancers and frequencies

Tumors can be divided into two major forms: noncancerous (benign) and cancerous (malignant) (Macdonald *et al.*, 2004). Benign tumors grow within a defined location with

limited size, and rarely cause death; they usually maintain the genomic characteristic of the original cell. For instance, seborrheic keratosis (SK) is a common benign epidermal lesion; it contains two keratinocytic components including basaloid cells and monomorphous squamous epithelial cells (Hafner and Vogt, 2008). Malignant cancers acquire the ability to invade locally and subsequently to lymph nodes, and eventually metastasize to distant organs of the organism. It is mostly the metastasis stage that contributes to cancer mortality (Macdonald *et al.*, 2004; Ruddon, 2007). The most common cancer types can be classified as follows: carcinoma, which is derived from epithelial cells such as skin, prostate, breast and lung; leukemia and lymphoma, which arise from cells of hematopoietic lineage; and sarcomas, which tumor cells originate from the mesenchymal layer (Ponten *et al.*, 2008).

In 2011, there will be approximately 5,000 new cases of leukemia diagnosed in Canada (CanadianCancerSociety, 2011). They will contribute to 3.7 % and 2.8 % of cancer deaths in males and females respectively (CanadianCancerSociety, 2011). The most common feature of leukemia is chromosomal abnormalities; such alteration usually occurs in or close to an oncogene. Although additional types of genomic changes may be involved in tumor initiation and development, chromosomal translocation or alteration may act as markers to identify disease clinical outcomes, progression and treatment effects of leukemia, such as chronic lymphocytic leukemia (Macdonald *et al.*, 2004; Ruddon, 2007).

Lung cancer is the third most common cancer type in Canada. There will be approximately 25,300 new cases of this type of cancer diagnosed in Canada in 2011. More importantly, it will contribute to the highest mortality rate at 28.3 % of all the cancer deaths in the country (CanadianCancerSociety, 2011). Lung cancer is further divided into non-small cell lung carcinoma (NSCLC) and small cell lung cancer (SCLC). SCLC accounts for 20 %

of all primary lung cancers whereas NSCLC accounts for 80 % of all the cases with the most common subtype known as adenocarcinoma followed by squamous cell carcinoma, large cell carcinoma, adenosquamous carcinoma, sarcomatoid carcinoma, neuroendocrine tumors, and unclassified carcinomas (Macdonald *et al.*, 2004).

Prostate cancer is the second most common malignancy in Canada in 2011; there will be approximately 25,500 new cases diagnosed in the country, and will lead to 10.2 % of cancer deaths (CanadianCancerSociety, 2011). It has been shown that men with ages between 45 to 64 have the highest mortality rate from this malignancy (Post *et al.*, 1999). A family history of prostate cancer is the most consistent predisposing factors of the disease, and is associated with 10 % to 15 % of all cases (Narod, 1999). Moreover, the clinical outcome and severity of the disease are extremely diverse, ranging from non-invasive to rapid metastasis and even death shortly after diagnosis (Macdonald *et al.*, 2004).

Skin cancer is divided into non-melanoma skin cancer (NMSC) and cutaneous melanoma. NMSC is the most common cancer type in humans. According to Canadian Cancer Statistics, NMSC has the highest incident rate as expected; 74,100 new cases will be diagnosed in 2011 in the country, which accounts for 42 % of all new cancer cases estimated in Canada (CanadianCancerSociety, 2011). Melanoma, on the other hand, is more aggressive but with a lower incidence rate; there will be only about 5,500 new cases diagnosed in Canada in 2011 (CanadianCancerSociety, 2011; Madan *et al.*, 2010). The incidence of skin cancer is increasing rapidly; every 1 in 6 males or females will develop such carcinoma during his or her lifetime in the United States (Gloster and Brodland, 1996). As such, laboratory investigation of the pathogenesis and mechanisms, as well as development and improvement of clinical trials and treatment of the disease, is required.

1.2 NMSC – basal cell carcinoma and cutaneous squamous cell carcinoma

NMSC primarily includes basal cell carcinoma (BCC) and cutaneous squamous cell carcinoma (SCC), which accounts for 80 % and 16 % of all the cases respectively (Madan *et al.*, 2010; Miller and Weinstock, 1994; Wenzel *et al.*, 2008). Other less common NMSCs include Merkel cell carcinoma, cutaneous lymphoma and adnexal tumors (Madan *et al.*, 2010). The lifetime risk of developing SCC is 7 % to 11 % while that of BCC is 28 % to 33 % in the United States (Walling *et al.*, 2004; Wong *et al.*, 2003). BCC rarely causes death and seldom metastasizes with a metastatic rate ranging from 0.003 % to 0.55 % (Wong *et al.*, 2003). However, it can behave aggressively with deep invasion, recurrence and resistance to standard treatments. Also, because this cancer typically affects sun-exposed skin of the head and neck, cosmetic disfigurement is common (Epstein, 2008; Walling *et al.*, 2004; Wong *et al.*, 2003). SCC, on the other hand, is more aggressive. Epstein and colleagues reported that the metastatic rate of cutaneous SCC was 2 % at the time of diagnosis (Epstein *et al.*, 1968); Rowe and colleagues demonstrated that rates increased as the duration of patient follow-up increased (from 2.3 % in < 5 years to 5.2 % in > 5 years) (Rowe *et al.*, 1992). Several outpatient-based studies revealed the rate of nodal metastasis of head and neck cutaneous SCC ranged from 4.9 % to 5.8 % (Bumpous, 2009; Czarnecki *et al.*, 1994; Joseph *et al.*, 1992). Although the mortality rate of SCC is about 1 %, it accounts for approximately three-quarters of deaths due to NMSC (Clayman *et al.*, 2005; Devesa *et al.*, 1999; Dunn *et al.*, 1965).

BCC and SCC are composed of proliferating mutated keratinocytes from the basal and suprabasal layer of the epidermis respectively (Figure 1.2) (Bernstein *et al.*, 1996;

Epstein, 2008; Nakayama, 2010). Unlike BCC, which develops *de novo* and has no pre-cancerous lesions, SCC may be preceded by pre-malignant lesions such as actinic keratosis (AK) and Bowen's disease (BD) (Epstein, 2008; Madan *et al.*, 2010). The risk of an individual AK to progress to invasive SCC is 1 % to 10 % over 10 years while that of BD (also known as SCC *in situ*) is 3 % to 5 % (Cox *et al.*, 2007; Glogau, 2000).

Figure 1.2 Origin of the major type of skin cancers

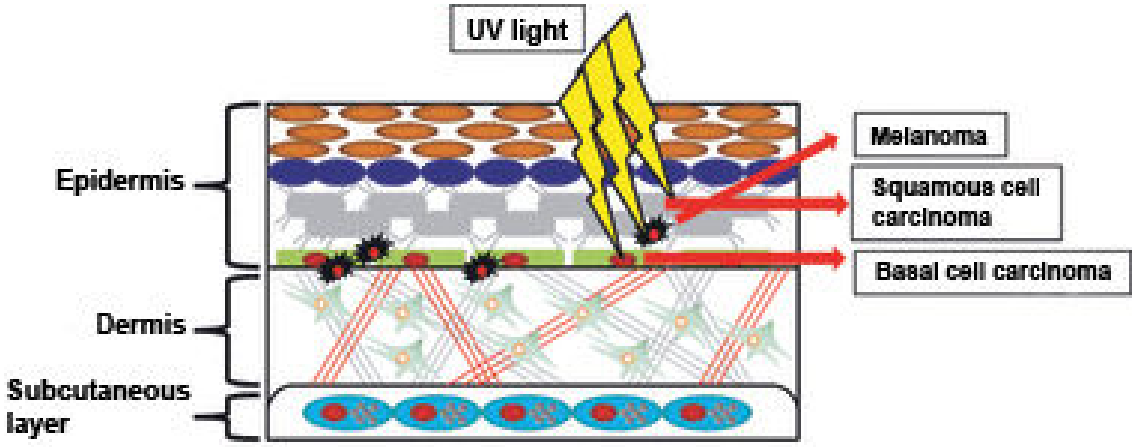

Skin is formed by the layers of cells, the epidermis, dermis, and subcutaneous layers. Three major types of skin cancer, basal cell carcinomas, squamous cell carcinomas, and melanomas originate from keratinocytes or melanocytes residing in the epidermis. UV light is one of the main causes of skin cancer. Modified from Nakayama K. 2010 with permission to reprint.

1.3 Epidemiology and frequency of NMSCs

It has been shown that the annual incidence rate of NMSC has increased 3 % to 8 % among the white population since 1960 in Canada, the United States, Australia and Europe (Madan *et al.*, 2010). The rapidly increasing rate may be due to increasing awareness of skin cancer prevention campaigns, higher attention from clinical diagnosis and referral of patients to dermatologists, more exposure to sunlight (for example, for leisure or outdoor activities), increased longevity and a higher number of elderly individuals in populations as well as increased UV radiation intensity due to ozone depletion (Chinem and Miot, 2011; Garssen *et al.*, 1998; Jones, 1987). The occurrence of BCC is about 4 to 5 times more than SCC, and is about 8 to 10 time more than melanoma (Chinem and Miot, 2011). Australia has the highest rate of BCC in the world with 726 cases per 100,000 inhabitants per year, followed by the US with 191 cases and Canada with 155 cases (Chinem and Miot, 2011; Gloster and Brodland, 1996). The BCC frequency in regional populations is increasing at a rate of 2 % to 19 % per year, with a 4 % annual rate of increase in Canada (Gallagher *et al.*, 1990; Marks *et al.*, 1993; Urbach, 1991). Interestingly, the number of male BCC patients is higher than female patients, which may be due to the fact that women tend to seek dermatological care or consultation more often than men (Chinem and Miot, 2011). Moreover, about 40 % to 50 % of patients with a primary BCC will develop at least one or more new BCCs within 5 years (Madan *et al.*, 2010).

1.4 Clinical appearance of BCCs and cutaneous SCCs

1.4.1 BCC

Early BCC tumors are usually small (less than 1 cm diameter) and translucent. They consist of areas that are raised and telangiectic (Madan *et al.*, 2010; Randle, 1996; Wong *et al.*, 2003). There are several subtypes of BCC; the most common one is nodular BCC (50 % to 54 %) followed by superficial, pigmented, morpheiform, basosquamous and other subtypes (Vargo, 2003). In addition, 10 % to 40 % of BCCs have mixed patterns of 2 or more of the subtypes (Madan *et al.*, 2010).

1.4.2 BCC subtypes

Nodular BCC is a solid, shiny, red nodule with telangiectasias and well-defined raised border; ulceration and/or erosion are seen in the center. It is usually found on the face (Madan *et al.*, 2010; Vargo, 2003; Wong *et al.*, 2003). Superficial BCC is often flat and has one or more erythematous, scaly patches surrounded by a fine, thread-like, pearly border; it usually occurs on the trunk. Also, the superficial subtype can be difficult to differentiate from psoriasis, eczema or BD (Madan *et al.*, 2010; Vargo, 2003; Wong *et al.*, 2003). The pigmented subtype has similar features as nodular BCC but with blue, brown or black pigmentation; this subtype can be confused with melanoma (Madan *et al.*, 2010; Vargo, 2003). Morpheiform BCC appears as an indurated, whitish or yellowish scar-like plaque with ill-defined borders; its surface is smooth and shiny. This tumor can be very large in size, become aggressive, and invade into the dermis (Madan *et al.*, 2010; Vargo, 2003; Wong *et al.*, 2003). Basosquamous BCC contains areas of both BCC and SCC with a transition zone

in between; it has poor prognosis, and is more aggressive with greater tendency to metastasize (Vargo, 2003).

1.4.3 Cutaneous SCC

Cutaneous SCC has common features of induration with a hyperkeratotic, flesh-like nodule or plaque surrounded by an ill-defined border (Madan *et al.*, 2010; Vargo, 2003). This tumor type grows by expansion and infiltration into dermis (Bernstein *et al.*, 1996; Vargo, 2003). SCC can spread laterally along tissue planes, perichondrium or periosteum, as well as spread along vessels or nerves involving perineural invasion in a conduit fashion (Bernstein *et al.*, 1996; Vargo, 2003). SCC may metastasize to regional lymph nodes or through hematogenous spread (Bernstein *et al.*, 1996).

1.4.4 SCC precursors and subtypes

SCC can have precursor forms, such as AK and BD, as mentioned earlier (Epstein, 2008; Madan *et al.*, 2010). Although the rate of an individual AK to transform to SCC is low, a patient with multiple AKs may have high overall risk to develop SCC (Lohmann and Solomon, 2001; Madan *et al.*, 2010). AK can be a marker used for early detection and treatment of skin neoplasia, which can further prevent subsequent malignant transformation into SCC (Madan *et al.*, 2010). The most common subtype of SCC is generic or simplex SCC, which also has the greatest risk to metastasize, followed by other subtypes including bowenoid and adenoid / acantholytic subtypes which have similar metastasis risk (Lohmann and Solomon, 2001). BD usually appears as slow-growing, erythematous, scaly or crusted plaques with well-defined borders (Bernstein *et al.*, 1996; Lohmann and Solomon, 2001;

Madan *et al.*, 2010). It mainly occurs on head and neck, followed by lower limbs, upper limbs and trunk (Bernstein *et al.*, 1996; Lohmann and Solomon, 2001). When the neoplastic keratinocytes of BD invade into the dermis, it becomes the bowenoid SCC subtype (Lohmann and Solomon, 2001). Adenoid SCC presents as an ulcer or crusted nodule; it can be wart-like, and has a central plug or crater (Bernstein *et al.*, 1996; Lohmann and Solomon, 2001). It is usually found on the head and neck (Lohmann and Solomon, 2001).

1.5 Histology of BCCs and SCCs

1.5.1 BCC

BCC consists of proliferating basaloid cells with enlarging nuclei and loss of intercellular bridges (Chinem and Miot, 2011). BCC cells usually form clusters and arrange peripherally in palisades; there are gaps between stroma and the tumor nests (Chinem and Miot, 2011). BCC subtypes may have additional specific histological features. Nodular BCC usually expresses cystic differentiation, and may have central necrosis within tumor lobules (Chinem and Miot, 2011; Vargo, 2003). The superficial subtype has budding and irregular proliferation of BCC cells, which form tumor nests that arrange horizontally in the papillary dermis. In addition, fibroblasts are found surrounding tumor masses with chronic inflammatory infiltrates in the upper dermis (Chinem and Miot, 2011; Vargo, 2003). The histology of pigmented BCC is similar to that of the nodular form but with additional melanin production (Chinem and Miot, 2011; Vargo, 2003). Morpheiform BCC has fibroepitheliomatous strands of tumor lobules, which form finger-like projections; these tumor masses can progress along tissue planes and invade into the dermis (Vargo, 2003).

Basosquamous carcinoma contains separate BCC and SCC histological features in a biphasic pattern (Vargo, 2003).

1.5.2 SCC

As mentioned earlier, SCC tumors are also composed of proliferating keratinocytes from the suprabasal layer of the epidermis (Bernstein *et al.*, 1996). Generic SCC consists of tumor cells with enlarging, hyperchromatic and pleomorphic nuclei, and has prominent mitotic figures (Lohmann and Solomon, 2001). The epidermis of bowenoid SCC is characterized with hyperkeratosis and acanthosis, and may have psoriasiform hyperplasia. In addition, atypical mitoses may be detected in this SCC subtype (Lohmann and Solomon, 2001). Adenoid SCC is composed of strands of tumor lobules forming pseudoglandular or adenoid structures produced by acantholysis of cells. Those acantholytic keratincoytes are large and dysplastic, and are found as single or cluster of cells in the lumen (Bernstein *et al.*, 1996; Lohmann and Solomon, 2001).

1.6 Risk factors for NMSCs

1.6.1 Individual factors

The initiation and progression of NMSC is associated with the interaction of intrinsic and extrinsic factors. The etiological factors of BCC and SCC are similar including male sex, aging, family history of skin cancer, more sun sensitive skin type (ie. Skin type I - always burns, never tans), red or blond hair, blue or green eyes as well as freckling and sunburn in childhood (Chinem and Miot, 2011; Karagas *et al.*, 1992; Madan *et al.*, 2010). The ratio of

male patients to female patients of BCC ranges from 1.5:1 to 2:1 (Roewert-Huber *et al.*, 2007). Also, more than half of BCCs are diagnosed in patients with age between 50 to 80 years old (Table 1.1) (Chinem and Miot, 2011).

1.6.2 Environment factors

1.6.2.1 UV radiation

UV radiation is the most important environmental insult for both BCC and SCC (Madan *et al.*, 2010). UV radiation has been shown to have direct effect on DNA damage (Buzzell, 1996). Also, UV radiation can suppress local and systemic immune responses, which may alter and impair the host immune system to detect and suppress neoplastic keratinocyte proliferation and progression (Buzzell, 1996; Madan *et al.*, 2010). UV radiation is subdivided according to the wavelength: UVA (320 nm to 400 nm), UVB (280 nm to 320 nm), and UVC (200 nm to 280 nm) (Bowden, 2004). UVB contains the most important tumorigenic wavelengths as it has stronger penetrative power than UVA, and can directly damage DNA and other cellular compartments; UVC is filtered out by the ozone layer (Bowden, 2004; Buzzell, 1996; Gloster and Brodland, 1996). UV radiation results in production of DNA adducts, such as cyclobutane dimers. Failure to repair or remove those DNA adducts lead to replication of pyrimidine-dimers in DNA, i.e. CC to TT or C to T transitions (Bowden, 2004; Buzzell, 1996; Gloster and Brodland, 1996). Such UV light signature mutations have been found in many tumor growth-associated genes, for example, patched (*PTCH*) and *p53* (Bowden, 2004; Buzzell, 1996; Gloster and Brodland, 1996; Vargo, 2003).

It has been indicated that the intensity of cumulative lifetime sun exposure is proportional to the susceptibility of SCC growth; especially when the total cumulative sun exposure hours approaches 100,000 hours. Interestingly, BCC development is associated with intermittent sun exposure and particularly during childhood; BCC incidence rate is the highest when the cumulative sun exposure time is 10,000 hours to 35,000 hours with no further increased risk rate under longer exposure times (Table 1.1) (Epstein, 2008; Kricker *et al.*, 1995; Madan *et al.*, 2010; Rosso *et al.*, 1996).

1.6.2.2 Ozone depletion and others

Other environmental predisposing factors include ozone depletion, which leads to higher amounts of UVB radiation penetrating to the earth's surface (Gloster and Brodland, 1996; Jones, 1987). Every 2 % decrease of ozone concentration leads to 4 % elevation of biologically effective radiation from the sun reaching the earth, and subsequently enhances the chance of individuals to develop NMSC over their lifetime by 6 % to 12 % (Gloster and Brodland, 1996; Kripke, 1988). Further environmental insults that promote skin cancers include ionizing radiation and arsenic exposure (Table 1.1) (Guo *et al.*, 2001; Jones, 1987; Karagas *et al.*, 2001; Karagas *et al.*, 2002).

1.6.3 Genetic factors and co-morbidities

1.6.3.1 Human papillomavirus

Human papillomavirus (HPV) has been shown to be associated with NMSCs (Chinem and Miot, 2011; Madan *et al.*, 2010). Approximately 90 % of immunocompromised

individuals and 50 % of immunocompetent individuals with NMSCs were detected with DNA from cutaneous HPV or β HPV types (Karagas *et al.*, 2006; Madan *et al.*, 2010). Harwood and colleagues found that HPV DNA was detected in 84.1 % of SCC and 75 % of BCC patients that were immunocompromised as well as in 27.2 % of SCC and 36.7 % of BCC of immunocompetent individuals (Table 1.1) (Harwood *et al.*, 2000).

1.6.3.2 Mutation of protein 53 gene

In addition, inactivation mutation of protein 53 (*p53*) has been shown to be important for the development of NMSC. *P53* encodes the protein p53, which is a tumor suppressor protein, and is involved in DNA repair and apoptosis (Madan *et al.*, 2010). Loss of function of *p53* causes cells to be resistant to apoptosis and leads to accumulation and expansion of cells with impaired DNA (Table 1.1) (Madan *et al.*, 2010). Such gene mutation is found in both BCC and SCC (Madan *et al.*, 2010).

1.6.3.3 Mutation of melanocortin 1 receptor gene

The melanocortin 1 receptor (*MC1R*) gene variants regulate the degree of skin pigmentation (Epstein, 2008; Madan *et al.*, 2010). The gene variants, agouti signaling protein (*ASIP*) and tyrosinase (*TYR*), contribute to red hair and fair pigmented skin, and are associated with cutaneous melanoma and BCC (Gudbjartsson *et al.*, 2008). More importantly, increasing evidence has shown that *MC1R* gene variants might be independent risk factors for NMSC (Table 1.1) (Bastiaens *et al.*, 2001).

1.6.3.4 Basal-cell nevus syndrome

Although most of the BCCs develop sporadically, there are some cases that are associated with an autosomal dominant disorder, basal-cell nevus syndrome (BCNS), also known as Gorlin syndrome (Epstein, 2008). BCNS results from mutation of *PTCH*, which is a tumor suppressor gene (Chinem and Miot, 2011; Epstein, 2008; Madan *et al.*, 2010). The patients are characterized by having multiple BCCs, bone deformation, disproportion of head to body ratio with elongated limbs as well as other tumors such as cerebellar medulloblastomas (Table 1.1) (Chinem and Miot, 2011).

1.6.3.5 Xeroderma pigmentosum

Xeroderma pigmentosum (XP) is a rare autosomal recessive syndrome (Madan *et al.*, 2010). Patients are found to have inactivating mutations of *XPC*, which encodes XPC protein to detect helix-distorting lesions in DNA, and participates in the genome repair pathway (Madan *et al.*, 2010). XP patients are susceptible to development of BCC and SCC (Table 1.1) (Chinem and Miot, 2011; Epstein, 2008; Madan *et al.*, 2010).

Table 1.1 Risk factors for the development of NMSC cancers

Individual Factors	• Male (1.5-2.1 fold higher than female) (Roewert-Huber *et al.*, 2007) • Old age (50 % of BCC patients are 50-80 years old) (Chinem and Miot, 2011) • Family history (Chinem and Miot, 2011; Karagas *et al.*, 1992; Madan *et al.*, 2010) • Sun sensitive, skin type I (Chinem and Miot, 2011; Karagas *et al.*, 1992; Madan *et al.*, 2010) • Red/blonde hair (Chinem and Miot, 2011; Karagas *et al.*, 1992; Madan *et al.*, 2010) • Blue/green eyes (Chinem and Miot, 2011; Karagas *et al.*, 1992; Madan *et al.*, 2010) • Childhood freckling and sunburn (Chinem and Miot, 2011; Karagas *et al.*, 1992; Madan *et al.*, 2010)
Environmental Factors	• UVB most dangerous (UVA has weak penetration, UVC gets filtered by ozone layer) (Bowden, 2004; Buzzell, 1996; Gloster and Brodland, 1996) • SCC risk increases proportional to length of childhood sun exposure; BCC is associated with intermittent sun exposure (Epstein, 2008; Kricker *et al.*, 1995; Madan *et al.*, 2010; Rosso *et al.*, 1996) • Ozone depletion, ionizing radiation and arsenic exposure (Gloster and Brodland, 1996; Guo *et al.*, 2001; Jones, 1987; Karagas *et al.*, 2001; Karagas *et al.*, 2002)
Genetic Factors and Co-morbidities	• Human papillomavirus DNA found 90 % of immunocompromised individuals with NMSC (Madan *et al.*, 2010) • Inactivation mutation of *p53* is associated with NMSC tumorigenesis (Madan *et al.*, 2010) • Gene variants of *MC1R*, such as *ASIP* and *TYR*, are associated with cutaneous melanoma and BCC (Epstein, 2008; Gudbjartsson *et al.*, 2008; Madan *et al.*, 2010) • Patients of BCNS (a.k.a. Gorlin syndrome) are highly susceptible to develop multiple BCCs (Chinem and Miot, 2011; Epstein, 2008; Madan *et al.*, 2010) • Xeroderma pigmentosum patients are predisposed to have BCC and SCC development (Chinem and Miot, 2011; Epstein, 2008; Madan *et al.*, 2010)

1.7 Pathogenesis of BCCs and SCCs

1.7.1 Sonic hedgehog signaling pathway

The fundamental mechanism of BCC initiation is mainly due to gene mutation of the sonic hedgehog (SHH) signaling pathway (Figure 1.3) (Epstein, 2008; Madan *et al.*, 2010). SHH is a morphogene, and is the human homolog of the Drosophila extracellular ligand hedgehog (Epstein, 2008). It is essential for the development of various organs including the skin and hair follicles (Athar *et al.*, 2006; Boukamp, 2005). SHH plays a key role in regulating stem cell populations; mutations in genes of this signaling pathway can result in inhibition of epithelial cell cycle arrest, neoplasia, and perturbation of other associated cell-cycle events (Athar *et al.*, 2006; Fan and Khavari, 1999; Nilsson *et al.*, 2000). Besides the patched gene, which encodes the protein PTCH and is a 12-domain transmembrane protein receptor of SHH, this pathway consists of genes smoothened (*SMO*), which encodes another 7-domain transmembrane protein SMO, suppressor of fused (SUFU) and the gliotactin (*GLI*) family of transcription factors, *GLI1*, *GLI2* and *GLI3* (Figure 1.3) (Epstein, 2008). Under normal conditions, PTCH interacts with SMO which keeps SMO in its inactive state. When SHH binds to PTCH, the latter can no longer attach to SMO, which leads to relief of the inhibition of SMO. Subsequently, SMO triggers its downstream signaling targets and activates transcription factor GLI proteins, which in turn induce expression of target genes such as transforming growth factor β (*TGF-β*) and *PTCH* (Figure 1.3) (Epstein, 2008). It has been shown that overexpression and upregulation of these downstream targets were detected in BCNS and BCC patients, as the result of SHH overexpression, activating mutations of *SMO*, or inactivating mutations of *PTCH* (Aszterbaum *et al.*, 1998; Athar *et al.*, 2006;

Epstein, 2008; Hahn *et al.*, 1996; Ji *et al.*, 2007; Nilsson *et al.*, 2000; Xie *et al.*, 1998). Such genomic alteration has been found in > 70 % of BCC cases studied (Boukamp, 2005; Gailani *et al.*, 1996; Xie *et al.*, 1998).

Figure 1.3 Hedgehog signaling pathway under normal and BCC tumorigenesis conditions

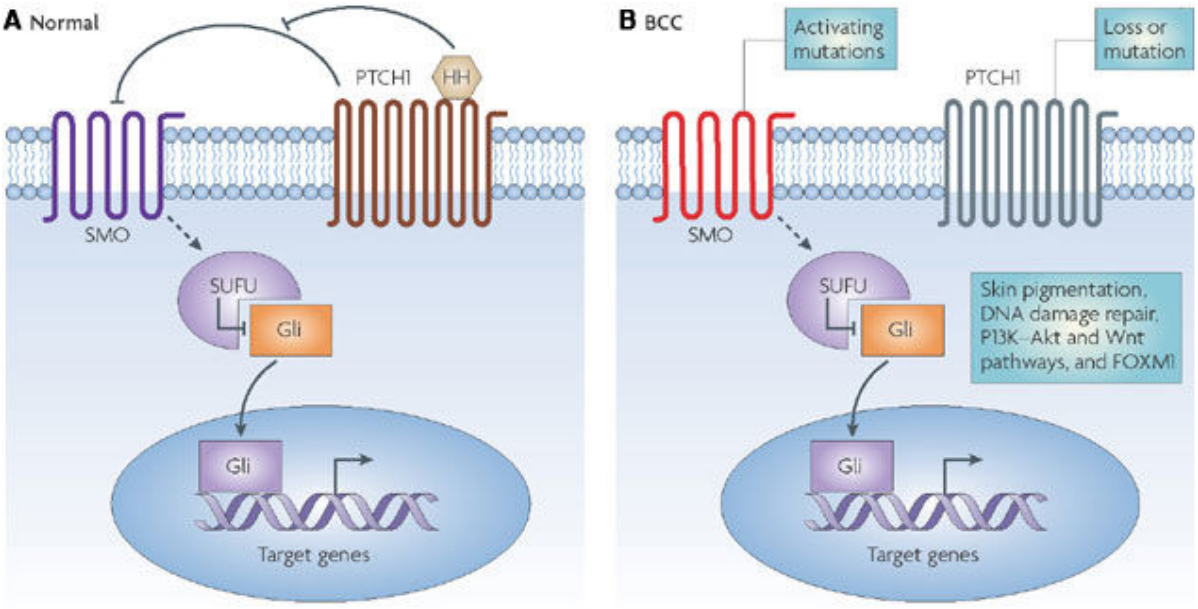

(A) The family of human hedgehog (HH) includes sonic hedgehog (SHH), Indian hedgehog (IHH) and desert hedgehog (DHH), which bind to transmembrane protein receptor PTCH1. Such binding relieves the inhibition of another transmembrane protein receptor, smoothened (SMO) by PTCH1. Activated SMO subsequently triggers and activates downstream targets, including suppressor of fused (SUFU) and the Gli transcriptional factor family. (B) In BCC, loss of function of PTCH1 or activating mutation of SMO is detected, which ultimately lead to activation of the HH signaling pathway and transcription of tumor progressor genes. Modified from Epstein, E.H. *et al.* 2008 with permission to reprint.

1.7.2 p53

Mutation of *p53* has been shown to be the most common genetic alteration in humans (Buzzell, 1996). It is involved in cell cycle regulation and apoptosis by binding to a specific sequence in DNA and triggering expression of regulatory proteins (Buzzell, 1996). Under normal conditions, *p53* is not detected in cells. Upon exposure to tumor promoting agents, such as UV radiation, posttranslational p53 molecules are stabilized and accumulation of the proteins results. The p53 molecule binds to a specific DNA sequence and causes cell cycle arrest in the G_1 phase which allows DNA repair before the replication and mitosis stages start (Buzzell, 1996). Mutation of *p53* leads to conformational change of the protein, which enhances the stability and half-life of the mutated molecule (Buzzell, 1996). Abnormal p53 acts in a dominant manner and prevents wild-type p53 from binding to DNA and activating transcription. Thus, replication of altered DNA and elevation of genomic instability result (Buzzell, 1996).

While there is no gene mutation of the SHH pathway in SCC, mutation of *p53* is an early event during the development of SCC and is involved in > 90 % of all the cases as well as 40 % to 66 % of premalignant BD and AK forms respectively (Madan *et al.*, 2010); such mutation is only found in 33 % to 50 % of BCC cases (Benjamin and Ananthaswamy, 2007; Reifenberger *et al.*, 2005).

1.8 Current treatments of NMSCs

The goals of NMSC treatment are to remove tumors completely, prevent recurrence and preserve as much non-lesional tissue as possible with good cosmetic outcome (Madan *et al.*, 2010). Due to significant morbidity of both BCC and SCC, the cost of treating NMSCs is

over 500 million dollars each year in the United States (Preston and Stern, 1992). Decision on treatment methods depends on several factors including the clinical and histological appearance of tumors, size and site of tumors, comorbidities, availability of treatment-specific practitioners and resources, and cost (Madan *et al.*, 2010). The treatment modalities for NMSC are mainly divided into surgical (Table 1.2) and medical methods (Table 1.3) (Madan *et al.*, 2010). Although surgery is considered a destructive technique, it is by far the most efficient cure for NMSC (Madan *et al.*, 2010).

1.8.1 Surgical methods

Surgical excision is removal of lesions with predetermined margins; marginal tissues are examined by histological analysis to ensure tumors are completely removed (Madan *et al.*, 2010). 95 % clearance of small BCC and SCC can be achieved with excisional margins of 4 mm to 5 mm while 3 mm to 15mm is required to reach the same level of clearance for morpheiform or large BCC (Madan *et al.*, 2010). High-risk and/or large SCCs usually require at least 6 mm of excisional margin (Madan *et al.*, 2010). This method is indicated for small, low-risk BCC and SCC tumors (Vargo, 2003). Surgery excision allows for histological examination of excised tissues and assessment of surgical margins, and results in acceptable cosmetic outcomes (Madan *et al.*, 2010; Vargo, 2003). The primary lesion cure rates of less than five years are 96.8 % to 99 % for BCC, 85 % to 87 % for SCC and 50 % to 75 % for high-risk SCC (Vargo, 2003). The 5-year recurrence rate for primary BCC ranges from 5.7 % to 8.1 % while that of recurrent BCC is 17.4 % (Randle, 1996).

Mohs micrographic surgery excises tumors one layer at a time followed by immediate histopathological analysis of removed tissues (Arora and Attwood, 2009). Its

indication includes tumors on the central face, ears and other locations where non-lesional tissue preservation is important for cosmesis and functional issues (Arora and Attwood, 2009). This method is also for NMSCs that are recurrent, with ill-defined borders or aggressive growth patterns (e.g. morpheiform, micronodular and basosquamous BCC) (Arora and Attwood, 2009; Madan *et al.*, 2010; Vargo, 2003). The advantages of this method are; allowing examination of all tumor margins, improved cure rates, and availability of results and/or reconstruction on the same day of surgery (Vargo, 2003). The cure rates of primary tumors less than five years duration are 99 % for BCC, 94 % to 97 % for SCC and 90 % for high-risk SCC; the recurrent rates of primary and recurrent BCC are 1 % and 5.6 % respectively (Randle, 1996; Vargo, 2003). However, both excision and Mohs micrographic surgeries require treatment-related equipment and advanced practitioners, and the cost is high (Epstein, 2008; Madan *et al.*, 2010).

Electrodessication and curettage is to remove tumors by scraping followed by cauterization (Vargo, 2003). This technique can be used for low-risk primary BCC, *in situ* SCC, and SCC on locations where cosmesis concern is not important (Arora and Attwood, 2009; Madan *et al.*, 2010; Vargo, 2003). However, it is contraindicated for recurrent or aggressive tumors (Madan *et al.*, 2010; Vargo, 2003). The cure rates for primary lesions are 94.7 % to 96.7 % for BCC, 90 % to 95 % for SCC and 50 % to 75 % for high-risk SCC (Vargo, 2003). The five-year recurrence rate for primary BCC is 7.7 % (Randle, 1996).

Cryosurgery is a cold-induced liquid nitrogen spraying and destruction method to remove tumors (Madan *et al.*, 2010). The duration and number of freeze – thaw cycles required to obtain optimal results varies depending on the nature of the individual lesions (Madan *et al.*, 2010). It is indicated for small, low-risk BCC and SCC (Madan *et al.*, 2010).

This method is not suggested for tumors on locations with cosmesis concerns (Vargo, 2003). Also, unpredictable scars due to necrosis and swelling may result (Arora and Attwood, 2009). The primary tumor cure rates are 87 % to 92.5 % for BCC, 90 % to 95 % for SCC and 50 % to 75 % for high-risk SCC (Vargo, 2003). The five-year recurrence rate for primary BCC is 7.5 % (Randle, 1996). Both electrosurgery and cryosurgery do not allow excisional tissues for histological examination (Arora and Attwood, 2009; Vargo, 2003).

Table 1.2 Surgical treatments

Treatment	Indication	Contraindication	Advantage	Disadvantage	<5-year cure rate of primary lesion	5-year cure rate of recurrent lesion
Surgical excision	• Small, low-risk BCC • SCC with 4-8mm deep (Arora and Attwood, 2009; Vargo, 2003)	• Large tumors (>1cm) • Aggressive growth pattern • Recurrent tumors (Vargo, 2003)	• Allow for histological examination of excised tissues and surgical margins • Good cosmetic outcome (Madan *et al.*, 2010)	• Time consuming • Require skilled surgical techniques • Cost • Excision sometimes incomplete (Epstein, 2008; Vargo, 2003)	• 96.8-99% for BCC • 85-87% for SCC • 50-75% for high-risk SCC (Vargo, 2003)	• 82.6% for BCC • 85-87% for SCC (Vargo, 2003)
Mohs micrographic surgery	• Tumors on central face, ears, and other locations where cosmesis and tissue function are concerned • Tumor large in size or with ill-defined border • Recurrent tumors • Morpheiform, micronodular or basosquamous BCC • Aggressive tumor (Arora and Attwood, 2009; Madan *et al.*, 2010)	None	• Examination of all tumor margins (tissue sparing) • Improved cure rate • Local anesthesia • Results available as well as reconstruction (if needed) same day • Office procedure (Vargo, 2003)	• Labor intensive • Require well-trained and advanced practitioners • Equipment and resources for tissue processing • Cost (Madan *et al.*, 2010; Vargo, 2003)	• 99% for BCC • 94-97% for SCC • 90% for high-risk SCC (Vargo, 2003)	• 94.4% for BCC • 84% for SCC (Vargo, 2003)

Treatment	Indication	Contraindication	Advantage	Disadvantage	<5-year cure rate of primary lesion	5-year cure rate of recurrent lesion
Electrodessication and curettage	• Locations where cosmesis concern is not important • Low-risk and small NMSC lesions at sites other than head and neck • Primary BCC, SCC in situ, SCC in actinic skin with defined border (Arora and Attwood, 2009; Madan *et al.*, 2010; Vargo, 2003)	• Recurrent tumors • Tumors >0.5 cm in high-risk areas, >1cm in middle-risk area, >2cm in low-risk areas • Tumor with aggressive growth pattern (Madan *et al.*, 2010; Vargo, 2003)	• Minimal equipment required • Local anesthesia • Office procedure (Vargo, 2003)	• Induce wounds that heal by secondary intention • Do not improve quality of life • No surgical specimens and margins for histological analysis • Hypertrophic scars • Use with caution if patients are with demand cardiac pacemakers (Arora and Attwood, 2009; Madan *et al.*, 2010; Vargo, 2003)	• 94.7-96.7% for BCC • 90-95% for SCC • 50-75% for high-risk SCC (Vargo, 2003)	• 60-80% for BCC (Vargo, 2003)
Cryosurgery	• Low-risk BCC and SCC • SCC in situ and SCC in actinic skin with defined-border • Best on skin with fixed undersurface	• Large tumor with ill-defined border • Tumor with aggressive growth pattern • High-risk tumors • Tumors at hair	• Office procedure • Require some specialized equipment (Vargo, 2003)	• Unpredictable scars due to necrosis and swelling • No excisional specimens for histology and	• 87-92.5% for BCC • 90-95% for SCC • 50-75% for high-risk SCC (Vargo,	

Treatment	Indication	Contraindication	Advantage	Disadvantage	<5-year cure rate of primary lesion	5-year cure rate of recurrent lesion
	(e.g. temple, trunk) (Madan *et al.*, 2010; Vargo, 2003)	bearing sites • Locations with cosmesis concerns (Vargo, 2003)		margin analysis • Wound is painful with inflammation and blistering (Arora and Attwood, 2009; Vargo, 2003)	2003)	

1.8.2 Medical methods

Fluorouracil is an antineoplastic antimetabolite that inhibits thymidylate synthetase, which prevents purine and pyrimindine from adding to the DNA sequence during the S phase of cell cycle. Thus, inhibition of DNA and RNA synthesis results (Madan *et al.*, 2010). It has been used as treatment for AK, BD, and small superficial BCC (Madan *et al.*, 2010). BCNS patients with subclinical BCC can be treated by this method as well (Arora and Attwood, 2009). However, it is not suggested as a cure for nodular BCC due to the high recurrence rate (21.4 % in 10 years), and is not used for SCC (Arora and Attwood, 2009; Madan *et al.*, 2010). The side-effects include local irritation, erythema, swelling, skin peeling and tenderness (Madan *et al.*, 2010).

Imiquimod is a synthetic immune response modifier that induces expression of toll-like receptor 7 in dendritic cells and monocytes. As such, production of cytokines and chemokines results, which in turn promotes both innate and adaptive immune responses (Madan *et al.*, 2010). It has been used as treatment for multiple AKs (Arora and Attwood, 2009). Application of topical 5 % imiquimod cream leads to response rates of 69 % to 100 % for superficial BCC and 42 % to 76 % for nodular BCC (Madan *et al.*, 2010). Side-effects include erythema, swelling, itchiness, ulceration, dyspigmentation and scabbing (Madan *et al.*, 2010).

An agent derived from the plant *Euphorbia peplus*, ingenol mebutate (PEP005 gel) induces necrosis of tumor cells and is involved in recruitment of leukocytes, mainly neutrophils to lesion sites to prevent tumor relapse (Challacombe *et al.*, 2006; Hampson *et al.*, 2008; Ogbourne *et al.*, 2004). It was tested at a concentration of 0.05 % for its effects on AKs (face, scalp, arm, chest and back of hand) in a Phase III trial (Patel *et al.*, 2011). The

preliminary data indicated that such treatment led to complete and partial clearance rates of AK at 27.8 % to 42.0 % and 44.4 % to 55.0 % respectively; minimal adverse effects were reported (Patel *et al.*, 2011). In addition, PEP005 gel was evaluated for its effects on superficial BCC on arms in a Phase II study, in which, the 0.05 % treatment resulted in a histological clearance rate of 63 % (Siller *et al.*, 2010). However, adverse effects including severe flaking/scaling/dryness beyond the application site, application site pain, headache and other severe local skin responses, were reported in the patients using the 0.05 % treatment (Siller *et al.*, 2010).

Photodynamic therapy can be topical and systemic treatment. It introduces photosensitizers to neoplastic tissues followed by photoexcitation with specific wavelengths of light and the presence of oxygen, which results in production of reactive oxygen species and leads to cell death and destruction of tumor tissues (Arora and Attwood, 2009; Madan *et al.*, 2010). Topical treatment can be used for AK, nodular and superficial BCCs. Systemic application has been used for high-risk BCC and BCNS; this treatment is contraindicated for SCC though (Arora and Attwood, 2009; Madan *et al.*, 2010). This method leads to better cosmetic outcomes than surgical excision and cryosurgery; however, it causes burning and a stinging burn under the sun, erythema, swelling, and hypo- or hyperpigmentation (Madan *et al.*, 2010).

Other non-destructive methods include perilesional or intralesional injection of recombinant interferon-α (IFN-α) 2b into BCC, which leads to approximately 98 % cure rate over 12 years of treatment (Madan *et al.*, 2010). The disadvantages of this method are that many treatment sessions are required which results in high cost (Madan *et al.*, 2010). A hedgehog signaling inhibitor, GDC-0449, from Curis-Genetech has been under a Phase I trial

for BCC treatment, in which 8 out of 9 patients had clinically significant benefits from it with minimal toxicity (Epstein, 2008). Further studies will be needed to investigate any side-effects or to improve efficacy of these therapies.

Table 1.3 Medical treatments

Treatment	Indication	Contraindication	Advantage	Side-effects
Fluorouracil	• Well established for AK and BD • Small superficial BCC • BCNS patients with subclinical BCC (Arora and Attwood, 2009; Madan *et al.*, 2010)	• SCC • Nodular BCC (Arora and Attwood, 2009; Madan *et al.*, 2010)		• Local irritation, erythema, swelling, desquamation and tenderness (Madan *et al.*, 2010)
Imiquimod	• Topical 5 % imiquimod cream for superficial and nodular BCC • Multiple AK (Arora and Attwood, 2009; Madan *et al.*, 2010)			• Erythema, oedema, pruritus, erosion, ulceration, dyspigmentation and scabbing (Madan *et al.*, 2010)
Photodynamic therapy	• Topical treatment for nodular BCC with 3-and 5-year recurrent rates at 30.3 % and 14 % respectively • Similar treatment and recurrent outcomes for superficial SCC • Systemic therapy with intravenous porfimer for BCC with cure rates of 50 – 100 % • Systemic method for high-risk BCC and BCNS • AK (Arora and Attwood, 2009; Madan *et al.*, 2010)	• SCC (Madan *et al.*, 2010)	• Better cosmetic outcome compared to surgical excision and cryosurgery (Madan *et al.*, 2010)	• Burning and stinging burn under the sun • Erythema, oedema • Temporarily post-inflammatory hypo- or hyperpigmentation (Madan *et al.*, 2010)
Perilesional or intralesional IFN-α 2b	• BCC (Arora and Attwood, 2009; Madan *et al.*, 2010; Vargo, 2003)		• High cure rate with 98 % after 12-year treatment (Madan *et al.*, 2010)	• Many treatment sessions and office visits • Cost (Madan *et al.*, 2010)
GDC-0449	• Oral administration for metastatic or high-risk BCC in Phase I trial (Epstein, 2008)			
PEP005 gel	• 0.05 % topical treatment for facial		• Promising	• BCC patients experienced

Treatment	Indication	Contraindication	Advantage	Side-effects
	and non-facial AKs in Phase III trial • Topical treatment for superficial BCCs in Phase II trial (Patel *et al.*, 2011; Siller *et al.*, 2010)		complete and partial clearance rates of AKs • Adverse effects resolved within 2 – 4 weeks in AK patients • High histological clearance rate of superficial BCC (Patel *et al.*, 2011; Siller *et al.*, 2010)	adverse effects of severe flaking, scaling and dryness beyond application site, application site pain, headache and other severe local skin responses (Siller *et al.*, 2010)

1.9 Mouse models of NMSCs

In order to improve and develop interventions and treatments of NMSCs, development of *in vivo* models is important. Most of the classical spontaneous mouse models of skin cancers are for SCC, but none for BCC (Epstein, 2008). For example, the SKH-1 mice, which are hairless and euthymic strains, have been used for developing models of human photocarcinogenesis and UVB-induced skin cancer (Bowden, 2004; Cooper *et al.*, 2003). The mice were irradiated with increasing doses of UVB light three times a week for 25 weeks. At the end of the treatment, approximately 100 % of the mice developed skin tumors; the average number was 7 to 9 tumors per mouse. Most of the tumors were SCC, which mostly arose from benign papillomas (Bowden, 2004).

The discovery of SHH signaling pathway being the fundamental mechanism of BCC initiation led to development of novel strategies to obtain BCC mouse models via manipulation of Shh-associated gene expression (Epstein, 2008). Certain gene targets and variables when designing *in vivo* BCC models should be taken into account. For instance, introduction of overexpression of *Gli1* or *Gli2*, activating mutation of *Smo*, or inactivated mutation of one of the alleles of *Sufu*, to murine models have been indicated to cause BCC-like proliferation in mouse skin (Epstein, 2008; Grachtchouk *et al.*, 2000; Nilsson *et al.*, 2000; Svard *et al.*, 2006; Xie *et al.*, 1998). Grachtchouk and colleagues used a triple-transgenic mouse model of Cre-*lox* and tet-regulated gene-switch technology to tightly control the transgene expression of *GLIN2ΔN*, which is one of the major downstream targets of the SHH pathway in both spatial and temporal manners (Grachtchouk *et al.*, 2011). By generating the triple transgenic mouse models combined with a *K5-CreER* driver, which could be specifically activated in the basal layer of the epidermis, high levels of Shh/Gli-signaling in

the interfollicular epidermis of the mice (*iK5;rtTA;GLI2ΔN*) led to the development of superficial BCC whereas in the hair follicle stem cell region led to nodular BCC growth (Grachtchouk *et al.*, 2011). Moreover, by using K5 promoter to drive the expression of mutated *Smo* in the skin of transgenic mice, human BCC features were found in the mouse models including absence of cornification in the surface epithelium and keratohyalin granules in the stratum granulosum, presence of hyperproliferation of basal cell layer, as well as formation of irregular branching islands and ribbons of cells bordered by palisading basal cells (Xie *et al.*, 1998).

Also, $Ptch^{+/-}$ mice which involve deletion of wild-type *Ptch1* and constitutive activation of the Shh signaling pathway, are more susceptible to BCC development (Aszterbaum *et al.*, 1999; Epstein, 2008). It has been shown that the degree of *Shh* pathway activation is associated with specific features in the histology and morphology of the mouse model; i.e. higher activation of the signaling pathway in mice leads to a stronger resemblance to human BCC tumors (Epstein, 2008). Oro and colleagues demonstrated that with generating transgenic mice by fusing *Shh* to the K14 promoter, multiple BCC-like epidermal proliferations were detected throughout the skin (Oro *et al.*, 1997). In addition, induction of *p53* mutations in conjunction with *Shh* activating mutations resulted in enhancement of BCC tumorigenesis in mouse models (Epstein, 2008).

1.10 Initial BCC studies

Previously, our laboratory conducted a detailed microarray-based analysis of genes in nodular, superficial and morpheiform BCC tissues to detect specific gene sets with significant differential expression as compared to non-lesional skin epithelium samples (Yu

et al., 2008). Those specific gene sets were further analyzed by incorporating them with the corresponding gene ontology annotation. The results indicated that genes associated with cell motility, cellular morphogenesis, positive and negative regulation of cellular processes, and cellular metabolism were commonly expressed in all three BCC subtypes. In addition, gene expression patterns between nodular and superficial BCCs were relatively more similar whereas morpheiform subtype had a more distinct gene expression pattern that was associated with more aggressive tumor cell behaviors (Yu *et al.*, 2008).

Furthermore, the data from this microarray study indicated that chemokines *CXCL9*, *CXCL10* and *CXCL11* as well as an immunosuppressive agent indoleamine 2,3-dioxygenase (*IDO*) showed significant upregulation in BCC samples. However, the roles and mechanisms of these genes in the immunoregulation of BCC and other skin cancers are still not known.

1.11 Chemokines CXCL9, CXCL10 and CXCL11

The chemokines CXCL9, CXCL10 and CXCL11 are small secretory chemoattractant proteins (Giuliani *et al.*, 2006). They interact with the heptahelical G-protein complex receptor CXCR3 and exert signaling effects in a paracrine or autocrine fashion (Baggiolini, 2001; Hall *et al.*, 1999). They have been well established as chemoattractive for activated $CXCR3^+$ T cells (Pellegrino *et al.*, 2004). Recently, increased expression of these chemokines, together with their receptor CXCR3, have been found to be associated with advanced-stage tumors, such as malignant melanoma, ovarian carcinoma, and B-cell lymphoma (Furuya *et al.*, 2007; Jones *et al.*, 2000; Monteagudo *et al.*, 2007). The roles of CXCR3 and its ligands during the development of BCC are elucidated in this dissertation.

1.12 Immune privilege and tumorigenesis

Immune privilege (IP) is a mechanism to tolerate the presence of foreign antigens at specific sites by suppressing the host immune response (Meyer *et al.*, 2008; Wahl *et al.*, 2006). Major factors to establish IP are production of immunosuppressive agents, low expression of major histocompatibility complex (MHC) class I molecules, reduction of MHC class II-dependent antigen presentation, and absence of lymphatics (Meyer *et al.*, 2008). Increasing evidence has shown that certain cancer types adopt IP characteristics to inhibit immunosurveillance, which leads to promotion of tumor initiation and progression (Mellor and Munn, 2008; Waldmann, 2010). For example, indoleamine 2,3-dioxygenase (IDO) is an immunosuppressive enzyme (Fallarino *et al.*, 2002). It catalyzes the catabolism of tryptophan, which results in suppression of T cell proliferation (Fallarino *et al.*, 2002). IDO expression has been detected in various types of cancers and has been shown to be involved in tumor development (Uyttenhove *et al.*, 2003).

1.13 Hypothesis and objectives

Based on our microarray analysis results, we further examined the gene ontology of the data set (Gene Expression Omnibus database series record GSE6520), and subsequently identified 27 immunoregulatory genes with significant differential expression in BCCs including *CXCL9*, *10* and *11* (unpublished). To verify the microarray results, we conducted quantitative real-time RT-PCR (qPCR) analysis of those 27 selected genes in BCC using non-lesional skin tissues as control. We found that *CXCL11* was significantly upregulated at the highest level of all the genes tested followed by *CXCL9*, *CXCL10* and *IDO* (Figure 1.4) (unpublished). In this thesis project, I wanted to elucidate the role of the chemokine receptor

CXCR3 signaling during the development of NMSC, especially BCC. Also, I wanted to determine if immune privilege, potentially via IDO, was involved in BCC growth.

I hypothesized that CXCR3 and its ligands were important for the growth of BCC. I found that CXCR3 and its ligands were significantly upregulated in human BCC tissues at both mRNA and protein levels. More importantly, I demonstrated that CXCR3 signaling was essential to support the growth, survival and migration of primary human BCC keratinocytes.

After that, I pursued the study of CXCR3 signaling in other non-melanoma skin lesions. **I hypothesized that CXCR3 signaling played a role in the development of NMSCs including SCC and its pre-malignant forms.** I determined that *CXCR3* and its ligands were upregulated at a much higher level in SCC than in BCC and other pre-malignant lesions. Also, I showed that CXCR3/CXCL11 signaling supported the cell proliferation, survival as well as migration and invasion of a human immortalized keratinocyte cell line; HaCaT cells.

I further examined if other tumorigenic associated features could be involved in BCC, such as immunoregulation, and determined if CXCR3 signaling may have any impact on it. **I hypothesized that expression of immune privilege-related genes are associated with BCC tumorigenesis**. I identified a panel of upregulated genes in nodular BCC tissues that have been shown to exert immunosuppressive signaling effects, such as cluster of differentiation 200 (*CD200*) and its receptor *CD200R*. Also, I showed that CD200 was expressed by BCC cells while CD200R was expressed by the surrounding stromal cells including T cells. Moreover, **I hypothesized that CXCR3 signaling promoted expression of functional IDO in BCC.** I found that IDO was significantly upregulated in human BCC tissues at both mRNA and protein levels. I found that CXCL11 treatment significantly induced IDO catalytic activity in primary human BCC cells and that such treatment

significantly enhanced the expression of *IDO2*; such outcomes were not seen in normal keratinocytes under same treatment condition.

Figure 1.4 The quantitative real-time RT-PCR analysis of immunoregulatory genes in human BCC tissues

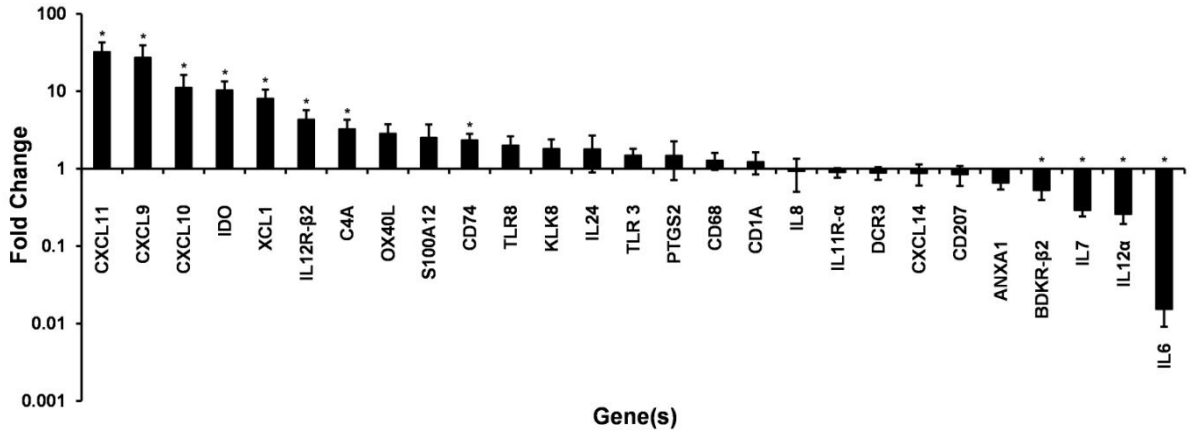

Twenty seven immunoregulatory genes were selected based on previous microarray analysis of BCCs. The qPCR analysis was used to determine the expression of those genes in human BCC tissues as compared to non-lesional skin epithelium samples. *CXCL11* was upregulated at the highest level in the tumor samples followed by *CXCL9*, *CXCL10* and *IDO*.

Chapter 2. Materials and methods

2.1 Human tissue samples

All tissue samples were obtained from the Mohs Surgery Clinic of the Department of Dermatology and Skin Science, the University of British Columbia. Tissue collection complied with the Declaration of Helsinki and was approved by the University Clinical Research Ethics Board. Specific patient consent was not required as surgically removed tissues are considered as discarded materials according to Canadian law.

In chapter 3A, 48 human BCC tumor samples from 21 female and 27 males patients were utilized along with 15 non-lesional skin epithelium (NL) tissues excised from 8 female and 6 male patients. In chapter 3B, there were 10 NL samples from female patients, 10 SCC tumor samples from 3 females and 7 males, 6 AK samples from male patients, 5 BD samples from 2 females and 3 males, 5 nodular BCC tumor samples from 1 female and 4 males as well as 10 SK samples from 5 females and 5 males. In chapter 4, hair follicles of 5 patients (2 females; 3 males), 32 nodular (14 females; 18 males) and 5 morpheiform (1 female; 4 males) BCC tumors were studied along with 26 NL tissues (16 females; 10 males). The sample size for each experiment is stated in the following protocol sections.

2.2 HaCaT and MCF-7 cell cultures

Human immortalized HaCaT keratinocyte cells and human breast cancer cell line MCF-7 cells were maintained at 37^0C in a humidified incubator with 5 % CO_2. They were propagated in Dulbecco's Modified Eagle's Medium (DMEM) (Fisher Scientific, Ottawa, Ontario) with 5 % heat inactivated fetal bovine serum (Fisher), 100 U/mL penicillin (Invitrogen, Burlington, Ontario), and 100 ug/mL streptomycin (Invitrogen). When the cells

reached 80 % confluence, HaCaT cells were transferred to multi-well plates for experimental assays in chapter 3A and chapter 3B while MCF-7 cells were transferred to 12-well plates for quantitative real-time RT-PCR analysis in chapter 3A.

2.3 Human BCC and NL cell isolation and culture

Cells were isolated from human nodular BCC and NL tissues using protocols as described (Lo *et al.*, 2010). In brief, patient samples were washed in Ca^2 and Mg^2-free Dulbecco's phosphate-buffered saline, cut into 2 mm^3 pieces, and incubated with 25.0 caseinolytic units/mL dispase (Invitrogen) containing 1 % antibiotic-antimycotic solution (Invitrogen) at 4^0C overnight. Tissues were further incubated with 0.05 % trypsin-EDTA at 37^0C for 15 minutes and a single cell suspension was obtained using a 40 μm cell strainer (BD Bioscience, Mississauga, ON, Canada). The trypsin activity was neutralized by adding an equal volume of 10 mg/mL soybean trypsin inhibitor (Invitrogen). After centrifugation and cell resuspension, the cells were seeded in flasks or multiwell-plates coated with collagen I (Invitrogen). Complete growth medium was prepared by mixing base medium M154 with the Human Keratinocyte Growth Supplement, 0.08 mM $CaCl_2$, 100 units Penicillin, 100 μg Streptomycin, and 0.25 μg/mL Amphotericin B (all Invitrogen).

In chapter 3A, the isolated BCC cells were treated with CXCL11 peptide (Peprotech, Dollard des Ormeaux, QC, Canada) and monitored for cell proliferation response (Section 2.4), and treated with 10 nM CXCL11 peptide for 1 month prior to the cyclic adenosine monophosphate study (Section 2.5). In chapter 4, the isolated BCC and normal keratinocyte (KC) cells were propagated in complete growth medium supplemented with 10 nM CXCL11 peptide (Peprotech) for 1 month, which would be proved to be necessary for primary BCC

cell culture in chapter 3A (Lo *et al.*, 2010). While CXCL11 is not necessary for normal KC cell culture, we used the same complete growth media for both BCC and normal KC cells for consistency. After that, primary human BCC and normal KC cells were used for further studies.

2.4 CXCL11 peptide treatment

HaCaT cells were seeded at 4 x 10^4 cells in 24-well plates to which CXCL11 peptide was added (Cat. No. 300-46; Peprotech Inc., Rocky Hill, New Jersey) at 1 nM, 5 nM, 10 nM or 20 nM dissolved in phosphate-buffered saline (PBS) in triplicate wells for 24 or 48 hours. As a control, the same amount of PBS alone was added to the cell cultures. A minimum of 8 x 10^4 human nodular BCC cells from each tissue sample were aliquoted for cytospin preparations on day 0 as controls for immunohistochemistry; the remainder were plated in 24-well plates (> 2.9 x 10^4 cells/well). The seeded cells were treated with 0 nM, 5 nM, 10 nM or 20 nM of CXCL11 peptide for 7, 14 and 21 days. All cell cultures were incubated at 37^0C with 5 % CO_2. Cell populations from each tissue sample were investigated separately. Cell proliferation was analyzed by cell counting using Trypan blue exclusion test.

In another study to compare the growth response of BCC cells and normal keratinocytes under CXCL11 supplementation, both of the cell types were treated with 0 nM, 5 nM, 10 nM and 20 nM CXCL11 peptide for 1 month and analyzed by cell counting using the Trypan blue exclusion test.

Moreover, another set of HaCaT cells were seeded at 1 x 10^5 cells per well of a 12-well plate, and were treated with 0 nM, 5 nM, 10 nM and 20 nM CXCL11 peptide (Peprotech) for 48 hours. Each peptide dosage setup was done in triplicate and the

experiment was repeated in three individual trials. The treated cells were further analyzed by quantitative real-time RT-PCR.

2.5 BCC-isolated cells cultured with cyclic adenosine monophosphate

Human nodular BCC cells were isolated from 3 patient samples as stated in Section 2.3. Cyclic adenosine monophosphate (cAMP) has been shown to facilitate cell proliferation of primary epidermal keratinocytes (Delecluse *et al.*, 1976; Marcelo and Tomich, 1983). Experiments were conducted to determine optimal treatment setup to induce BCC keratinocyte proliferation and prevent cytotoxicity, terminal cell differentiation and death. To accomplish this, BCC-isolated cells were treated with 0.1 μM, 1 μM and 10 μM cAMP monitored for cell growth for 10 to 20 days. Photographs of the cell cultures were taken as observational data.

2.6 Treatment of cAMP in BCC-derived cells prior to further analyses

Cells from nodular BCC patients (n = 6) were isolated and cultured in complete growth medium as stated in Section 2.3. In addition, the cells were supplemented with 1 μM cAMP for 10 days to obtain enough cell numbers for immunohistochemistry (cells from 3 of the 6 BCC patients) and CXCR3 neutralization experiments (cells from the remaining 3 BCC patients).

2.7 Neutralization of CXCR3 bioactivity

The HaCaT cells and the cAMP-treated BCC-isolated cells were seeded in 24-well plates at 7×10^4 cells and 5.6×10^3 cells per well respectively. Blockade of CXCR3 signaling

was obtained by treating the cells with monoclonal mouse anti-human CXCR3 neutralizing antibody (Cat. No. mab160) (R&D Systems, Minneapolis, MN). CXCR3 neutralizing antibody was applied at 0 μg/mL, 25 μg/mL and 50 μg/mL for BCC cells as well as 0 μg/mL, 50 μg/mL and 100 μg/mL for HaCaT cells for 24, 48 and 72 hours. Media and antibody were replenished every 24 hours. Cell growth and death assays were carried out as in Section 2.9.

To further examine the effects of CXCR3 inhibition with exogenous ligand stimulation, HaCaT cells were treated with 10 nM recombinant CXCL11 peptide (Ca. No. 300-46) (Peprotech, Rocky Hill, NJ) in addition to 0 μg/mL, 50 μg/mL and 100 μg/mL CXCR3 neutralizing antibody for 24, 48 and 72 hours. Cell cultures were replenished with CXCL11 peptide and CXCR3 neutralizing antibody every 24 hours.

In addition, control experiments were conducted by replacing CXCR3 neutralizing antibody with IgG_1 isotype antibody (Cat. No. mab002) (R&D Systems) to ensure the specificity of the neutralizing anti-CXCR3 antibody. Such studies were done using in HaCaT cell culture.

2.8 Recovery from CXCR3 suppression in previously treated HaCaT cells

For the recovery study, cell culture plates were prepared with anti-CXCR3 antibody (R&D Systems) with or without CXCL11 peptide (Peprotech) for 72 hours as above. Some of the cultured cells were harvested and their cell numbers were used as baseline for calculating cell proliferation rate later. For the rest of the treated cells, CXCR3 neutralizing antibodies were removed, and were further cultured in complete growth medium or complete growth medium with recombinant CXCL11 for analysis at 24, 48 and 72 hours. Cell numbers

were counted to obtain cell proliferation rates and dead cell percentages; the results plotted are the mean of each triplicate setup.

2.9 Cell growth and death evaluation assays

HaCaT cells BCC-isolated cells and normal KC cells exposed to each CXCL11 concentration were counted from three wells for each time-point, with evaluation repeated three times. Cell counting using the Trypan blue exclusion test was conducted, in which, dead cells in the cell culture were stained as blue and viable cells remained unstained (Levin *et al.*, 2005; Pradelli *et al.*, 2009; Yang *et al.*, 2010). The growth rate was calculated by dividing the number of viable treated cells at each time point by the cell number originally seeded on day 0. Values higher than 1 indicated a cell population increase whereas a value between 0 and 1 indicated a reduction of cell numbers. The values presented were mean cell growth rate ± SE of three independent experiments. Differences in cell growth rates between the untreated and treated HaCaT cells and normal KCs were analyzed by Student's t-test, and a p-value < 0.05 was considered as statistically significant. The BCC cell growth rates of all the treatment setups were compared to each other and the statistical significance was analyzed by analysis of variance (ANOVA) with a p-value of 0.05.

The cell growth and death rates in CXCR3 neutralization assays (Section 2.1.2.7) were evaluated with the Trypan blue exclusion test as well. The cell proliferation rates were obtained by dividing the live cell number determined for each treatment by the cell number originally seeded and converting the ratio to a percentage. The cell death frequency was measured by calculating the fraction of dead cells in the whole cell population after each

treatment and converting to a percentage. Statistical significance was measured by Student's t-test. P-value < 0.05 was considered significant and indicated by *.

2.10 Migration and invasion assays

The cell numbers and medium supplementation setup were the same for both of the assays, except that Transwell culture chambers were used for migration assays while Boyden chambers were used for invasion assays (BD Biosciences, Mississauga, Ontario). Primary human BCC- (n = 6) derived cells were prepared as stated in Section 2.3, and were propagated with 10 nM CXCL11 peptide for 1 month to obtain homogeneity of $K17^+$ BCC keratinocytes prior to analyses (Lo *et al.*, 2010).

The BCC cells and HaCaT cells were suspended in complete growth medium without CXCL11 peptide, and 2 x 10^4 cells and 5 x 10^4 cells per well (250 µL) respectively were seeded in the upper compartment of the chamber. In the lower compartment, 750 µL complete growth medium plus 0 nM, 5 nM, 10 nM or 20 nM CXCL11 peptide (Peprotech) was added. After 48 (HaCaT cells) or 72 hours (BCC cells) of incubation at 37^0C, HaCaT cells and BCC cells were fixed with 10% trichloroacetic acid, and the transmigrated cells on the lower side of the membrane were further stained with 0.5 % crystal violet, air-dried and photographed. Only stained cells transmigrated to the lower side of the membrane, and were counted in order to calculate the percentages of cell migration and invasion.

2.11 Total RNA isolation and cDNA synthesis

Human BCC, SCC, actinic keratosis, Bowen's disease, seborrheic keratosis, non-lesional interfollicular skin epithelium, hair follicle bulb and shaft tissues were excised and

preserved in a RNA stabilization reagent (Qiagen, Mississauga, Ontario) and stored at -80^{0}C before use. Samples were removed from the stabilization reagent, and homogenized using a QIAshredder^{TM} kit (Qiagen) according to the manufacturer's instructions. In addition, human primary BCC cells, normal keratinocytes, HaCaT cells and MCF-7 cells were trypsinized by 0.05 % trypsin-EDTA (Invitrogen) followed by homogenization.

Total RNA of the lysates was isolated using the RNeasy^{TM} Mini Kit (Qiagen) according to the manufacturer's instructions. DNase digestion was conducted using RNase-Free DNase Set (Qiagen) after the first buffer washing step of the RNA-bound RNeasy membrane. Total RNA was subsequently eluted in a volume of 25 μL RNase-free water.

The synthesis of cDNA was performed using the SuperScript First Strand Synthesis System^{TM} for RT-PCR kit (Invitrogen). Briefly, 500 ng of each RNA sample was reverse transcribed in the presence of 50 ng/μL random hexamers, 10 mM dNTP mix, 10X RT buffer, 25 mM $MgCl_2$, 0.1 M DTT, and RNaseOUT recombinant ribonuclease inhibitor. The synthesis of cDNA reactions was catalyzed by SuperScript II reverse transcriptase at 42^{0}C for 50 minutes, and was terminated at 70^{0}C for 15 minutes. Any remaining RNAs were removed by incubating samples with RNase H at 37^{0}C for 20 minutes. Reactions were programmed and carried out in a Mastercycler Gradient (Eppendorf, Mississauga, Ontario).

2.12 Quantitative real-time RT-PCR (qPCR)

The qPCR was performed using an MJ Research DNA Engine Opticon real-time cycler (Bio-Rad Laboratories, Mississauga, Ontario) using the QuantiTect^{TM} SYBR Green RT-PCR kit (Qiagen). All reactions were carried out in technical duplicate for all biological replicates. The sequences of synthesized primers (Invitrogen) were obtained by using the

online software Primer3 at http://frodo.wi.mit.edu/cgi-bin/primer3_www.cgi (Lo *et al.*, 2010; Yu *et al.*, 2008), and their specificities were determined by the online Blast program from the National Center for Biotechnology Information website (http://www.ncbi.nlm.nih.gov/blast/Blast.cgi) and compared with the Genbank database. The forward (f) and reverse (r) primer sequences of each gene are shown in Table 2.1.

The relative quantization of each targeted gene was normalized to the housekeeping gene 18S expression level in the samples and was determined by the comparative C_T method (Livak and Schmittgen, 2001). Gene expression levels are presented in terms of fold change using the formula $2^{-\Delta\Delta Ct}$. Each tissue sample was examined separately and analyses conducted in duplicate. Data is presented as the mean of individual samples within each tissue group. Statistical analysis was done by Student's t-test; p-value < 0.05 was indicated as *, <0.005 as **, and < 0.0005 as ***.

Table 2.1 Primer sequences

Gene	Forward primer	Reverse primer
CXCL11	AGAGGACGCTGTCTTTGCAT	TGGGATTTAGGCATCGTTGT
XCL1	GACTGCCGGTTAGCAGAATC	GTTGGCTTGGTCTGGATCAT
CXCL9	TTTTCCTCTTGGGCATCATC	GAACAGCGACCCTTTCTCAC
CXCL10	CCAATTTTGTCCACGTGTTG	TTCTTGATGGCCTTCGATTC
CXCL14	AAGCTGGAAATGAAGCCAAA	GGCGTTGTACCACTTGATGA
CXCL4	GCTGTTCCTGGGGTTGCT	CCAAAAGTTTCTTAATTATTTT CTTGT
CXCL16	TACACGAGGTTCCAGCTCCT	CACAATCCCCGAGTAAGCAT
CXCL12	AGAGCCAACGTCAAGCATCT	CTTTAGCTTCGGGTCAATGC
CXCL5	TCTGCAAGTGTTCGCCATAG	TTGTTTCCACCGTCCAAAAT
XCR1	AGCTGGGGTCCCTACAACTT	GACCCCCACGAAGACATAGA
CXCR6	CAGATGCCCTTCAACCTCAT	GGCTGACAAAGGCATAGAGC
CXCR4	GGTGGTCTATGTTGGCGTCT	CTCACTGACGTTGGCAAAGA
CXCR3	GTGGACATCCTCATGGACCT	CGGAACTTGACCCCTACAAA
CXCR3A	TGGTCCTTGAGGTGAGTGAC	AAGAGGAGGCTGTAGAGGGC
CXCR3B	AAGTACGGCCCTGGAAGACT	GGCGTCATTTAGCACTTGGT
CXCR3 alt	TACAACTTCCCACAGGGGTC	CTCACAAGCCCGAGTAGGAG
IL8Rβ	ACTTTTCCGAAGGACCGTCT	GTAACAGCATCCGCCAGTTT
IL8	GTGCAGTTTTGCCAAGGAGT	AAATTTGGGGTGGAAAGGTT
MMP1	GCAGCCCAGATGTGGAGTGC C	TGTGTTTGCTCCCAGCGAGGG

Gene	Forward primer	Reverse primer
MMP2	CCCTCGCAAGCCCAAGTGGG	CCATGCTCCCAGCGGCCAAA
MMP3	CTGTTGCTGTGCGTGGCAGTTT	GTCGGAGTCCAGCTTCCCCGT
MMP9	GCAGCTGGCAGAGGAATACCTGT	ATGGCCTTCAGCGTGGCGCTAT
CCL2	TCTGTGCCTGCTGCTCATAG	CAGATCTCCTTGGCCACAAT
CD200	GGAGAGGCTGGTGATCAGG	CTGCTCTCTTTCATCCTGGG
CD200R	CCATTTGACTGGCAACAAGA	TAGGGCTGCATTTCATCCTC
CD46	ACCACTTTACACTCTGGAGC	GCTACCTGTCTCAGATGACG
CD55	CAGCACCACCACAAATTGAC	CTGAACTGTTGGTGGGACCT
CD59	GGAATCCAAGGAGGGTCTGT	TGCAGGCTATGACCTGAATG
CD80	CACCTCTCCTGGTTGGAAAA	GGGCGTACACTTTCCCTTCT
CD86	AGACGCGGCTTTTATCTTCA	ATCCAAGGAATGTGGTCTGG
DCR3	TGCTCCAGCAAGGACCATGA	GTGCTGCTGGCTGAGAAGGT
Fas	AGGAAAGCTAGGGACTGCAC	GCACTTGGTATTCTGGGTCC
FasL	GGAAAGTGGCCCATTTAACA	CAAGATTGACCCCGGAAGTA
HLA-A	GGAGCAGAGATACACCTGCC	TGCTTGCAGCCTGAGTGTAA
HLA-B	AGCTTGTGGAGACCAGACCA	TCCGATGACCACAACTGCTA
HLA-C	GAGCAGAGATACACGTGCCA	CCTCCTACACATCATAGCGGT
HLA-DPα1	CCATGTGTCAACTTATGCCG	GAGCCTCAAAGGAAAAGGCT
HLA-DPβ1	TTTCTACCCAGGCAGCATTC	GTCAATGTCTTACTCCGGGC
HLA-	GACCACGTTGCCTCTTGTG	ATTTGCTGAACTCAGGCCAC

Gene	Forward primer	Reverse primer
DQα1		
HLA-DQβ1	ACAACTACGAGGTGGCGTTC	AACCACCGGACTTTGATCTG
HLA-DRα1	AGCACTGGGAGTTTGATGCT	GTCCCAATAATGATGCCCAC
HLA-DRβ1	ATGGTGTGTCTGAAGCTCCC	ACTCCCTCTTAGGCTGCCAC
HLA-E	GCCCGTCACCCTGAGATGGA	GCTGTGAGACTCAGACCCCT
IDO1	GGCAAAGGTCATGGAGATGT	CTGCAGTCTCCATCACGAAA
IDO2	AGGTCCTGCCAAGGAATCTT	CAGCACCAAGTCTGAGTGGA
IGF1	CCGGAGCTGTGATCTAAGGA	CCTGCACTCCCTCTACTTGC
IK	GATCCTCACTCCTTCCACCA	CTTTTTCCTCCTTCGTGCAG
IL10	TTACCTGGAGGAGGTGATGC	GGCCTTGCTCTTGTTTTCAC
IL1R antagonist (IL1RA)	GGAATCCATGGAGGGAAGAT	CCTTCGTCAGGCATATTGGT
MICA	GCCATGAACGTCAGGAATTT	TTCCAGGGATAGAAGCCAGA
MICB	TCTGCTGCTATGCCATGTTT	CTCACAAGCTCTGGACCCTC
MIF	GGTTCCTCTCCGAGCTCAC	TGCTGTAGGAGCGGTTCTG
PRLH	CACCCCTGACATCAATCCTG	ATCCTGGGACGACATAGCAC
TGFβ1	CACGTGGAGCTGTACCAGAA	GAACCCGTTGATGTCCACTT
TGFβ2	TTGACGTCTCAGCAATGGAG	TCGCCTTCTGCTCTTGTTTT
VIP	CCCGCCTTAGAAAACAAATG	TCTTCTGGAAAGTCGGGAGA

Gene	Forward primer	Reverse primer
α-MSH	AGAGCAGCCAGTGTCAGGA	GAAGTGGCCCATGACGTACT
β2M	GTGCTCGCGCTACTCTCTCT	TCTCTGCTGGATGACGTGAG

2.13 Immunohistochemistry

Patients' biopsies were embedded in Optimal Cutting Temperature compound (Sakura, Torrance, California), frozen in liquid nitrogen, and stored at -80^{0}C before use. Frozen samples were processed by cryostat sectioning, air drying, and fixation in acetone at 4^{0}C. For HaCaT cell cultures, a sterilized glass coverslip was placed in each well, which was seeded with a minimum of 4 x 10^5 cells. For both CXCL11-treated and cAMP-treated BCC cells, they were used for cytospin preparations, in which 8 x 10^4 cells in 150 µL culture media were added in glass slide-loaded concentrator cuvettes and were centrifuged at 48.5 x g for 4 minutes. The cells were fixed with 4 % v/v paraformaldehyde (Cedarlane Laboratories, Hornby, Ontario) in PBS and were permeabilized by 0.1 % v/v triton X-100 (Cedarlane) in tris-buffered saline (TBS).

Single color labeling was performed using the Avidin: Biotinylated enzyme Complex (ABC) System (Vector Laboratories, Burlington, California). In brief, after washing the sections in PBS, endogenous peroxidase activities in the tissue samples were inhibited by incubating them in PBS with 0.3 % H_2O_2 and 0.3 % normal serum. The sections were treated with protein block serum-free solution (Dako, Mississauga, Ontario), followed by avidin/biotin blocking (Vector Laboratories Inc.) and further treated with diluted normal blocking serum (Vector). Preliminary titration experiments indicated optimal dilutions for primary antibodies (data not shown). Primary antibody was diluted in DakoCytomation Antibody Diluent (Dako) with 5 % normal serum, and was applied to the sections overnight at 4^{0}C. After washes in TBS, the slides were exposed to diluted biotinylated secondary antibody (Vector) with 5 % normal serum at room temperature for 1 hour. Subsequently, the labeling was revealed by peroxidase-based reaction using the Vectastain *Elite* ABC reagent

and Vector NovaRed substrate solution (Vector). Hematoxylin (Fisher Scientific) was used for counterstaining. Control experiment was conducted by replacing the primary antibody with TBS.

For double labeling procedures, the sections were further rinsed in TBS, and treated with protein block serum-free solution, avidin/biotin blocking reagent, as well as normal blocking serum again. The second primary antibody was prepared in the antibody diluent (Dako) with 5 % normal serum, and was incubated with the sections overnight at 4^0C, followed by treatment of diluted biotinylated secondary body with 5 % normal serum at room temperature. The signals were detected by the alkaline phosphatase-based reaction of Vectastain ABC-AP reagent and Vector Blue substrate solution (Vector). Finally, the slides were dehydrated and mounted in Permount (Fisher). Two different control experiments were set up to ensure specific labeling for both markers. The first control setting replaced the second primary antibody with TBS while the second one replaced the second secondary antibody with TBS. The information of primary antibodies used was shown in Table 2.2.

Table 2.2 Primary antibodies

Antibody	Manufacturer	Dilution
Monoclonal mouse anti-human keratin 17	Santa Cruz Biotechnology, Santa Cruz, CA (Cat. No. sc-58726)	1:200
Monoclonal mouse anti-human CXCL9	R&D Systems Inc., Minneapolis, Minnesota (Cat. No. MAB392)	1:33
Polyclonal goat anti-human CXCL10	R&D Systems Inc. (Cat. No. AF-266-NA)	1:200
Polyclonal goat anti-human CXCL11	Santa Cruz Biotechnology (Cat. No. sc-34784)	1:75
Polyclonal goat anti-human CXCR3	Santa Cruz Biotechnology (Cat. No. sc-9900)	1:20
Monoclonal mouse anti-human keratin 13	Abcam Inc., Cambridge, MA (Cat. No. ab101001)	1:120
Polyclonal rabbit anti-human IDO	Dr. Ghahary, University of British Columbia	1:200
Monoclonal mouse anti-human CD200	Abcam Inc. (Cat. No. ab23552)	1:150
Monoclonal mouse anti-human CD200R	Abcam In. (Cat. No. ab17225)	1:300
Monoclonal mouse anti-human CD3	Dako Canada, Inc., Burlington, Ontario, Canada (Cat. No. M7254)	1:75

2.14 Immunohistochemistry analysis

Ten randomly selected areas of BCCs in dual IHC labeled tissue sections, that coexpressed the chemokines (labeled blue) and K17 (labeled red), were evaluated for the chemokines' label intensity using a protocol modified from previous publications (Kokolakis *et al.*, 2008; Robinson *et al.*, 2000; Sompuram *et al.*, 2002). Each area had an average size of 131.57 μm^2 containing approximately two cells. Optical color density in BCC keratinocytes was calculated and compared to equivalent regions of cells in the BCC-adjacent stroma within the same images. The immunolabel color of the chemokine antibodies was isolated from other colors in the images using Adobe Photoshop CS2 software (Adobe Systems, Etobicoke, Ontario). The immunolabeling intensities in positive cells were then quantified using the software Scion Image (Scion, Frederick, Maryland). The analysis was done by converting the label color intensity of the images to grey scale (256 levels). The average label intensity for each antibody was calculated as mean pixel optical density, i.e. the sum of gray values of all pixels within a selected area divided by the number of pixels.

For cytospin cell culture preparations, the numbers of cells labeled as $K17^+/CXCR3^-$, $K17^+/CXCR3^+$, and $K17^-/CXCR3^+$ were counted in six random fields of view for each IHC dual label slide for each BCC cell culture. The percentage of cells with each expression presentation in the total cell population observed was calculated. Statistical significance was determined for CXCL11-treated BCC cells, and was evaluated by ANOVA.

2.15 Western blot

The total protein from human nodular and morpheiform BCC, as well as NL interfollicular skin tissues (n = 5 for each tissue type), were obtained using a Total Protein

Extraction kit according to manufacturer's protocols (Millipore, Etobicoke, ON, Canada); tissue samples were treated with the protease inhibitor solution mixed with tris-HCl magnesium chloride lysis buffer. Equal amounts of protein (100 µg) from each sample were separated by SDS-PAGE, and electrotransferred to PVDF membrane (Millipore). Immunoblotting of the membrane was performed by using polyclonal rabbit anti-human IDO antibody (provided by Dr. Ghahary; University of British Columbia), which has been shown to have specific Western blot labeling in previous studies (Forouzandeh *et al.*, 2008; Sarkhosh *et al.*, 2004). The membrane was probed with goat anti-rabbit secondary antibody conjugated to horseradish peroxidase (Bio-Rad). Immunolabeling was conducted using an ECL plus Western blotting detection kit (GE Healthcare, Baie d'Urfe, QC, Canada). The experiment was repeated by replacing the primary antibody with a monoclonal rabbit anti-human IDO antibody (Cat. No. ab76157) (Cedarlane Laboratories, Burlington, ON, Canada).

2.16 Kynurenine assay

The enzymatic activity of IDO was evaluated by measuring the amount of tryptophan catabolite, L-kynurenine (kyn) in the conditioned medium of cell cultures as described in a previous publication (Li *et al.*, 2006). Conditioned medium from BCC and normal KC cell cultures was collected after treatment with different CXCL11 peptide concentrations. Protein precipitation was obtained by mixing the media with 30 % v/v trichloroacetic acid. After centrifugation, supernatant of the mixture was added to an equal volume of Ehrlich's reagent (Sigma-Aldrich, Oakville, ON, Canada). Absorbance values of the resultant solutions were recorded at 490 nm by spectrophotometer. A standard curve of known concentrations (0 µg

to 20 µg) of kyn was conducted to determine the amount of kyn in the conditioned medium. Absorption of unused culture media with CXCL11 was used as the baseline control.

Chapter 3. CXCR3 signaling effects on basal cell carcinoma and other non-melanoma skin tumors

3.1 CXCR3/ligands are significantly involved in the tumorigenesis of basal cell carcinomas

3.1.1 Introduction

3.1.1.1 Chemokines

Chemokines are short for "chemotactic cytokines", as defined by the International Immunology Meeting in Budapest in 1992 (Baggiolini, 2001; Kunkel *et al.*, 1995). They are small secretory molecules that exert chemoattractive effect via their corresponding heptahelical G protein-coupled receptor (GPCR) (Baggiolini, 2001). Such signaling effect has been shown to be involved in a wide spectrum of biological and physiological activities, including cell proliferation and migration (Aksoy *et al.*, 2006). Chemokines consist of four reserved cysteines and are divided into four subgroups: CXC, CC, CX_3C and C. The "X" represents any amino acid between the preserved cysteines at the amino-terminal of the molecule (Baggiolini, 2001; Vandercappellen *et al.*, 2008). CXC and CC subgroups are also known as α and β chemokines respectively; they differentiate from each other depending on the position of the first two cysteines, in which CXC group cytokines have one amino acid in between the cysteines whereas CC group cytokines have those cysteines adjacent to each other (Baggiolini, 2001). Fractalkine (CX_3CL1) and neurotactin belong to the CX_3C or δ group, and have three amino acids between the first two cysteines (Baggiolini, 2001;

Vandercappellen *et al.*, 2008). Lymphotactin (XCL1) is under the C or γ subgroup, which has two conserved cysteines instead of four (Baggiolini, 2001; Vandercappellen *et al.*, 2008).

3.1.1.2 CXCR3 signaling and cancers

The CXC subgroup is further divided into ELR^+ and ELR^- depending on the presence or absence of a tripeptide motif, glutamic acid-leucine-arginine (ELR), preceding the CXC domain (Vandercappellen *et al.*, 2008). The ELR motif has been shown to be involved in ligand/receptor binding on neutrophils (Clark-Lewis *et al.*, 1993; Vandercappellen *et al.*, 2008). The ELR^- CXC chemokines, CXCL9, 10, and 11 are IFN-γ induced, small secretory proteins that are synthesized and released by leukocytes, as well as epithelial, endothelial, and stromal cells (Pellegrino *et al.*, 2004). They interact with the common receptor CXCR3, which is a seven helical transmembrane G-protein coupled receptor; such binding exerts signaling effects in a paracrine or autocrine fashion (Baggiolini, 2001; Booth *et al.*, 2002; Hall *et al.*, 1999). The major regions of CXCL9, 10 and 11 include the first pair of conserved cysteines on the N-terminal followed by the "N-loop" and the first β-strand (Booth *et al.*, 2002). It has been shown that chemokines bind to their receptors in a "two-step interaction" manner (Fernandez and Lolis, 2002; Loetscher and Clark-Lewis, 2001). The first step involves the N-loop region of a chemokine that interacts with the N-terminal of the receptor, which is known as the "docking" step. Such initial contact of the chemokine and receptor facilitates subsequent binding of the N-terminal of the chemokine to the extracellular loops of the receptor, which is known as the "triggering" step and leads to activation of the G protein and downstream signaling pathway (Booth *et al.*, 2004; Fernandez and Lolis, 2002; Loetscher and Clark-Lewis, 2001). It has been indicated that the triggering of CXCR3

requires its extracellular loops 1 and 2 by CXCL11, loops 1 to 3 by CXCL10 and loops 2 and 3 by CXCL9 (Xanthou *et al.*, 2003).

CXCL9, 10 and 11 are presumed to have anti-tumor functions due to their chemoattractive properties on $CXCR3^+$ T cell migration into inflammatory and/or neoplastic sites (Baggiolini, 2001; Pellegrino *et al.*, 2004). However, recent research has proposed that CXC chemokines and their receptors, particularly CXCR3 and its ligands, may participate in tumor progression and metastasis (Chen *et al.*, 2006; Moller *et al.*, 2003). CXCR3 and its ligands have been shown to enhance the progression of ovarian carcinoma and multiple myeloma (Furuya *et al.*, 2007; Moller *et al.*, 2003; Oppenheim *et al.*, 1997; Pellegrino *et al.*, 2004), and to facilitate the metastasis of malignant melanoma (Kawada *et al.*, 2004; Monteagudo *et al.*, 2007; Oppenheim *et al.*, 1997; Robledo *et al.*, 2001). Also, on exposure to inflammatory cytokines, leukocytes typically lose their chemokine receptor expression (Balkwill and Mantovani, 2001; Sica *et al.*, 2000). In the cases of malignant melanoma and ovarian carcinoma, CXCR3 is expressed at a much higher level in the tumor cells than in the infiltrating immunocompetent cells (Kawada *et al.*, 2004; Monteagudo *et al.*, 2007; Oppenheim *et al.*, 1997). Consequently, tumor cells may be relatively more receptive and responsive to chemokines, whether expressed by tumors or inflammatory cells (Balkwill and Mantovani, 2001).

3.1.1.3 Rationale

In addition to genetic defects, depletion of host immune responses and the development of a more permissive tissue environment may act as pivotal forces for BCC progression and transformation (Kaur *et al.*, 2006; Walling *et al.*, 2004). However, the

molecular profile of the immune response during BCC development has not been fully established. Based on our preliminary quantitative real-time RT-PCR analysis of immunoregulatory genes in human BCC tissues as compared to non-lesional skin epithelium samples, the CXCR3 ligand, *CXCL11* was significantly upregulated at the highest level in the tumors (Figure 1.3). We hypothesized that the upregulation of CXCR3 and its ligands could be a key BCC growth promotion event. In this study, we investigated the potential impact of CXCR3/ligand signaling on BCC development. Our findings suggest that the chemokines CXCL9, 10, and 11 are potent signaling mediators via CXCR3 for BCC keratinocyte proliferation, and may be significantly involved in the regulation of BCC tumor development.

3.1.2 Results

3.1.2.1 mRNA for CXCR3/ligands were upregulated in BCCs

The expression levels of mRNA for 18 chemokine genes and their receptors in seven nodular, five superficial, and five morpheiform BCC tumors were analyzed by qPCR (Figure 3.1; Table 3.1). The expression levels for these chemokines in BCCs were compared with those in ten non-lesional skin epithelium samples. The analysis provides an overall indication of mRNA expression present in both keratinocytes and inflammatory cells in the tissue samples. Twelve of the 18 mRNAs exhibited significant differential expression (p-value < 0.05) in BCCs as compared to the controls. *CXCL11*, *CXCL10*, and *CXCL9* were the 3 most upregulated genes in the tumor samples, and were increased by an average 26.62-fold, 9.24-fold, and 22.56-fold respectively. Their common receptor, *CXCR3*, was increased (4.93-fold)

in the BCCs with statistical significance. Separate examination of specific CXCR3 isotypes *CXCR3A, CXCR3B* and *CXCR3 alternative (CXCR3 alt)* revealed all types to be significantly upregulated in BCCs (4.25-fold, 8.02-fold and 3.16-fold average respectively).

Examination of differences in mRNA expression fold change associated with BCC subtypes revealed that all nodular, superficial, and morpheiform BCCs showed a uniform increase of the 12 upregulated genes (Table 3.1A). In comparison to superficial and morpheiform BCCs, nodular BCCs exhibited the greatest levels of differential gene expression for *CXCL11* at 35.50-fold, *CXCL9* at 36.22-fold, and *CXCL10* at 16.67-fold mean increase above control tissue levels (Table 3.1A). For the chemokines identified as down-regulated, there was a less consistent gene expression pattern associated with BCC subtypes (Table 3.1B). However, statistically significant reductions in expression in some BCC subtypes were observed for *CXCR4*, *CXCL4*, and *CXCL12* (Table 3.1B). For instance, *CXCR4* was significantly downregulated in morpheiform BCC at 0.33-fold, *CXCL12* was substantially reduced in morpheiform and nodular BCC at 0.29-fold and 0.35-fold respectively, and *CXCL4* was significantly decreased in nodular BCC at 0.37-fold while insignificantly declined in superficial and morpheiform subtypes (0.45-fold and 0.84-fold respectively (Table 3.1B).

Table 3.1 Expression levels of chemokines and their receptors in nodular, superficial and morpheiform BCCs

(A)	Upregulation							
	All BCCs		Nodular		Superficial		Morpheiform	
Gene	Fold change [a]	P-value [b]	Fold change [a]	P-value [b]	Fold change [a]	P-value [b]	Fold change [a]	P-value [b]
CXCL11	* 26.62	2.60×10^{-6}	* 35.46	4.48×10^{-5}	* 32.08	8.49×10^{-6}	* 15.37	1.12×10^{-4}
CXCL9	* 22.56	2.18×10^{-8}	* 36.21	1.63×10^{-4}	* 16.53	3.79×10^{-3}	* 17.46	8.85×10^{-5}
CXCL10	* 9.24	5.33×10^{-6}	* 16.67	6.84×10^{-4}	* 9.95	0.012	* 3.88	0.026
XCL1	* 6.65	1.45×10^{-5}	* 12.23	5.47×10^{-5}	* 4.96	1.92×10^{-3}	* 3.60	0.028
CXCR3	* 4.93	1.76×10^{-4}	* 7.08	3.96×10^{-4}	2.70	0.136	* 5.05	2.86×10^{-3}
CXCR3A	* 4.25	4.35×10^{-3}	* 6.03	1.47×10^{-3}	* 3.34	0.013	* 3.56	0.011
CXCR3B	* 8.02	9.51×10^{-8}	* 9.31	3.19×10^{-6}	* 8.96	6.02×10^{-6}	* 6.01	3.87×10^{-5}
CXCR3 alt	* 3.16	4.07×10^{-3}	* 4.36	0.014	* 2.80	0.010	* 2.44	0.033
CXCL5	* 3.88	0.013	* 4.78	7.47×10^{-3}	* 10.21	7.17×10^{-3}	1.02	0.847
CXCR6	* 2.62	0.033	2.74	0.082	* 3.06	0.039	1.84	0.112

(B)	Downregulation							
	All BCCs		Nodular		Superficial		Morpheiform	
Gene	Fold change [a]	P-value [b]	Fold change [a]	P-value [b]	Fold change [a]	P-value [b]	Fold change [a]	P-value [b]
XCR1	0.96	0.911	0.71	0.290	1.99	0.127	0.94	0.604
CXCL16	0.78	0.174	0.71	0.109	0.74	0.112	0.99	0.738
IL8	0.76	0.797	1.88	0.641	0.90	0.944	0.14	0.118
CXCL14	0.72	0.424	1.13	0.817	1.33	0.334	0.19	0.147
IL8Rβ	0.68	0.283	0.59	0.141	1.15	0.728	0.61	0.139
CXCR4	0.55	0.049	0.60	0.127	0.77	0.410	* 0.33	0.002
CXCL4	0.49	0.072	* 0.37	0.021	0.45	0.098	0.84	0.661
CXCL12	* 0.38	7.66 x 10-5	* 0.35	6.36 x 10-5	0.57	0.139	* 0.29	0.004

[a] Fold change is evaluated using the $2^{-\Delta\Delta Ct}$ equation.

[b] Statistical analysis was done by Student's t-test to obtain p-value.

* indicates p-value < 0.05 and is considered as statistically significant

Figure 3.1 Quantitative real-time RT-PCR analysis of the chemokine expression levels in BCCs as compared to non-lesional skin epithelium

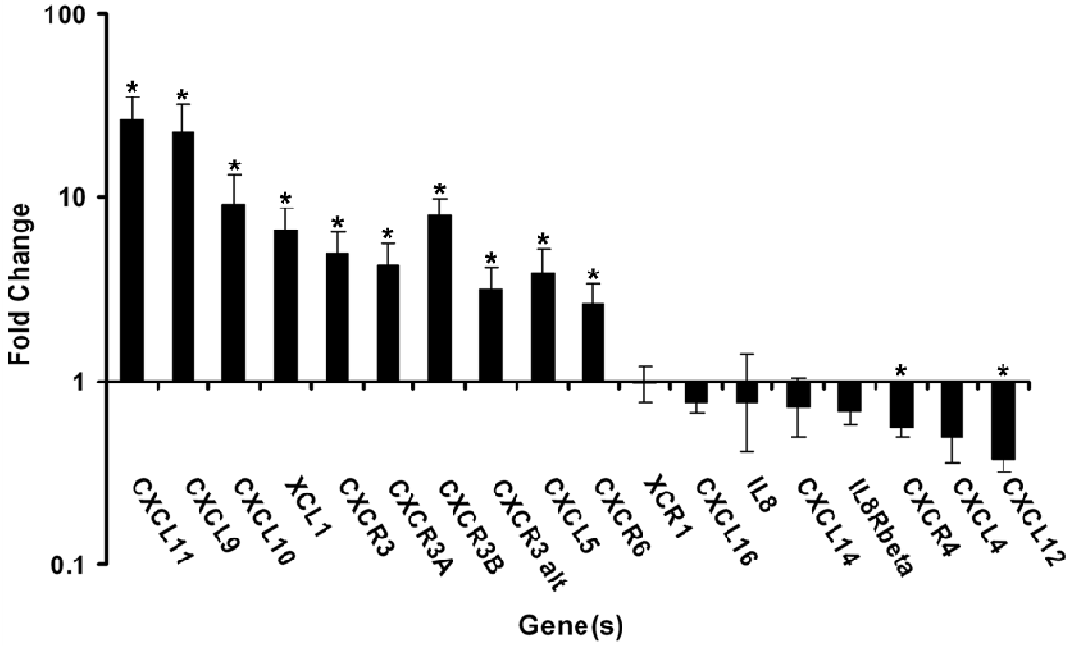

BCC tumors (7 nodular BCCs, 5 superficial BCCs, and 5 morpheiform BCCs) were studied. The gene expression levels in each BCC subtype were analyzed separately and were calculated in terms of fold change by using the $2^{-\Delta\Delta Ct}$ equation. The average fold change values of the 3 BCC subtypes are presented. Error bars represent the range factor difference ($2^{-\Delta\Delta Ct - \Delta Ct\ SE}$ and $2^{-\Delta\Delta Ct + \Delta Ct\ SE}$). Statistical significance was calculated by Student's t-test, and * indicates p-value < 0.05.

3.1.2.2 CXCR3/ligands colocalized with K17 in BCC tissues

IHC serial staining of CXCL9, 10, 11, and CXCR3 indicated that these chemokines were more prevalent with wider distribution in five nodular BCC tissue samples than in corresponding five control skin tissues when processed in parallel (Figure 3.2). CXCL10, 11 and CXCR3 were mainly localized in the tumor masses, though some expression was detected in the surrounding stroma (Figures 3.2C, E and G). However, CXCL9 was largely not expressed specifically in the BCC tumor nests; its immunolabeling was mainly distributed in the inflammatory infiltrate of the adjacent stromal region (Figure 3.2A).

Double labeling of K17 and the chemokines using five BCC biopsy samples was subsequently performed (Figure 3.3). It has been shown that K17 is expressed in BCC subtypes, including nodular, superficial, and morpheiform BCCs (Alessi *et al.*, 2008; Apaydin *et al.*, 2005; Asada *et al.*, 1993; Kurzen *et al.*, 2001; Schirren *et al.*, 1997), and it has been used as a histological diagnostic BCC marker (Alessi *et al.*, 2008). The coexpression patterns of the antibodies were consistent among the BCC subtypes. The IHC labeling revealed that K17 expression was positive in BCC keratinocytes and negative in non-follicular normal epithelium. K17 expression was localized close to the perimeter of the BCC cells consistent with a structural protein (Figure 3.3).

While CXCL9 was expressed by inflammatory cells in the interstitial area and stroma, CXCL9 was not expressed by $K17^+$ BCC keratinocytes (Figures 3.3A and E). In contrast, CXCL10 was positive in most $K17^+$ BCC keratinocytes, and localized in the cell cytoplasm (Figures 3.3B and F). Image analysis of label intensity demonstrated that $K17^+$ BCC cells expressed a significantly higher level of CXCL10 than inflammatory cells (Figure 3.4). CXCL11 was present throughout the tissue sections with $K17^+$ BCC cells exhibiting

higher expression intensity than the inflammatory cells (Figures 3.3C and 3.4). CXCL11 was predominantly localized in cytoplasm of the keratinocytes, but some expression was detected in interstitial regions between the BCC cells and the stroma (Figures 3.3C and G). CXCR3 was also labeled at a significantly higher intensity in $K17^+$ BCC cells than in the inflammatory infiltrate (Figures 3.3D and 3.4). Unlike its chemokine ligands, CXCR3 was not only present throughout the whole cell, but was also detected at the BCC cell surface (Figures 3.3D and H).

Figure 3.2 Serial immunohistochemistry of CXCL9, 10, 11 and CXCR3 in nodular BCCs and non-lesional skin

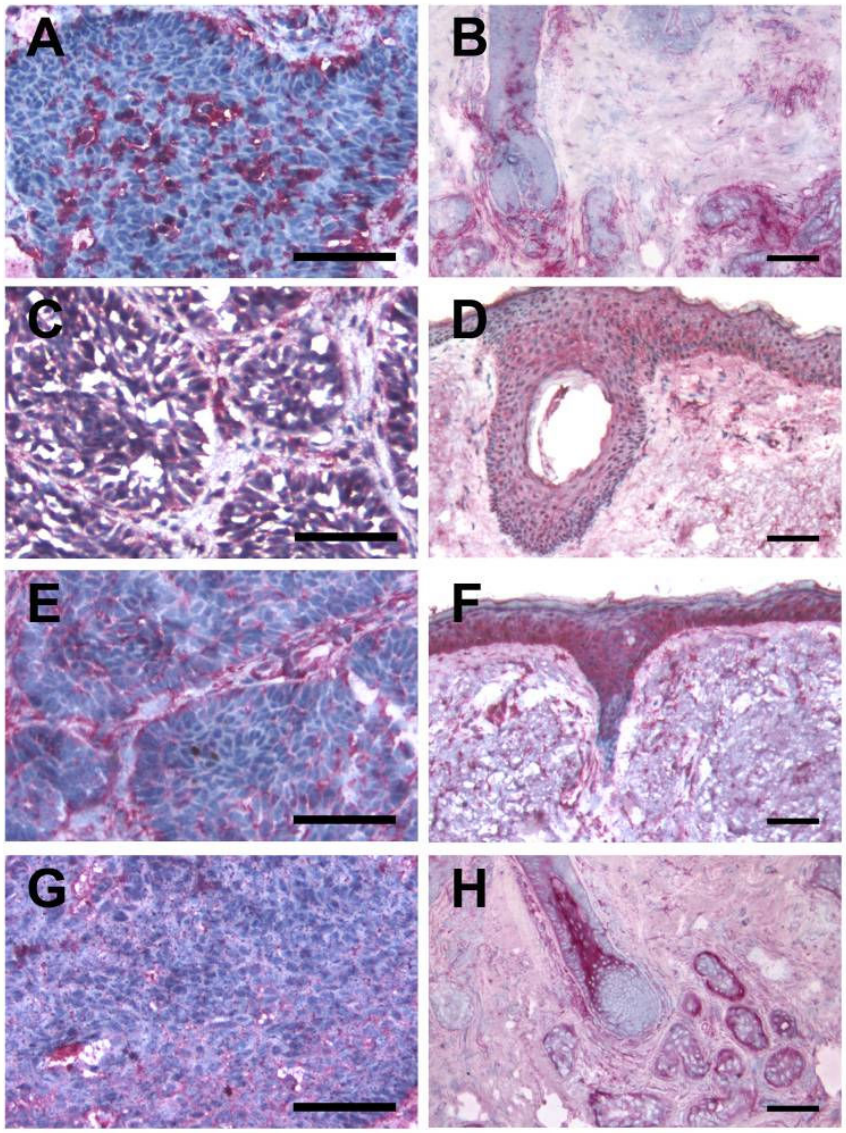

Five frozen sections of BCC tumors (A, C, E, G) and normal skin (B, D, F, H) tissues were analyzed for the protein expression patterns of CXCL9 (A and B respectively), CXCL10 (C and D respectively), CXCL11 (E and F respectively) and CXCR3 (G and H respectively). Positive labeling is indicated in red; the frozen sections were counterstained with hematoxylin (blue). Scale bar = 80 μm (A – H).

Figure 3.3 Dual immunohistochemistry of K17 with CXCL9, 10, 11 and CXCR3 in nodular BCCs

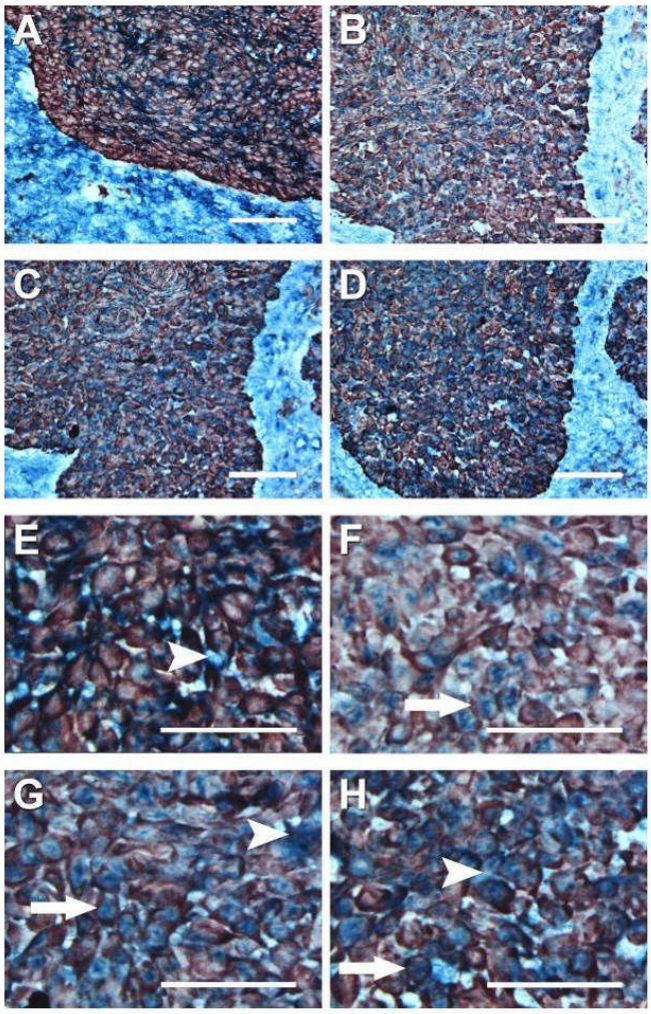

Five frozen BCC biopsies were studied for the colocalization of K17 with CXCL9 (A, E), CXCL10 (B, F), CXCL11 (C, G), and CXCR3 (D, H). K17 is shown as red, while CXCR3 and its ligands are indicated as blue. Arrows indicate representative cells with dual label of $K17^+$ co-expression with CXCL10 (F), CXCL11 (G), or CXCR3 (H). Arrowheads indicate representative cells with CXCL9 (E), CXCL11 (G) or CXCR3 (H) labeling in the absence of $K17^+$ co-expression in the BCC tumor masses. Scale bar = 80 μm (A – D). Scale bar = 55 μm (E – H).

Figure 3.4 Quantitative analysis of immunohistochemistry label intensities for CXCL10, 11 and CXCR3 in K17+ BCC keratinocytes as compared to cells in the stromal area

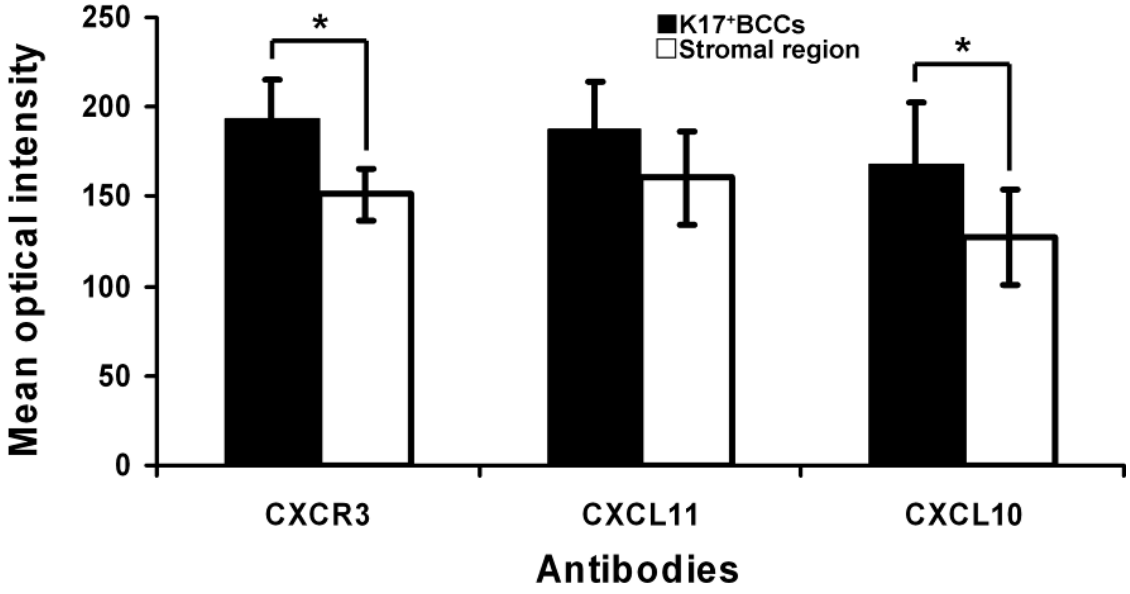

The mean immunolabeling intensities of the chemokines were evaluated using Scion Image software. The label intensities were derived from image pixel values (grey scale = 0 to 255), and are presented as mean optical intensity. In each of the 5 BCC biopsies, 10 randomly selected areas from each of the $K17^+$ BCC cell nests and the stromal regions were measured and compared for each IHC label by Student's t-test. * indicates p-value < 0.05.

3.1.2.3 CXCR3/ligands and K17 were expressed by HaCaT cells

Human immortalized HaCaT keratinocytes were examined by IHC analysis for K17, CXCR3, and its ligands. All of the factors evaluated were positively identified in the cells (Figure 3.5) though CXCL9 exhibited minimal expression. The localization of K17 was cytoplasmic as anticipated though expression was variable from cell to cell. Cells overlying other cells were more likely to express K17 as compared to cells adherent to the glass substrate (Figure 3.5E). The presence of K17 was distributed with less coherence in the cultured HaCaT cells as compared to BCC keratinocytes (Figures 3.5E and 3.3).

Figure 3.5 Immunohistochemistry analysis of CXCL9, 10, 11, CXCR3 and K17 in HaCaT cells

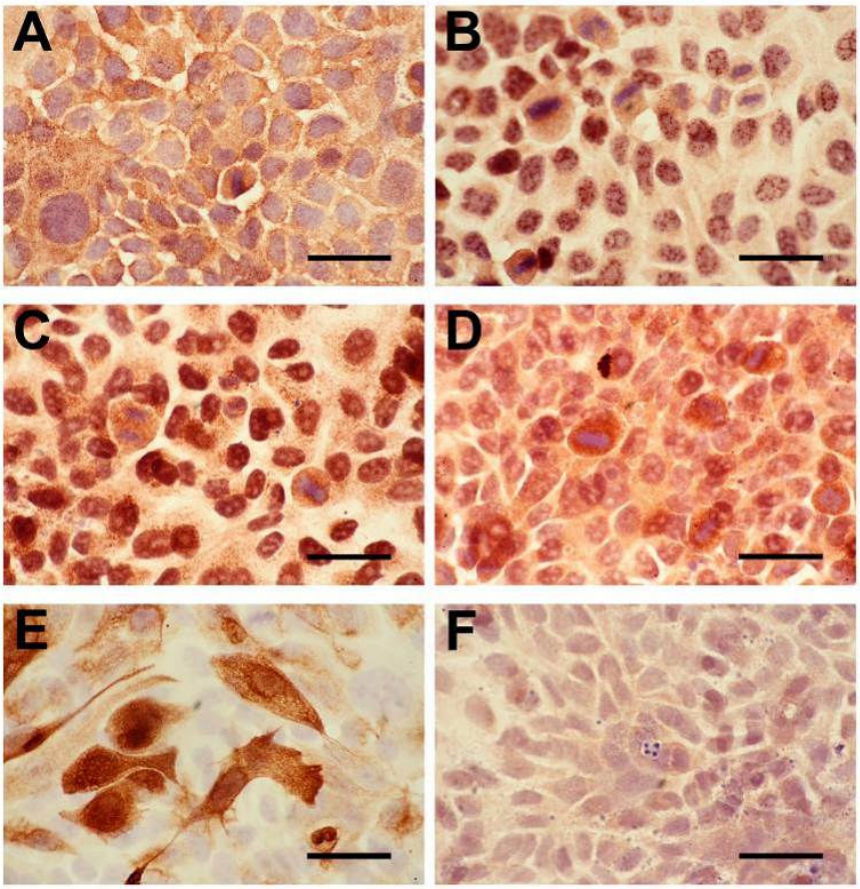

HaCaT cells were cultured on coverslips until 80 % confluency. Cell fixation and permeabilization were conducted, followed by overnight incubation of primary antibodies against CXCL9 (A), CXCL10 (B), CXCL11 (C), CXCR3 (D), and K17 (E). HaCaT cells were counterstained with hematoxylin. The negative control was performed in parallel (F). Scale bar = 45 μm (A – F).

3.1.2.4 CXCL11 enhanced proliferation of HaCaT cells

Based on the observations of HaCaT cell expression of K17, CXCR3 and ligands above, an *in vitro* functional assay of CXCR3 ligand effect was performed with HaCaT cell cultures. Because previous qPCR analysis revealed that CXCL11 mRNA was expressed with greatest fold increase in BCC tissues, and given CXCL9, 10, and 11 all act through the same CXCR3 receptor (Baggiolini, 2001; Hall *et al.*, 1999; Pellegrino *et al.*, 2004), this study examined CXCL11-regulated HaCaT keratinocyte cell growth.

Growth rates of HaCaT cells incubated with 1 nM, 5 nM, 10 nM and 20 nM of CXCL11 peptide for 24 and 48 hours were compared to that of non-treated cells. The y-axis represents the mean of growth rate of three individual experiments. The immortalized keratinocytes proliferated in response to all concentrations of CXCL11 at both time-points in a dose-dependent manner (Figure 3.6). HaCaT cells proliferated at a significantly faster rate as compared to controls ($p < 0.05$) at a minimum concentration of 5 nM after 24-hour incubation. Significant difference in cell proliferation was observed with 1 nM CXCL11 exposure after 48 hours (Figure 3.6). The 48-hour incubation yielded approximately double the number of cells as compared to the 24-hour time-point (Figure 3.6).

Figure 3.6 Growth rates of HaCaT cells incubated with CXCL11

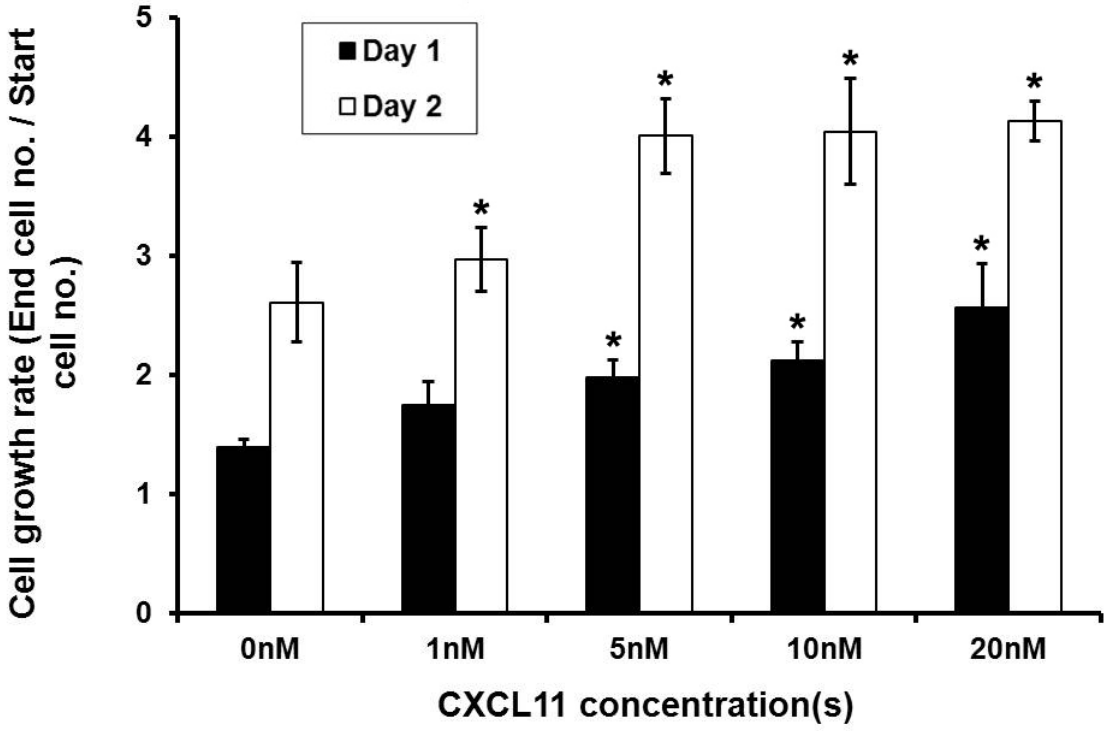

HaCaT cells were treated with different concentrations of CXCL11 peptide. The cell growth rate was calculated by the cell number at each time-point treatment by the cell number seeded on day 0. The y-axis represents the mean cell growth rate (± SE) of 3 individual experiments for each peptide concentration as shown on the x axis. Statistical significance of cell growth rate increased relative to untreated controls (i.e. 0 nM) was calculated by Student's t-test. * indicates p-value < 0.05

3.1.2.5 Human BCC-derived cells proliferation in culture media supplemented with CXCL11 peptide

Single cell suspensions of three human nodular BCC-derived cell cultures were treated with 0 nM, 5 nM, 10 nM and 20 nM CXCL11 peptide for 7, 14 and 21 days. When no CXCL11 peptide was added to the culture media, cell numbers did not increase (Figure 3.7). When BCC cells were treated with 5 nM CXCL11, the cell population exhibited a low, statistically insignificant, cell growth rate (Figure 3.7). With 10 nM peptide treatment, cell populations were expanded at all time-points, especially on day 21 where the cell growth rate was statistically significantly higher than with other peptide treatment concentrations (Figure 3.7). In addition, under the 10 nM CXCL11 condition, the higher cell growth rate at day 7, as compared to that of day 14, was statistically insignificant as the cell numbers increased at a similar rate for these two time-points (1.37 and 1.01 respectively) Notably, the cell number was reduced when the concentration of CXCL11 was increased to 20 nM suggesting 10 nM was the optimal concentration for BCC cell proliferation.

Figure 3.7 Human BCC-derived cell proliferation with or without CXCL11

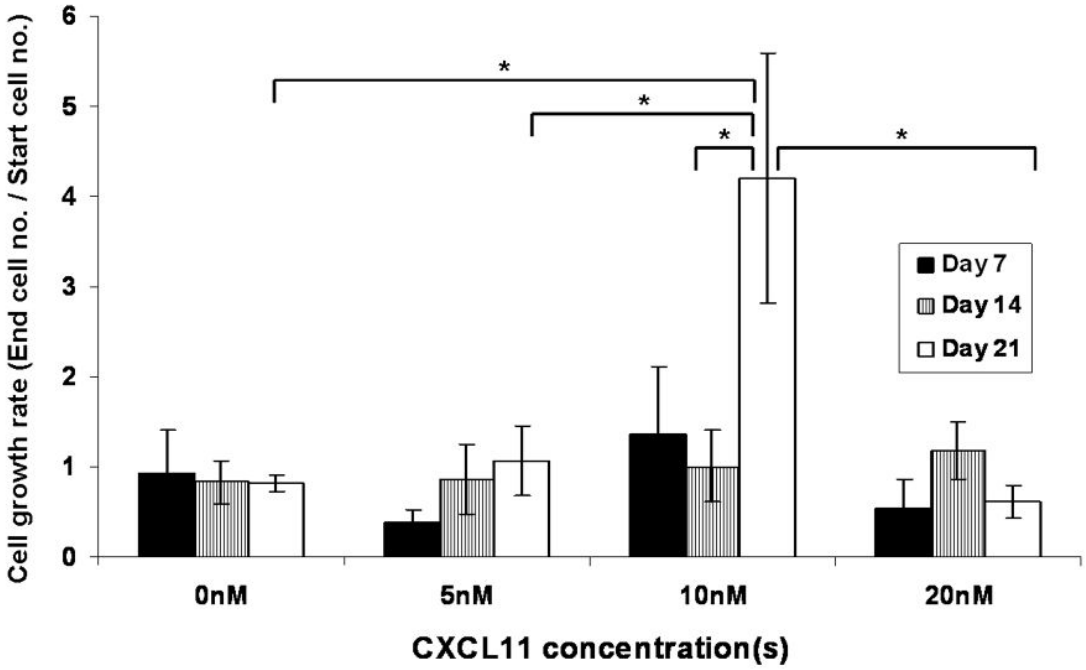

The y-axis represents the cell growth rate, which was calculated by dividing the cell number at the end of the treatment by the cell number seeded initially. A value less than 1 indicates a reduction of the cell population whereas a value greater than 1 represents the number of times more than the cell number started. The cell growth rates of all the treatments were compared among each other over 7, 14 and 21 days. Statistical significance was evaluated by ANOVA. * represents p-value < 0.05.

3.1.2.6 K17 and CXCR3 were detected in BCC cell cultures incubated with CXCL11

To characterize the nodular BCC derived cell cultures, cells incubated with 10 nM CXCL11 were examined by dual IHC labeling for K17 and CXCR3 at day 0, 7, 14 and 21. The results revealed 3 different cell presentations; $K17^{+}/CXCR3^{-}$, $K17^{+}/CXCR3^{+}$ or $K17^{-}/CXCR3^{+}$ cells (Figures 3.8 and 3.9). On day 0, the proportion of $K17^{-}/CXCR3^{+}$ cells (58.90 %) was significantly higher than the other 2 cell groups (Figure 3.9). On day 7, there was no significant difference among the cell numbers of the three marker groups. By day 14, $K17^{+}/CXCR3^{+}$ cells were more predominant (43.66 %) in the cultures (Figures 3.8 and 3.9). On day 21, both $K17^{+}/CXCR3^{+}$ and $K17^{+}/CXCR3^{-}$ cell groups were at significantly higher numbers (65.47 % and 33.09 % respectively) than the $K17^{-}/CXCR3^{+}$ group, which was reduced to 1.44 % of cells in the culture (Figures 3.8 and 3.9).

Figure 3.8 Dual immunohistochemistry of K17 and CXCR3 in human BCC-derived cells incubated with CXCL11

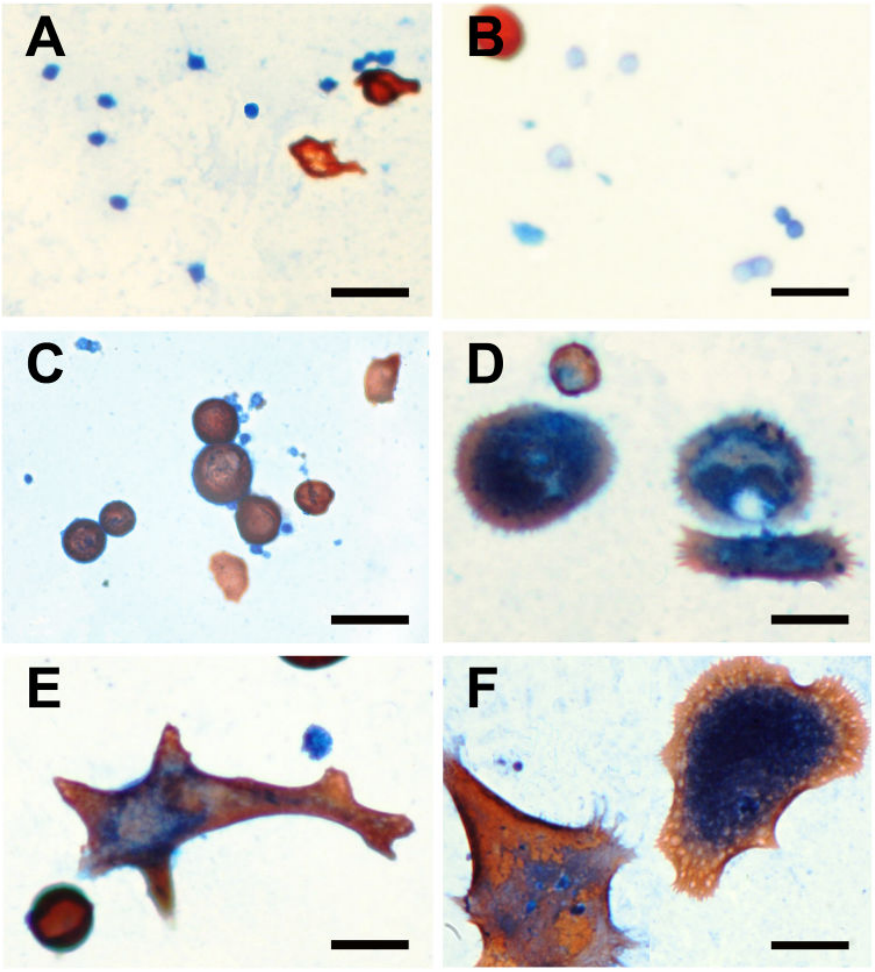

The BCC cells were cultured with 10 nM CXCL11 peptide and subsequently analyzed for the co-expression of K17 and CXCR3 at day 0 (A), 7 (B), 14 (C) and 21 (D – F). K17 labeling is indicated in red while CXCR3 labeling is shown in blue. Scale bar = 50 μm (A – F).

Figure 3.9 The proportion of cells representing as $K17^+/CXCR3^-$, $K17^+/CXCR3^+$, $K17^-/CXCR3^+$ in the BCC cell population after incubated with CXCL11

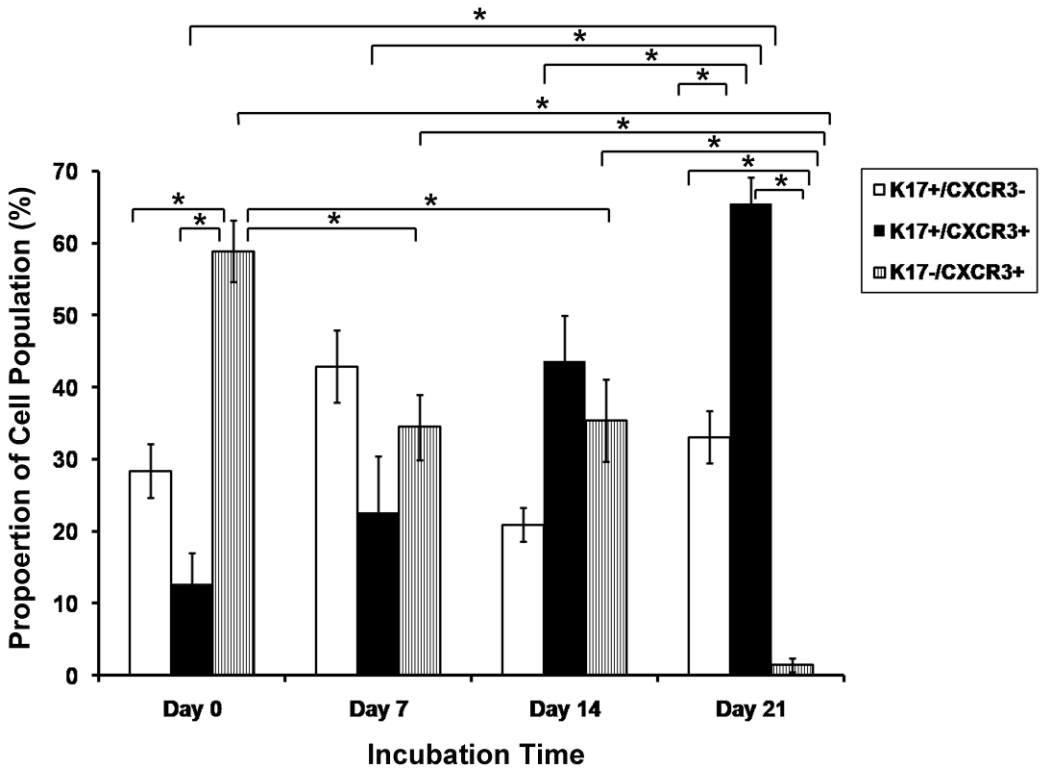

Cells derived from human BCCs were cultured in the presence of 10 nM CXCL11 and examined at day 0, 7, 14, and 21. The y-axis represents the percentage of the three cell groups in the cell population at each time-point. Statistical analysis was performed by ANOVA. * indicates p-value < 0.05.

3.1.2.7 Supplementation of cAMP maintained cell growth of $K17^+$ BCC-isolated cells

Various concentrations of cAMP were applied to three nodular BCC-isolated cell cultures, and cell growth and morphology were studied over 10 to 20 days. Doses of 0.1 μM and 10 μM of cAMP did not cause any cell settlement or growth after 10 days of incubation (Figures 3.10A and B respectively). The 1 μM concentration enhanced the isolated cells to settle and start to form colonies by 10 days of incubation (Figure 3.10C). The cells further proliferated up to 13 days with enlarging nucleus at the same cAMP treatment concentration (Figure 3.10D). However, by day 16 under 1 μM cAMP, the cells started to elongate and differentiate (Figure 3.10E). At day 20, the same dose of cAMP caused the cells to undergo stratification and cornification (Figure 3.10F). The observation suggested that 1 μM cAMP for 10 days of incubation may be the optimal setup for BCC-isolated cell proliferation. Cells under such treatment were further analyzed for marker expression.

After culturing with 1 μM cAMP for 10 days, another 3 nodular BCC-isolated cell cultures were examined by dual labeling IHC of K17 and CXCR3. The labeled cell cultures were categorized into four groups based on the markers they expressed. Positive labeling of K17 is shown as red while that of CXCR3 is indicated as blue (Figure 3.11 A). The data showed that 11.3 % of the cAMP-treated cells expressed K17 only, and that 85.8 % of the cells were $K17^+/CXCR3^+$ double positive. Also, there were some cells that were much smaller in size and were $CXCR3^+$ only and accounted for only 1.7 % of the cell culture. There was a small group of cells (1.2 %) that expressed neither of the markers (Figure 3.11B).

Figure 3.10 Different treatments of cAMP in BCC-isolated cells

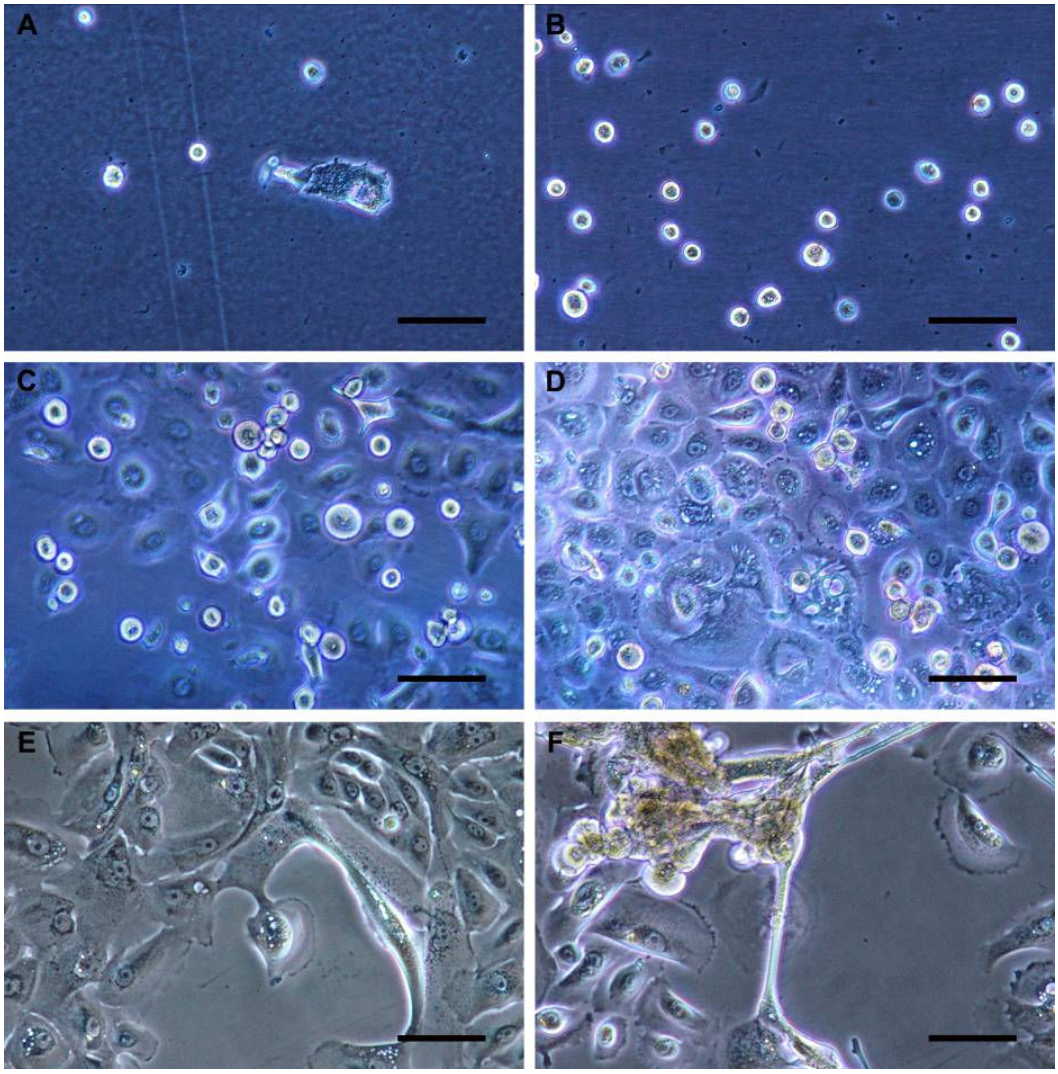

BCC patient samples (n = 3) were processed to obtain single cell suspension, which was further treated with 0.1 µM, 1 µM and 10 µM cAMP for 10 to 20 days. Cell growth and morphology were examined under inverted microscope and photographs were taken as observational data. Representative images of cell culture under 0.1 µM (A), 10 µM (B) and 1µM (C) for 10 days as well as 1 µM for 13 days (D), 16 days (E) and 20 days (F) were shown. The data suggested that the optimal setup for BCC-isolated cell growth was 1 µM cAMP for 10-day incubation (C). Scale bar = 100 µm (A – F).

Figure 3.11 Dual labeling of immunohistochemistry of K17 and CXCR3 in human BCC-isolated cells under cAMP treatment

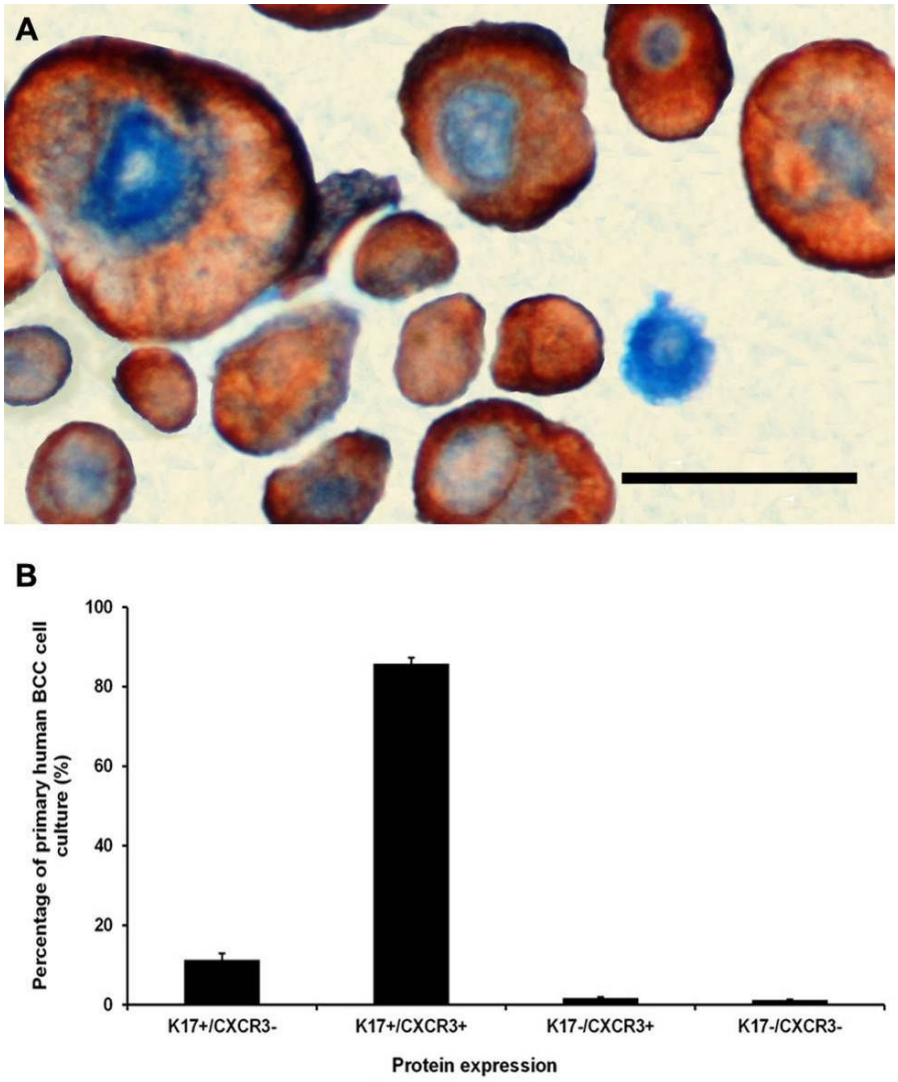

Cells were isolated from BCC tissues, and were treated with 1 μM cAMP for 10 days. The cells were analyzed for the expression of K17 (red) and CXCR3 (blue) by dual labeling immunohistochemistry; scale bar = 40 μm (A). The numbers of cells expressing markers $K17^{+}/CXCR3^{-}$, $K17^{+}/CXCR3^{+}$, $K17^{-}/CXCR3^{+}$, and $K17^{-}/CXCR3^{-}$ were counted. The data was presented as percentages of cell cultures (B). More than 80 % of the treated cells coexpressed K17 and CXCR3.

3.1.2.8 Anti-CXCR3 treatment increased primary human BCC cell death

To pursue the functional study further, loss of function of CXCR3 signaling in human BCC-isolated cells was conducted. After being isolated from three nodular BCC patient tissues, cells were not treated with any CXCL11 peptide to avoid any skew of gene expression towards CXCR3 and its ligands. Instead, cells were propagated with 1 μM cAMP supplementation for 10 days to obtain enough number of primary human nodular BCC cells for study. The cells were further treated with different amounts of CXCR3 neutralizing antibody, and were monitored for cell growth and death over 72 hours.

After 24 hours, the 50 μg/mL CXCR3 neutralizing antibody-treated BCC cells had a significantly lower fold change in cell proliferation (84.1 %) than the untreated control (109.3 %) (Figure 3.12A). By 72 hours, substantially reduced cell growth rates were observed in CXCR3 neutralizing antibody-treated cultures with the concentrations of 25 μg/mL (63.7 %) and 50 μg/mL (46.0 %) as compared to the untreated cells (118.0 %). For the cell death assays, all BCC cell cultures with CXCR3 antibody added exhibited a significantly higher proportion of dead cells than the untreated control at all time-points (Figure 3.12 B). At 72 hours, the CXCR3 antibody doses of 25 μg/mL and 50 μg/mL resulted in dead cell percentages of 37.1 % and 52.6 % respectively whereas the cell culture without any antibody added had 6.0 % dead cells.

Figure 3.12 Cell growth and death of primary human BCC cell culture under neutralization of CXCR3 signaling treatments

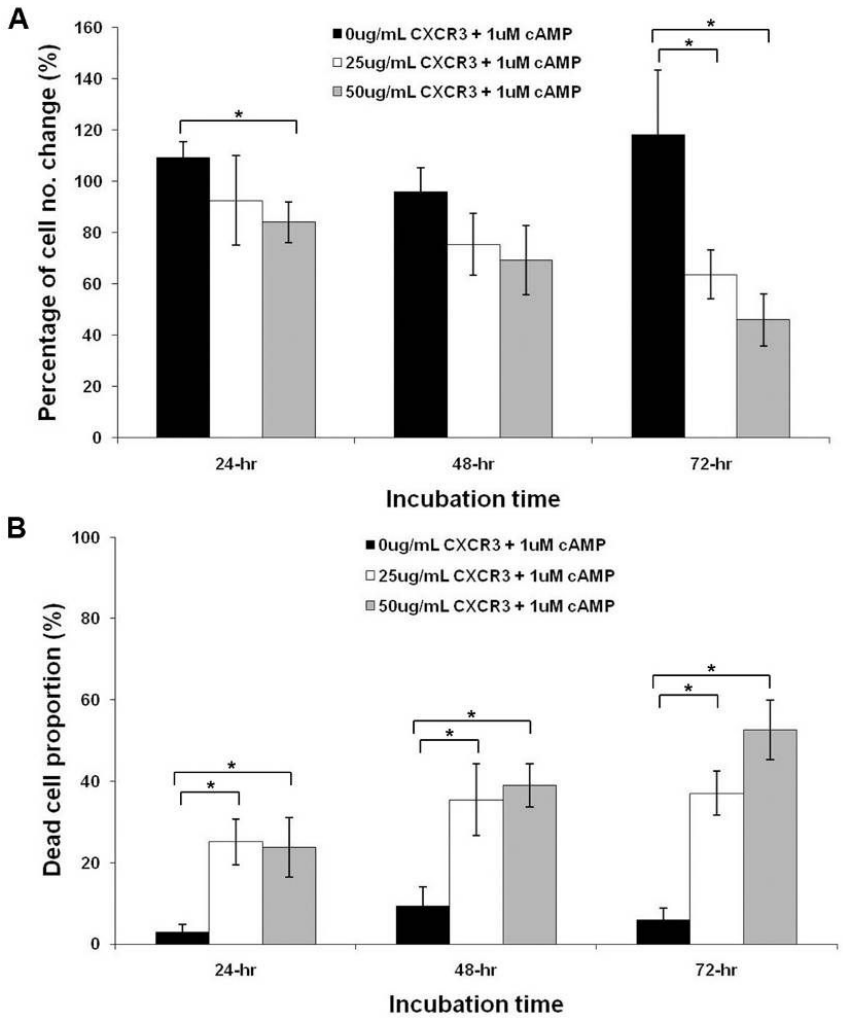

Human BCC tissue-isolated cells were treated with 1 μM cAMP for 10 days to obtain enough primary human BCC cell numbers for analysis. After that, the cells were treated with different concentrations of CXCR3 neutralizing antibody for 72 hours; cell cultures without any antibody added were used as control. Anti-CXCR3 treatment significantly reduced cell growth rates (A) and enhanced apoptosis (B). By 72 hours, more than 50 % of the cell culture under the 50 μg/mL treatment was dead. Statistical analysis was done by Student's t-test; p-value < 0.05 is indicated by *.

3.1.2.9 CXCL11 treatment stimulated primary human BCC cell migration

To determine if CXCR3 signaling had impact on any other BCC cellular activities, migration and invasion assays of BCC cells (three patient samples for each assay) in response to CXCL11 peptide were performed. After 72 hours of incubation, the migration rate of BCC cells increased significantly with the presence of CXCL11 in a dose-dependent manner. The percentage of migrated cells at 5 nM of the peptide was 5.5 %, 10 nM was 11.0 % and 20 nM was 20.8 % while that of 0 nM was 1.1 % (Figure 3.13 A).

However, BCC cells did not show much invasion response with CXCL11 peptide exposure. Even when 20 nM CXCL11 peptide was used, only 5.3 % of the cells invaded, while the invasion rate for 10 nM CXCL11 was only 4.3 %. When no peptide was applied, there was barely any cell invasion observed (1.0 %) (Figure 3.13B).

Figure 3.13 Migration and invasion assays of primary human BCC cells under CXCL11 treatments

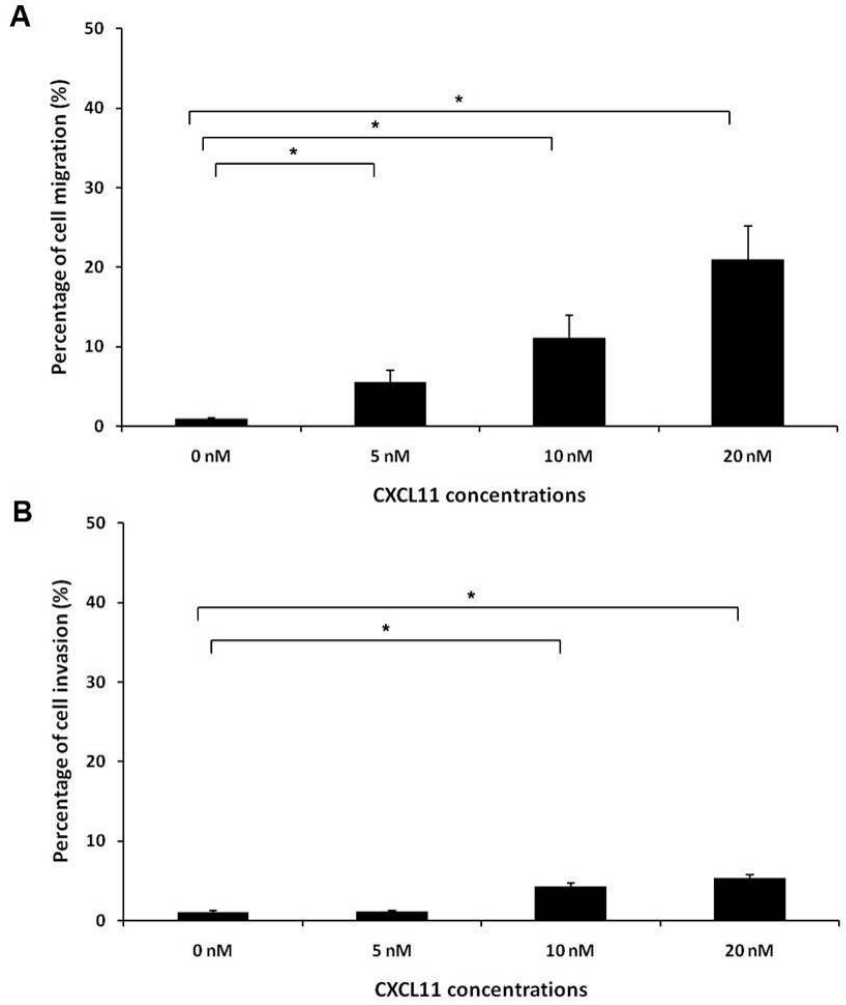

Primary human BCC cells were analyzed for their migration (A) and invasion (B) abilities in response to different concentrations of CXCL11 peptide by using Transwell culture chamber and Boyden chamber assays respectively after 72 hours of incubation. The BCC cells migrated towards CXCL11 peptide; such response increased significantly in a dose-dependent manner (A). However, the hBCC cells did not exhibit much invasion under the CXCL11 treatment (B). Statistical significance was measured by Student's t-test; p-value < 0.05 is indicated by *.

3.1.2.10 CXCL11 treatment of primary human BCC cells resulted in overall decrease of *MMP* expressions

To study the effects of CXCR3 signaling on BCC cell motility further, we decided to examine the expression of several matrix metalloproteinases (*MMPs*), *MMP1*, *2*, *3* and *9* in CXCL11-treated BCC cells from three patient samples by qPCR. Gene expression levels of cells without any treatment were used as baseline. After 72-hour of the peptide treatment, there was no upregulation of any of the *MMP* genes in BCC cells as compared to the untreated control (Figure 3.14). There was relatively less downregulation of most of the genes when higher concentrations of CXCL11 peptide, such as 20 nM, were applied. For instance, *MMP9* expression was significantly reduced when 5 nM and 10 nM CXCL11 was used (0.48- and 0.26-fold change respectively) as compared to the untreated control cells while such reduction of the expression level became insignificant when 20 nM peptide was applied (0.73-fold change) (Figure 3.14).

In addition, as 5.6 nM CXCL11 has been demonstrated to induce significant upregulation of *MMP9* and insignificant increase of *MMP2* expression in human breast cancer cells *in vitro* (Shin *et al.*, 2010), examining the expression of these two *MMPs* by qPCR in breast cancer cells treated with CXCL11 peptide would be a positive control for the protocol in this study. MCF-7 cells, which are a human breast cancer cell line, underwent the same treatments and qPCR analysis as in the BCC project. The y-axis represents the mean of fold change of three individual experiments. As expected, *MMP9* was upregulated at the highest level among all the genes tested especially when MCF-7 cells were supplemented with 5 nM and 10 nM CXCL11 peptide (3.6- and 2.5-fold change respectively); cells without any peptide supplementation were used as comparative control (Figure 3.15). *MMP2*

expression was only significantly increased under the 5 nM CXCL11 setup (2.1-fold change). The expression of *MMP1* and *MMP3* was insignificantly reduced in all the CXCL11 treatment concentrations.

Figure 3.14 Gene expression of *MMPs* in primary human BCC cells under CXCL11 supplementation

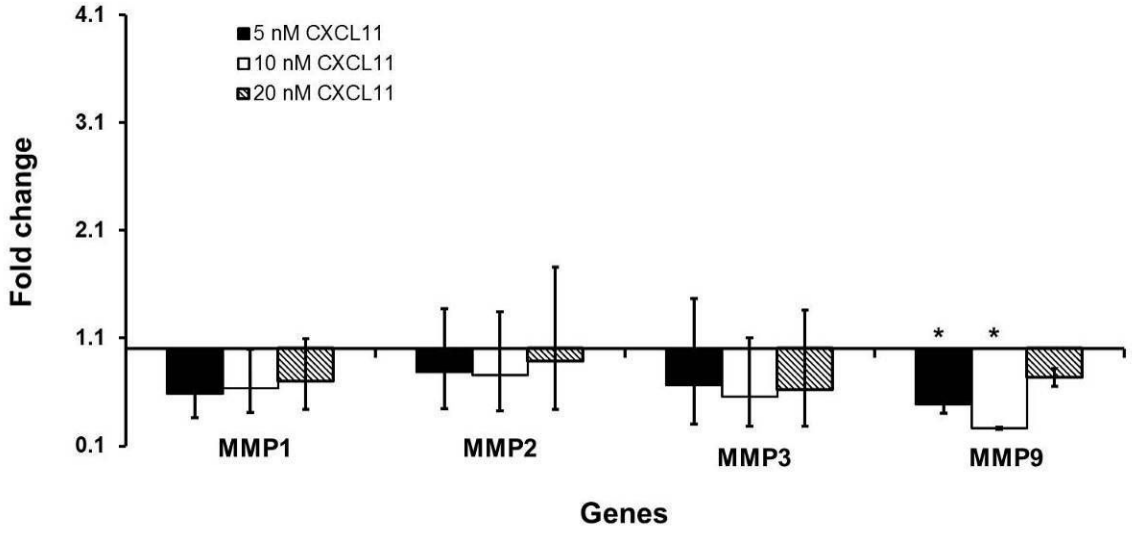

After being incubated with CXCL11 peptide for 72 hours, the primary human BCC cells (n = 3) were analyzed by qPCR for the expression of *MMP1*, *2*, *3* and *9*. There was no overall increase of expression of *MMPs* in the chemokine-treated hBCC cells. The gene expression levels were calculated in terms of fold change by using the $2^{-\Delta\Delta Ct}$ equation. The average fold change values of the patient cell samples were presented. Error bars represent the range factor difference ($2^{-\Delta\Delta Ct - \Delta Ct\ SE}$ and $2^{-\Delta\Delta Ct + \Delta Ct\ SE}$). Statistical significance was calculated by Student's t-test, and * indicates p-value < 0.05.

Figure 3.15 Expression of *MMPs* in CXCL11-treated MCF-7 cells

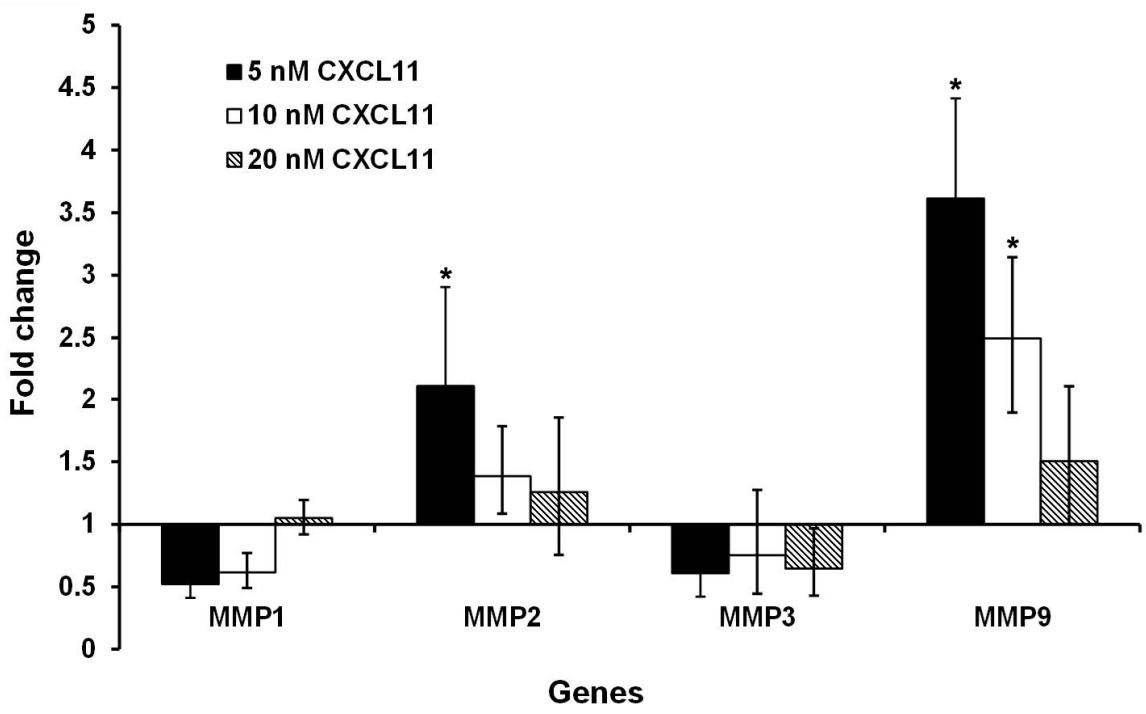

The human breast cancer cell line, MCF-7 was cultured with or without CXCL11 peptide for 72 hours. After that, the expression of *MMP1*, *2*, *3* and *9* in CXCL11-treated cells was evaluated by qPCR using untreated cells as the comparative control. Upregulation of *MMP2* and *MMP9* was detected in the cells under CXCL11 treatment while no significant differential expression of *MMP1* and *MMP3* was observed. The gene expression levels were calculated in terms of fold change by using the $2^{-\Delta\Delta Ct}$ equation. Error bars represent the range factor difference ($2^{-\Delta\Delta Ct - \Delta Ct\ SE}$ and $2^{-\Delta\Delta Ct + \Delta Ct\ SE}$). Statistical significance was calculated by Student's t-test, and * indicates p-value < 0.05.

3.1.3 Discussion

3.1.3.1 BCC tumors expressed CXCR3 and its ligands

It has been shown that certain cytokines and chemokines, commonly associated with immune system-activation, are involved in tumor cell growth and local immunosuppression rather than exerting anti-tumor functions (Furuya *et al.*, 2007; Jones *et al.*, 2000; Monteagudo *et al.*, 2007). As CXCL9, 10 and 11 have been suggested to play important roles in the development of other malignancies (Furuya *et al.*, 2007; Kawada *et al.*, 2004; Monteagudo *et al.*, 2007; Pellegrino *et al.*, 2004), we investigated the potential impact of chemokines, particularly the CXCR3 ligands, on the regulation of BCC etiopathology. In the current study, qPCR of 18 chemokines and their receptors in BCC tissues indicated significant increases in mRNA levels for selected chemokines. *CXCL11*, *9*, and *10* exhibited the greatest fold increase in expression in BCCs, which led us to consider the possibility that these CXC chemokines may play a significant role in BCC tumorigenesis. We also observed significant reduced expression of *CXCL12* in nodular and morpheiform BCCs and *CXCR4* in the morpheiform subtype, but insignificant downregulation of these genes in superficial BCCs. CXCL12-CXCR4 signaling has been shown to enhance the metastasis of solid tumors such as melanoma (Scala *et al.*, 2006). The relative decrease of *CXCL12-CXCR4* expression may be consistent with the low rate of metastasis observed in BCCs. CXCL4 has been indicated as an angiostatic molecule to affect tumor growth (Struyf *et al.*, 2011). Our data showed that *CXCL4* was substantially downregulated in nodular BCC only while in a less extent in morpheiform subtype, which may be consistent to the relatively non-aggressive nature of nodular BCC as compared to the more aggressive morpheiform BCC.

3.1.3.2 CXCR3 and its ligands were coexpressed with K17 by BCC keratinocytes

K17 is a marker of cell proliferation and follicular differentiation, and localizes in the lower hair follicle outer root sheath below the entry of the sebaceous duct (Alessi *et al.*, 2008; Leigh *et al.*, 1995; Moll *et al.*, 1982). It has also previously been shown that K17 is expressed in nodular, superficial, morpheiform, micronodular, fibroepithelial, and nodulocystic BCCs (Alessi *et al.*, 2008; Apaydin *et al.*, 2005; Asada *et al.*, 1993; Kurzen *et al.*, 2001; Schirren *et al.*, 1997; Yoshikawa *et al.*, 1998). In this study, our IHC analysis re-confirmed that BCCs strongly expressed K17, consistent with K17 as a marker of keratinocyte cell proliferation, and a specific marker of BCC keratinocytes.

The dual IHC labeling indicated that CXCR3, CXCL10 and CXCL11 proteins were represented at a high level in $K17^+$ BCC cells but at a relatively low level in the stroma infiltrating inflammatory cells. The distribution and expression intensity patterns of these chemokines suggest that the BCC keratinocytes may respond to CXCR3/ligands signaling more readily and efficiently than the stromal infiltrating cells, and that the tumor keratinocytes may synthesize and utilize these chemokines to direct autocrine signaling effects for cell proliferation and migration. Thus, in BCCs, CXCR3 and its ligands may be involved in tumor promotion rather than anti-tumor functions as seen in some other malignancies.

3.1.3.3 Human BCCs significantly expressed all three CXCR3 subtypes

The functional roles of CXCL9, 10, and 11 may depend on the subtype of CXCR3. There are at least 3 CXCR3 splice variants; CXCR3A, CXCR3B, and CXCR3 alt, which

may be expressed at different levels depending on the observed cell type (Ehlert *et al.*, 2004; Lasagni *et al.*, 2003). CXCR3A couples with $G_{\alpha i}$ of a GPCR to activate MAP kinase 1/2 (ERK1/2), p38/mitogen-activated protein kinase (MAPK) and phosphoinositide-3-kinase/v-akt murine thymoma viral oncogene (Akt) signaling pathways (Aksoy *et al.*, 2006; Ji *et al.*, 2008), and subsequently induces intracellular calcium influx, DNA synthesis and cell proliferation (e.g. normal human bronchial epithelial cells, astrocytes and glioma cells) (Aksoy *et al.*, 2006; Ji *et al.*, 2008; Loetscher *et al.*, 1998; Maru *et al.*, 2008). CXCR3B couples with $G_{\alpha s}$ of a GPCR to induce adenylyl cyclase, and results in inhibition of endothelial cell proliferation and migration (Kim *et al.*, 2002; Lasagni *et al.*, 2003); this receptor subtype does not induce chemotaxis (Ji *et al.*, 2008; Lasagni *et al.*, 2003). CXCR3 alt coexpresses with CXCR3A at a very low level (~5 % of CXCR3A mRNA) (Aksoy *et al.*, 2006). It has been shown that all three variants are expressed in colorectal carcinoma, breast cancer and multiple myeloma (Datta *et al.*, 2006; Giuliani *et al.*, 2006; Zipin-Roitman *et al.*, 2007). Our qPCR results indicated that all CXCR3 splice variants were significantly upregulated in all the BCC subtypes tested and that no strong bias in expression to a particular receptor variant was present. BCCs may employ the signaling effects of these CXCR3 subtypes in a similar fashion as in other cancers.

3.1.3.4 CXCR3 and its ligands may modulate tumor growth

In this study, IHC revealed that CXCL9 proteins were present in cells of the interstitial area and stroma, but not in $K17^+$ BCC keratinocytes. Further, while CXCL10 and CXCL11 were present in $K17^+$ BCC keratinocytes, expression at a lower level was also distributed in cells surrounding the tumor nests. The distribution patterns of these 3

chemokines suggest inflammatory cells in the tumor tissue biopsies also express the CXCR3 ligands. It is possible that, in addition to autocrine activity within BCC tumors, chemokines produced by adjacent inflammatory cells may have a further paracrine mode of action on BCC keratinocytes.

3.1.3.5 CXCL11 promoted dose-dependent HaCaT cell proliferation

HaCaT cells are spontaneously immortalized keratinocytes derived from human adult skin epithelium with UV-type specific mutations on both alleles of p53 (Boukamp, 2005; Boukamp *et al.*, 1988; Lehman *et al.*, 1993). They have been used extensively to study human skin carcinogenesis through over-expression or suppression of genes regulating cancer cell proliferation (Billings *et al.*, 2003; Boukamp, 2005; Boukamp *et al.*, 1995; Mudgil *et al.*, 2003; Mueller and Fusenig, 1999; Mueller *et al.*, 2001; Skobe and Fusenig, 1998). In this study, HaCaT cells exhibited similar expression patterns of K17, CXCR3 and its ligands as observed in BCC keratinocytes. Our data demonstrated that CXCL11 significantly enhanced the proliferation rate of HaCaT cells *in vitro*. Such findings, combined with the positive IHC results for CXCR3 and its ligands in HaCaT cells, suggests that both exogenous and endogenously produced CXCL11 can interact with $CXCR3^+$ HaCaT cells to activate cell growth pathways. Previous literature has suggested that the interaction of CXCL11 and CXCR3 can result in mitogenic effects and proliferation of human bronchial epithelial cells through the ERK1/2 and MAPK pathways (Aksoy *et al.*, 2006).

3.1.3.6 Human BCC-derived cells required CXCL11 supplementation for proliferation *in vitro*

To pursue the *in vitro* study of CXCR3-ligands in BCCs, we derived a modified BCC cell culture protocol from previous publications (Boyce and Ham, 1983; Brysk *et al.*, 1992; Sneddon *et al.*, 2006). We found that nodular BCC-isolated cells treated with 10 nM CXCL11 peptide showed significant increased cell growth at all observed time-points. Under this dosage of peptide supplementation, the duration of days 7 and 14 resulted in statistically insignificant differences between their cell growth rates due to the fact that these time-points were at the earlier stages of the establishment of BCC cell colonization and the cells proliferated at an unsteady rate. Notably, the BCC cells in the medium without CXCL11 peptide showed decreased cell growth rates and the remaining population number was progressively reduced as the incubation time increased. This suggests CXCL11 was needed for the growth of BCC cells, and that 10 nM was the optimal concentration of the peptide for cell culture.

Since K17 is a marker of BCC (Alessi *et al.*, 2008; Apaydin *et al.*, 2005; Asada *et al.*, 1993; Kurzen *et al.*, 2001; Schirren *et al.*, 1997; Yoshikawa *et al.*, 1998), the cell groups in BCC cell cultures expressing $K17^+$/ $CXCR3^-$ and $K17^+$/$CXCR3^+$ were BCC keratinocytes. $K17^-$/$CXCR3^+$ cells are likely infiltrating dendritic cells, lymphocytes or stromal cells (Chen *et al.*, 2009). The number of $K17^-$/$CXCR3^+$ cells progressively reduced with time in culture such that by day 21, $K17^+$ cells (with or without CXCR3 expression) accounted for ≥ 98 % of the cells. Ligands for CXCR3 may preferentially select for BCC keratinocyte survival and proliferation over non-keratinocytes. Based on our IHC and qPCR results of CXCL10 and CXCL11 being highly upregulated in $K17^+$ BCC cells, and the cell culture data here, it is

possible that the chemokines produced by BCC keratinocytes and stroma infiltrating inflammatory cells may bind with CXCR3 expressed by BCC cells to induce tumor cell proliferating signals. CXCR3 and its ligands may act as BCC tumor promoters.

3.1.3.7 CXCR3 signaling prevented cell death of primary human BCC cells

To further verify the growth support effects of CXCR3 signaling on BCC keratinocytes, loss of function studies were required. To accomplish that, neutralizing anti-CXCR3 antibody was used. Previous data showed that culturing primary BCC-isolated cells with 10 nM CXCL11 peptide for at least 21 days substantially enhanced the homogeneity of BCC keratinocyte culture, in which, the majority of the cells expressed CXCR3 (Sections 3.1.2.6 and 3.1.3.6) (Lo *et al.*, 2010). CXCL11 peptide treatment might distort gene expression, leading to the cells preferentially expressing CXCR3 and its ligands, and might bias the outcome of studies evaluating the blockade of CXCR3 signaling. As such, we decided to culture the nodular BCC-isolated cells with cAMP instead.

Cyclic AMP is a second messenger, and has been shown to be involved in the development of hyperproliferative skin lesions, such as psoriasis (Marcelo *et al.*, 1979). However, optimal doses of cAMP and duration of the treatment are critical to induce cell proliferation. It has been shown that cAMP can enhance DNA synthesis and proliferation of epidermal cells for short period of time (approximately 10 to 13 days); prolonged treatment induced differentiation and keratinization of the cells (Delecluse *et al.*, 1976). Also, it has been indicated that cAMP could facilitate proliferation of epidermal keratinocytes only at low dosage ranging from 0.01 μM to 1 μM; high dosage from 0.01 mM to 1 mM can have cytotoxic effects on the cells (Marcelo and Tomich, 1983). After multiple trials, an optimal

concentration of 1 μM cAMP and incubation time of 10 days for primary human nodular BCC cells (hBCC cells) were obtained for this study. Notably, our dual labeling IHC analysis confirmed that > 96 % of the cAMP-treated cells were indeed $K17^+$ BCC keratinocytes (Section 3.1.2.7), and that CXCR3 expression was detected in most of those cells even without any CXCL11 stimulation. As such, cAMP cultured hBCC cells could be used for the study of CXCR3 neutralization.

CXCR3 signaling has been shown to induce cell growth in various cancer types, such as osteosarcoma (Pradelli *et al.*, 2009). Pradelli and colleagues also demonstrated that treatment of CXCR3 antagonist, AMG487, to a mouse osteosarcoma cell line significantly reduced cell survival (Pradelli *et al.*, 2009). In this study, the loss of function experiment demonstrated that without the support of CXCR3 signaling, primary human nodular BCC keratinocytes were not able to proliferate. More importantly, neutralization of the chemokine signaling facilitated the cell death process in the culture. Even though CXCR3 and its ligands may not be the sole mediators for BCC initiation and progression, the data provide further support that the chemokine signaling may be required for BCC keratinocyte survival.

In addition, other cell death assays including TUNEL assay, caspase 3 assay or FACS analysis of Annexin V can be used as alternative methods to further confirm the effects of CXCR3 on BCC cell survival in the future studies.

3.1.3.8 CXCR3/CXCL11 induced cell migration of primary human BCC keratinocytes

Chemokine signaling has been shown to be associated with aggressiveness and metastasis in various cancers, such as aggressive natural killer cell leukemia and sporadic

breast cancer (Makishima *et al.*, 2005; Zafiropoulos *et al.*, 2004). Furthermore, it has been well established that CXCR4/CXCL12 chemokine signaling is involved in tumor cell migration, invasion and metastasis. Those studies demonstrated that $CXCR4^{+}$ tumor cells migrated to locations where its ligand, CXCL12 was present (Muller *et al.*, 2001; Murakami *et al.*, 2002). Similarly, CXCR3 signaling has been shown to be associated with metastasis to regional lymph nodes in melanoma and colon cancer as well as metastasis to lungs in breast cancer (Kawada *et al.*, 2007; Kawada *et al.*, 2004; Walser *et al.*, 2006).

In a study of murine osteosarcoma cells, CXCR3 ligands significantly induced cell migration whereas application of a CXCR3 antagonist reduced the tumor cell motility (Pradelli *et al.*, 2009). From this investigation, BCC cells were found to enhance their migration rate in response to CXCL11 peptide in a chemokine concentration dependent manner. The invasion of BCC cells in response to CXCL11 was relatively low, which was expected as BCC has been shown to have a very low metastatic rate (Walling *et al.*, 2004). The data implies that CXCR3/ligand signaling confers some neoplastic characteristics to BCC, such as cell migration, in addition to tumor cell proliferation and survival.

3.1.3.9 CXCR3 signaling did not induce MMP activity in BCC

Matrix metalloproteinases (MMPs) belong to the metzincins superfamily, and are zinc-based proteinases (Shiomi *et al.*, 2010). These enzymes are secreted as zymogens, which are inactive enzyme precursors, and require biochemical or configurational change to become active enzymes (Woessner, 1991). MMPs decompose at least one component of extracellular matrix and basement membrane (Shiomi *et al.*, 2010; Woessner, 1991). These proteinases are significantly involved in embryonic development, tissue remodeling,

ovulation, wound healing, and tissue destruction during pathological conditions (Shiomi *et al.*, 2010; Woessner, 1991). There are 23 MMPs discovered in humans, mainly categorized into 2 groups according to their structural properties and corresponding substrates: secreted-type MMPs and membrane-anchored MMPs (Shiomi *et al.*, 2010). Secreted-type MMPs contain several subgroups such as collagenases (e.g. MMP1), gelatinases (e.g. MMP2, MMP9) and stromelysins (e.g. MMP3) whereas membrane-anchored MMPs include type I and type II transmembrane-type MMPs (Shiomi *et al.*, 2010; Woessner, 1991).

Furthermore, MMPs are involved in tumor cell progression, invasion and metastasis (Egeblad and Werb, 2002; Shiomi and Okada, 2003). In fact, MMP expressions have been shown to be associated with aggressiveness of epithelial skin cancers (Kerkela *et al.*, 2001; Son *et al.*, 2008). Several studies of MMP expression in BCC have been published, in which, tissue array and IHC demonstrated that MMP1 and MMP3 were expressed in BCC tumor and stromal cells. MMP2 and MMP9 were found in the organ culture fluid of both aggressive and non-aggressive BCC subtypes by gelatinolytic activity assays (Son *et al.*, 2008; Varani *et al.*, 2000).

MMP expression and activity have been correlated with CXCR3 signaling in some cancers. Pradelli and colleagues demonstrated that CXCR3/CXCL10 signaling induced expression of active MMP2 and MMP9 in murine osteosarcoma cells (Pradelli *et al.*, 2009). Also, Shin and colleagues found that treatments of CXCL9, 10 and 11 upregulated the expression of *MMP2* and *MMP9* in human breast cancer cells (Shin *et al.*, 2010). Based on our previous data, CXCR3 signaling may be involved in BCC keratinocyte motility. As such, I wanted to elucidate if the chemokine signaling has any additional effects on MMP expressions, especially MMP1, 2, 3 and 9 in primary human BCC cells. The qPCR data

revealed that CXCR3/CXCL11 signaling did not enhance the expression of *MMPs* in the BCC cells. The outcome was distinct from other cancers as mentioned above. Such difference may be due to the possibility that MMP1, 2, 3 and 9 were not the key factors during CXCR3-induced cell migration in BCC cells, and that other MMPs or migration-associated molecules may be involved.

In order to verify the correctness of the protocol in this study, evaluation of MMP gene expression in breast cancer cells under CXCL11 supplementation was repeated. The data was consistent with previously published studies in that both *MMP9* and *MMP2* were upregulated in the breast cancer cells with the former being expressed at a higher level. *MMP1*, but not *MMP3*, expression has been detected in human breast cancer and has also been shown to be involved in bone metastasis (Okuyama *et al.*, 2008). However, neither *MMP1* nor *MMP3* expression was upregulated by CXCL11 in breast cancer cells here. By reproducing the qPCR results of *MMP2* and *MMP9* in breast cancer cells treated with CXCL11, it was concluded that the present study protocol was correct. The lack of significant changes in *MMP* expression in BCC cells in response to CXCL11 is distinct from the increased *MMP* expression seen in breast cancer cells. Such different response may be consistent with the absence of metastatic ability in BCC cells.

3.1.4 Conclusion

Taken together, CXCR3 and its ligands expressed by BCC keratinocytes, and to a lesser extent by inflammatory cells, may enable autocrine or paracrine signaling to induce BCC cell proliferation. Moreover, CXCR3 signaling may support cell survival and prevent cell death of BCC keratinocytes. CXCR3/CXCL11 may participate in other neoplastic

characteristics of BCC, such as tumor cell migration. Our results provide evidence for CXCR3 and its ligands being a novel mechanism for BCC growth and progression, and these chemokines may serve as potential targets in developing drug treatments against BCCs.

3.2 CXCR3 signaling effects on non-melanoma skin cancer keratinocytes

3.2.1 Background and rationale

Recently, studies have demonstrated that cancers such as malignant melanomas and ovarian carcinomas modulate CXCR3/ligand signaling for tumor progression and metastasis (Furuya *et al.*, 2007; Monteagudo *et al.*, 2007). Our previous studies revealed that CXCR3 and its ligands were significantly involved in primary BCC tumor cell proliferation (Chapter 3A) (Lo *et al.*, 2010). However, the impact of chemokine signaling on other NMSCs is not known.

In this study, we elucidated the roles of chemokines, especially CXCR3 and its ligands, during the development of NMSCs, including SCC and its pre-malignant skin lesions actinic keratosis (AK) and Bowen's disease (BD), as compared to BCC and the benign epithelial lesion seborrheic keratosis (SK). Our data revealed that *CXCR3* and its ligands were significantly upregulated in all NMSCs and skin tumors, but most significantly in SCC. Also, CXCR3 ligands supported the growth, survival, migration and invasion of HaCaT cells as a human neoplastic keratinocyte cell model. As such, CXCR3/ligand signaling may be crucial for the development of NMSC, especially SCC.

3.2.2 Results

3.2.2.1 Upregulation of *CXCR3* and its ligands *CXCL9*, *CXCL10* and *CXCL11* in non-melanoma skin cancer

The mRNA expression levels for 18 chemokines were analyzed in nine SCC, six AK, five BD, five nodular BCC and ten SK as compared to ten NL skin tissues using qPCR. The results demonstrated that *CXCR3* along with its ligands *CXCL9, CXCL10* and *CXCL11* exhibited a significant increase in all five lesions (Table 3.2; figure 3.16). In particular, SCC exhibited the highest increase in *CXCR3* expression level (1080.6-fold) as compared to normal skin epithelium (Figure 3.16A). AK (Figure 3.16B), BD (Figure 3.16C), BCC (Figure 3.16D) and SK (Figure 3.16E) had less than 100 fold increase in *CXCR3* expression (96.9-, 74.4-, 4.5- and 3.2-fold respectively) (Table 3.2). As for *CXCL11, CXCL10* and *CXCL9* mRNA expression levels, SCC showed the highest fold change among all the NMSC samples tested (2448.5-, 1290.5- and 1031.8-fold respectively) (Table 3.2; figure 3.16A). In addition, the *CXCR3* splice variants were all upregulated in the NMSC lesion samples (Table 3.2; figure 3.16); the expression levels of *CXCR3A, CXCR3B* and *CXCR3 alt* in SCC were 233.6-, 1547.0- and 151.6-fold respectively (Table 3.2; figure 3.16A). Furthermore, for SCC, *interleukin-8* (*IL8*) was substantially increased at the highest level (14588.1-fold) among all other chemokines evaluated; this gene was also significantly upregulated in the other lesion samples but to a lesser extent (Figure 3.16). Interestingly, SCC and AK showed significant upregulation of all chemokines tested.

In addition, *CXCL12* was significantly upregulated in SCC (5.6-fold) and AK (3.5-fold) (Figures 3.16A and B respectively); however, the chemokine expression was either

downregulated or neutral in BD, BCC and SK (Figures 3.16C – E respectively). Notably, the receptor for CXCL12, *CXCR4* was upregulated at the highest level in SCC (211.6-fold) followed by AK (11.1-fold), BCC (1.3-fold) and BD (1.2-fold); only SK demonstrated insignificant reduced expression of *CXCR4* (0.7-fold) (Figure 3.16).

Table 3.2 Expression level of *CXCL9*, *10*, *11* and *CXCR3* receptors in SCC, AK, BD, BCC and SK

	SCC		AK		BD		BCC		SK	
Gene	Fold change[a]	P-value[b]	Fold change[a]	P-value[b]	Fold change[a]	P-value[b]	Fold change[a]	P-value[b]	Fold change[a]	P-value[b]
CXCL9	* 1031.82	0.031	* 247.03	3.83×10^{-8}	* 22.54	1.54×10^{-4}	* 40.71	0.013	* 5.15	0.029
CXCL10	* 1290.49	1.71×10^{-6}	* 329.33	8.11×10^{-8}	* 357.49	3.06×10^{-7}	* 9.61	0.002	* 11.26	0.001
CXCL11	* 2448.45	4.85×10^{-8}	* 262.09	5.31×10^{-8}	* 3.97	0.008	* 10.00	0.003	* 19.09	0.001
CXCR3	* 1080.63	6.43×10^{-9}	* 96.87	1.21×10^{-10}	* 74.35	5.81×10^{-8}	* 4.45	0.031	* 3.17	6.18×10^{-5}
CXCR3A	* 233.60	6.60×10^{-10}	* 1889.78	2.87×10^{-9}	* 3145.05	9.13×10^{-8}	* 1.83	0.014	* 1.80	0.007
CXCR3B	* 1546.99	5.21×10^{-15}	* 888.60	6.48×10^{-10}	* 2616.99	1.07×10^{-7}	* 4.06	8.90×10^{-5}	* 16.11	4.30×10^{-9}
CXCR3 alt	* 151.59	3.50×10^{-8}	* 648.27	1.38×10^{-15}	* 1392.93	1.88×10^{-6}	* 2.34	0.043	2.02	0.17

[a] Fold change is evaluated using the $2^{-\Delta\Delta Ct}$ equation.

[b] Statistical analysis was done by Student's t-test to obtain p-value.

* indicates p-value < 0.05 and is considered as statistically significant.

Figure 3.16 Expression level of chemokines and their receptors in non-melanoma skin lesion samples

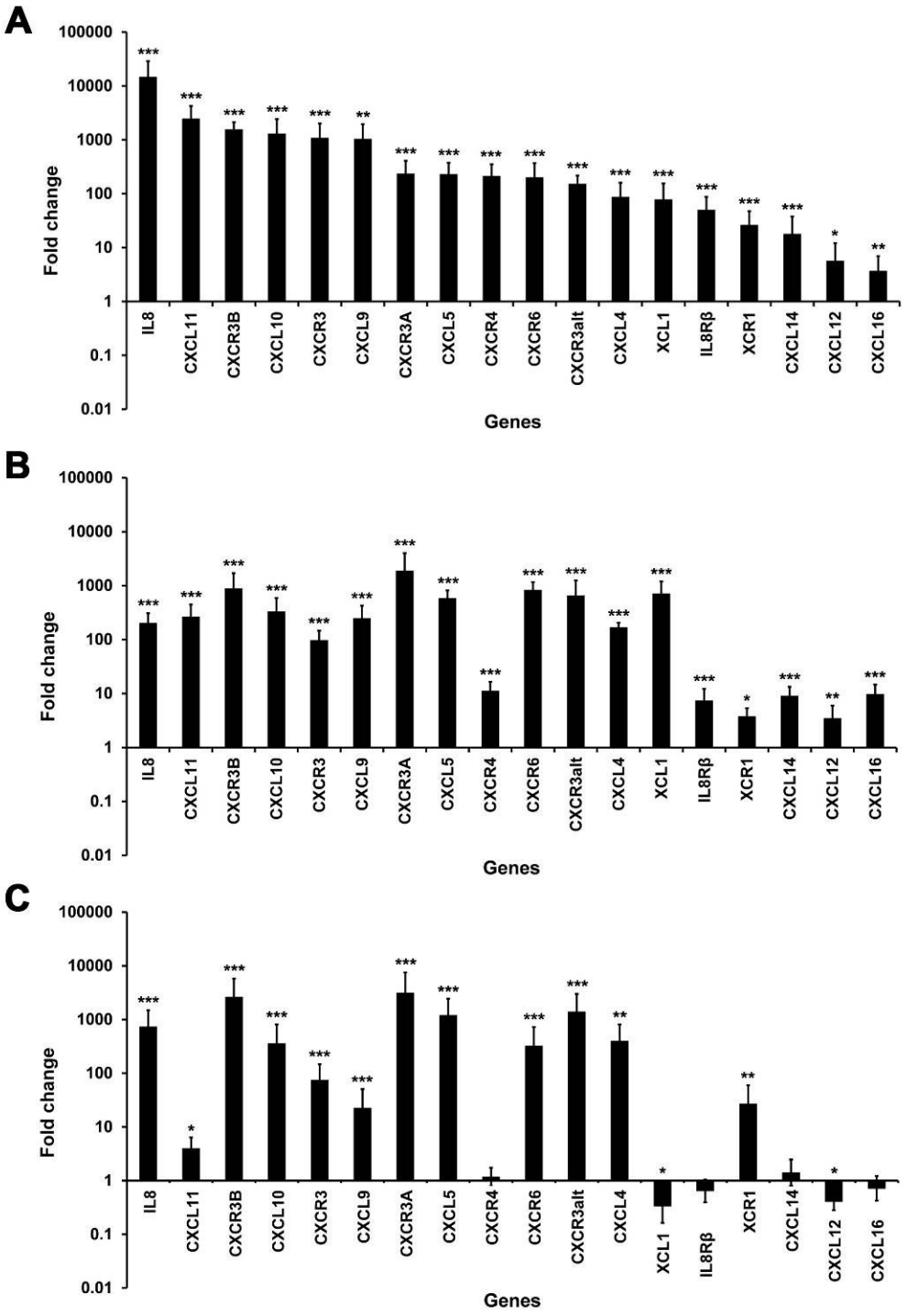

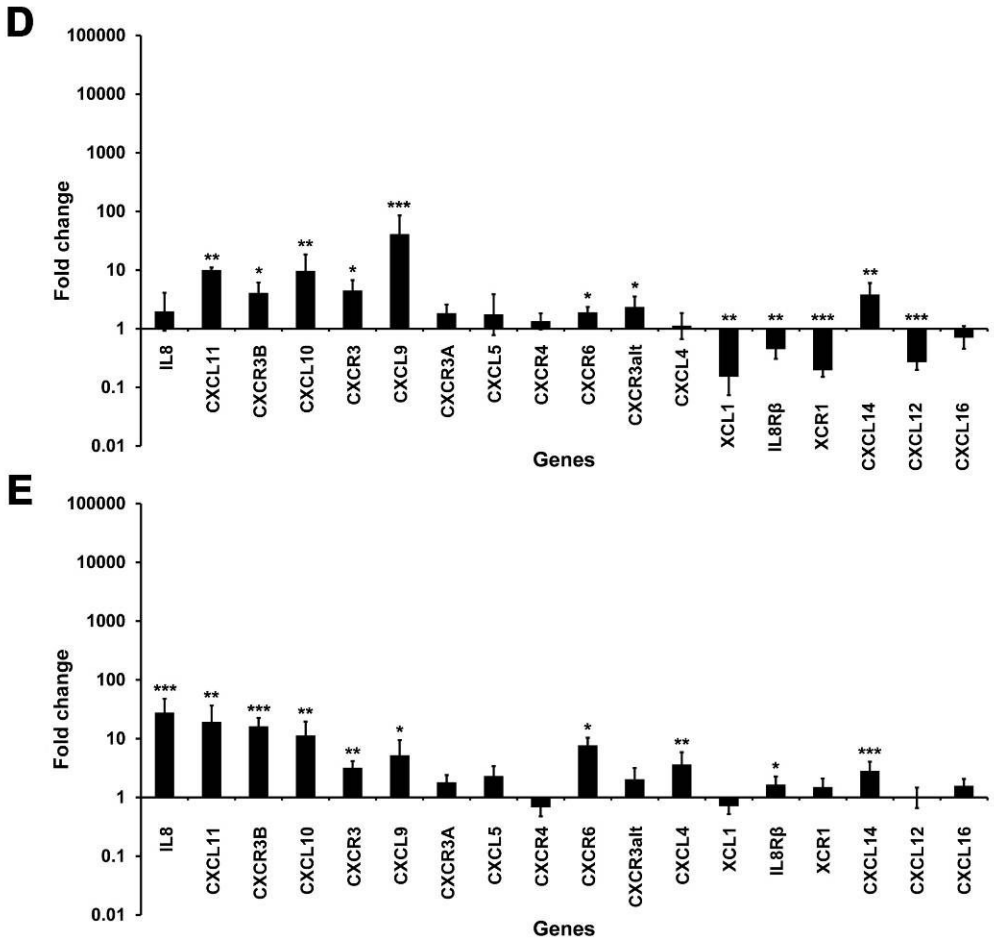

Tissue samples of SCC (n=9) (A), AK (n = 6) (B), BD (n = 5) (C), BCC (n = 5) (D) and SK (n = 10) (E) were analyzed by qPCR. The expression level for each gene in the skin lesion samples was compared to NL tissues (n = 10), and was presented as fold change using the equation $2^{-\Delta\Delta Ct}$. Error bar represents the range difference of fold change ($2^{-\Delta\Delta Ct - \Delta Ct\ SE}$ and $2^{-\Delta\Delta Ct + \Delta Ct\ SE}$). Statistical significance was measured by Student's t-test; p-value <0.05 was indicated as *, <0.005 as **, <0.0005 as ***.

3.2.2.2 Colocalization of CXCR3 and the SCC keratinocyte marker, K13, in cutaneous SCC tissues

Dual labeling IHC revealed that CXCR3 colocalized with K13 in all tumor masses of human SCC tissue sections (Figures 3.17A and B). Interestingly, the staining intensity of CXCR3 was not distributed evenly within the tumor nests; some cells exhibited a stronger labeling signal than the others. There was some non-specific staining of the chemokine in the stromal regions. K13 was specifically expressed by SCC keratinocytes as expected. In addition, K13 was localized in the suprabasal layer and select regions of the basal layer of the epidermis in SCC biopsies (Figures 3.17C and D). CXCR3 was not detected in the epidermis.

Figure 3.17 Dual labeling immunohistochemistry of K13 and CXCR3 in cutaneous SCC tissue samples

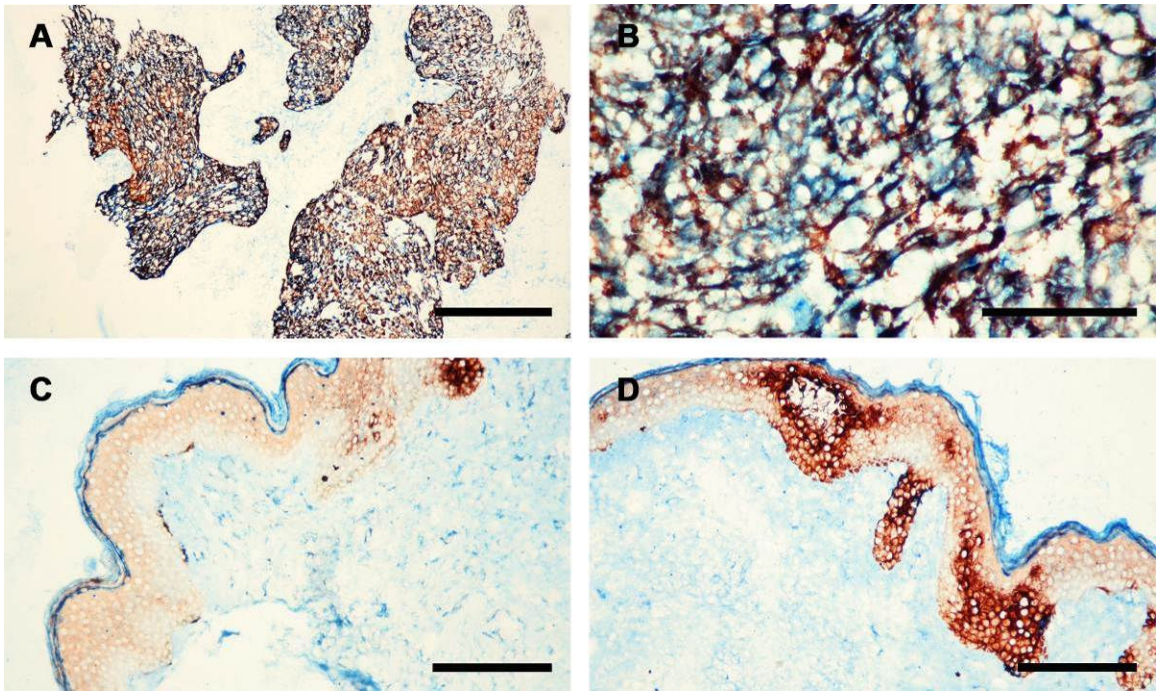

The positive labeling of K13 is indicated as red while that of CXCR3 is indicated as blue. Representative IHC photographic images are shown. Specific coexpression of K13 and CXCR3 was detected in SCC tumor nests (A and B). K13 localized in the suprabasal layer of the epidermis as well as in select regions of the basal layer; no specific staining of CXCR3 was found in the epidermis (C and D). Scale bars equal 280 μm (A), 60 μm (B) and 140 μm (C and D).

3.2.2.3 Blockade of CXCR3 signaling reduced cell growth and increased death of HaCaT cells

The y-axis of the graph of both cell proliferation and cell death assays represents the mean percentage of three individual experiments. Increasing concentrations of CXCR3 neutralizing antibody led to reduced HaCaT cell growth rates (Figure 3.18A) and increased cell death (Figure 3.18B) as compared to untreated controls as early as 24 hours after the treatments; such effects were further accentuated as the incubation time increased. By 72 hours, 100 μg/mL anti-CXCR3 antibody yielded an average 194.3 % growth rate and 11.9 % death rate in HaCaT cells compared to 241.0 % and 2.7 % respectively in untreated controls. Control experiments with mouse IgG_1 isotype antibody demonstrated no significant difference in HaCaT cell growth and death rates (Figures 3.18C and D respectively).

HaCaT cells treated for 72-hours with CXCR3 neutralizing antibody were further evaluated for the efficiency of their recovery by propagating them in complete growth medium only. Cells without prior antibody treatment showed a substantially higher cell growth rates and lower dead cell percentages than those cells that were previously exposed to CXCR3 neutralizing antibody (Figures 3.18E and F respectively).

Figure 3.18 Neutralization of CXCR3 bioactivity in HaCaT cell culture

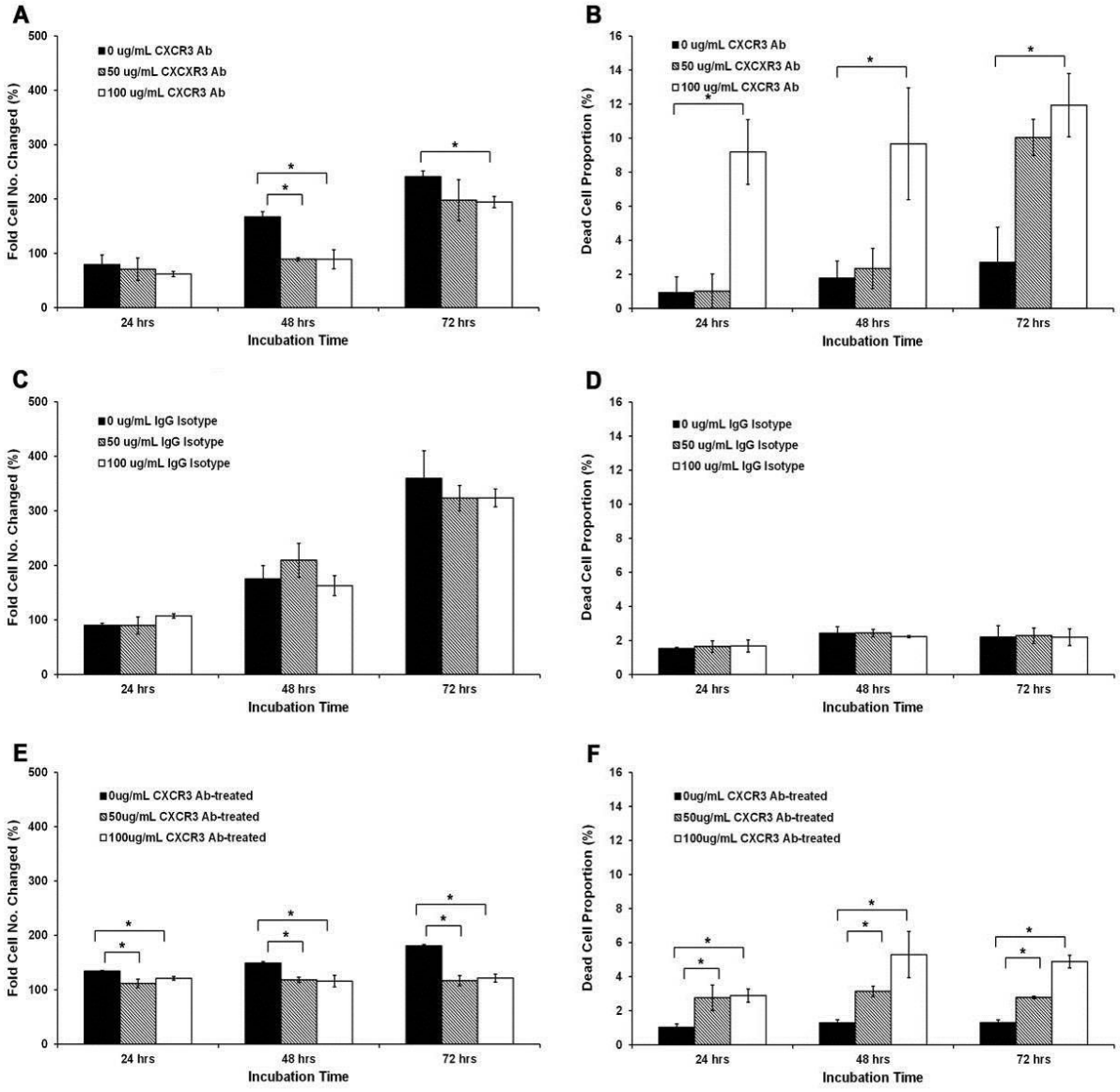

Growth rates are presented as percentage of original seeded cell number while dead cells are presented as percentage of the total population at each time point. CXCR3 neutralizing antibody treatment caused decreased cell growth rates and increased dead cell proportions (A and B respectively). The recovery studies indicated that HaCaT cells with previous CXCR3 neutralizing antibody exposure were not able to resume their growing and survival capacities (E and F respectively). IgG_1 isotype control antibody did not have any significant effect on

HaCaT cells (C and D respectively). The data shown is the mean value of triplicate setups. Error bars represented ± SE. Statistical significance was done by Student's t-test; * indicates p-value < 0.05.

3.2.2.4 HaCaT cells supplemented with CXCL11 peptide still exhibited a reduced cell survival rate with CXCR3 blockade

Suppression of CXCR3 signaling in the presence of 10 nM recombinant CXCL11 as an exogenous stimulator was examined; the y-axis of the graphs represents the mean percentage of three individual experiments. By 72 hours, cells in the CXCL11 peptide-only setup had substantially greater cell proliferation (366.3 %) as compared to 100 µg/mL CXCR3 neutralizing antibody plus CXCL11-treated cells (169.4 %) (Figure 3.19A). However, significant increase in cell death was only observed up to 48 hours, where the dead cell proportion in the antibody/peptide treated cell cultures was 7.6 % in comparison to 1.4 % for cells treated with CXCL11 only (Figure 3.19B). Treatments with mouse IgG_1 isotype control antibody plus CXCL11 peptide did not lead to significant difference in cell proliferation and death percentages among the different setups of each time-point study (Figures 3.19C and D).

HaCaT cells cultured with CXCL11 peptide plus anti-CXCR3 antibody for 72 hours were propagated with complete growth medium and 10 nM recombinant CXCL11 only to study recovery efficacy. HaCaT cells with previous CXCR3 antibody exposure were not able to fully recover (Figures 3.19E and F). At 72 hours, HaCaT cells without previous CXCR3 blockade showed significantly higher growth rates (260.7 %) and lower death percentages (1.9 %) (Figures 3.19 E and F respectively) than cells previously treated with the neutralizing antibody (204.4 % and 3.7 % respectively for 100 µg/mL CXCR3 antibody treated cells).

Figure 3.19 Treatment of anti-CXCR3 plus CXCL11 supplementation on HaCaT cells

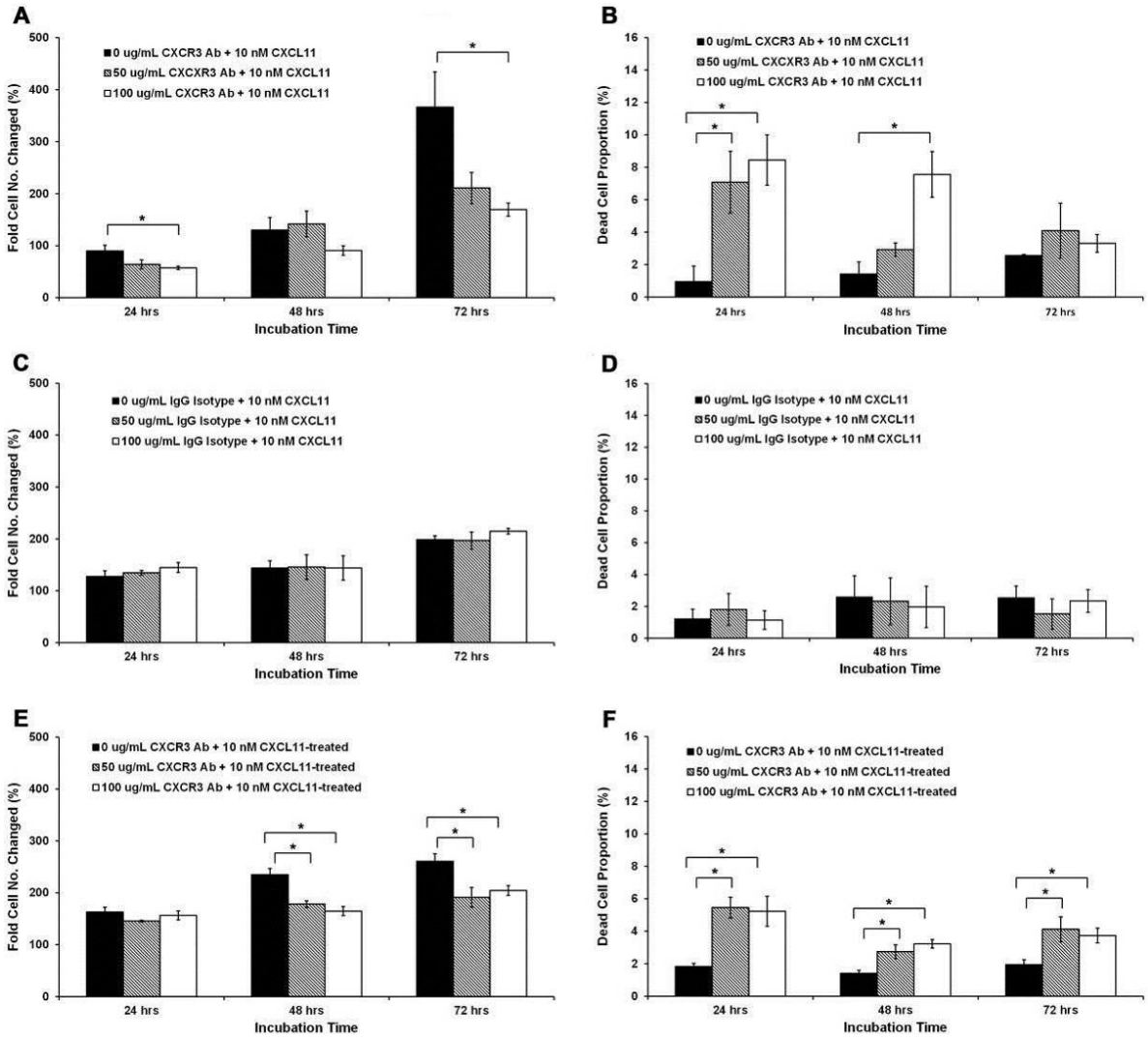

Cell proliferation rates and dead cell proportions were measured as per Figure 2.18. CXCR3 neutralizing antibody plus CXCL11 peptide led to reduced cell growth rates and enhanced dead cell percentages (A and B respectively). HaCaT cells under recovery, after neutralizing antibody removal and with CXCL11 supplementation, exhibited reduced cell growth and increased cell death (E and F respectively). IgG_1 isotype control antibody plus recombinant CXCL11 did not have any impact on HaCaT cell growth or death (C and D respectively).

Each treatment setup was conducted in triplicate. Error bars represented ± SE. Statistical significance was done by Student's t-test, and * indicates p-value < 0.05.

3.2.2.5 HaCaT cells migrated and invaded towards CXCL11 peptide in a dose-dependent manner

The y-axis of the graphs represents the mean percentage of cell motility of three individual experiments. The percentages of HaCaT cell population migration and invasion increased as the concentration of CXCL11 peptide increased (Figures 3.20A and B). 10 nM- and 20 nM-CXCL11 yielded 58.55 % and 73.12 % cell migration respectively and 57.95 % and 58.03 % cell invasion respectively, which were all significantly higher than untreated controls (migration: 44 %; invasion: 40.44 %).

Figure 3.20 Migration and invasion assays of HaCaT cells in response to CXCL11 peptide

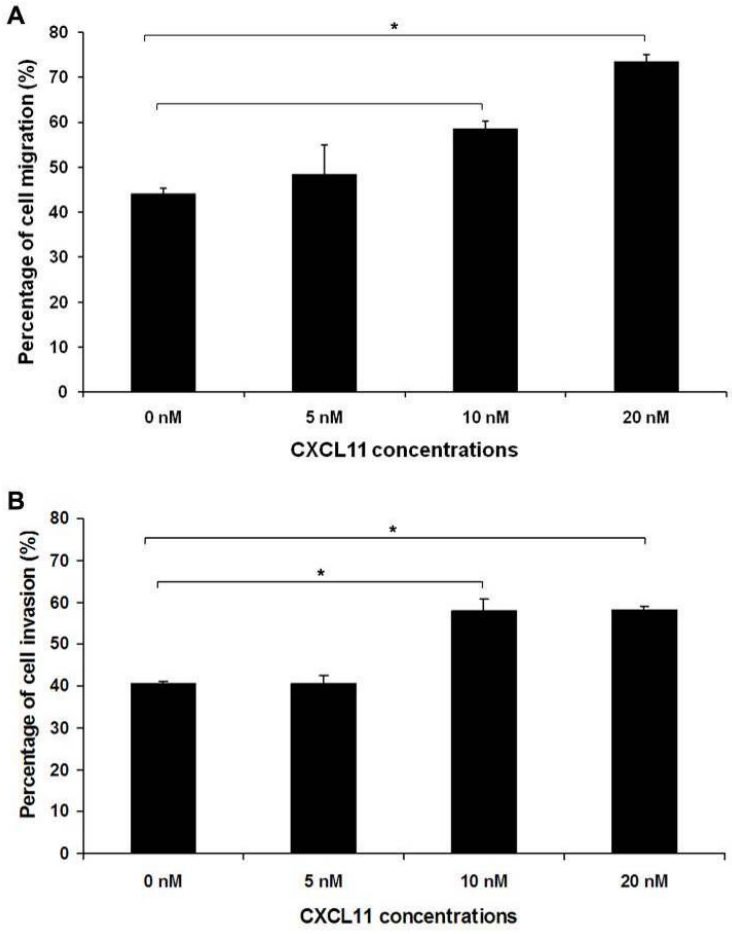

HaCaT cells were seeded in Transwell culture chambers or Boyden chambers for migration (A) and invasion (B) studies respectively. Various concentrations of CXCL11 peptide were applied to the lower compartments of the chambers. The percentages of cells transmigrated to the lower side of the insert membranes were calculated. HaCaT cells migrated and invaded towards recombinant CXCL11 in a dose-dependent manner (A and B respectively). Each treatment setup was conducted in triplicate, and the mean value was presented. Error bars represented ± SE. Statistical significance was done by Student's t-test and * indicates p-value < 0.05.

3.2.2.6 CXCL11 supplementation did not have significant impact on *MMP* expressions in HaCaT cells

HaCaT cells were treated with increasing concentrations of CXCL11 peptide for 48 hours; both technical and biological replicates were done in triplicate. The expression levels of *MMP1*, *2*, *3* and *9* were evaluated by qPCR. Cells without any peptide treatment were used as controls. *MMP1* was significantly upregulated (2.5-fold) in HaCaT cells only under the 10 nM CXCL11 treatment as compared to the untreated cells (Figure 3.21). Other than that, CXCL11 supplementation led to insignificant differential expression of *MMP1*, *2*, *3* and *9* in the cells.

Figure 3.21 Expression of *MMPs* in CXCL11-treated HaCaT cells

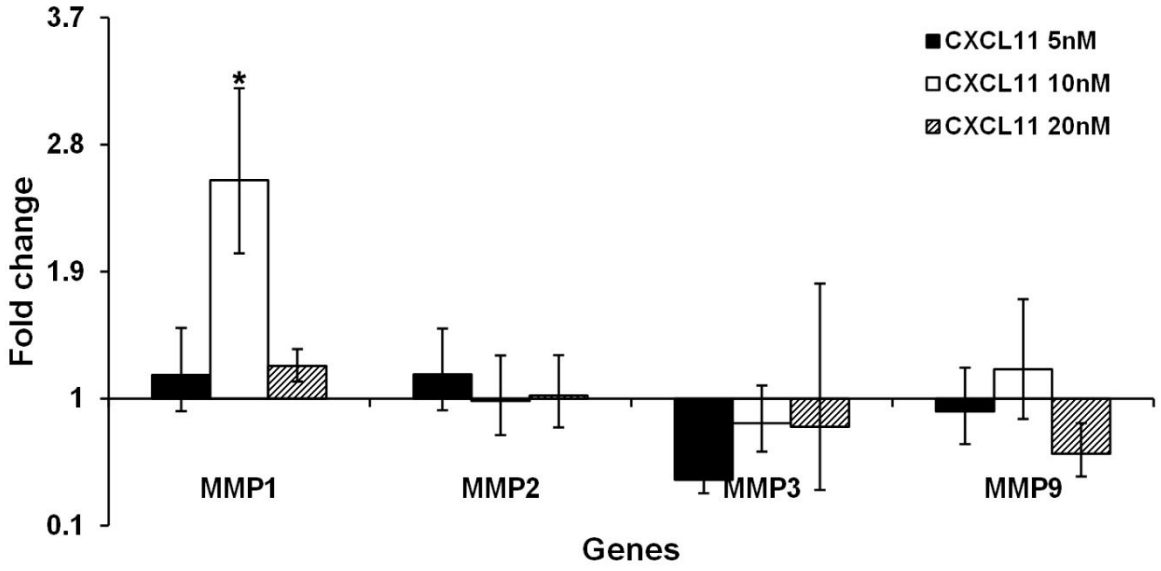

HaCaT cells were treated with 0 nM, 5 nM, 10 nM and 20 nM CXCL11 peptide for 48 hours prior to analysis. The expression of *MMP1*, *2*, *3* and *9* of the treated cells were evaluated by qPCR as compared to the untreated cell control. The gene expression level was presented as fold change using the equation $2^{-\Delta\Delta Ct}$. The y-axis represents the mean value of 3 individual experiments. Error bar represents the range difference of fold change ($2^{-\Delta\Delta Ct - \Delta Ct\ SE}$ and $2^{-\Delta\Delta Ct + \Delta Ct\ SE}$). Statistical significance was measured by Student's t-test; p-value <0.05 is indicated as *.

3.2.3 Discussion

3.2.3.1 The expression of *CXCR3* and other chemokines was associated with the aggressiveness of epithelial tumors

The CXC chemokine subgroup includes numerous ligands (Vandercappellen *et al.*, 2008). The binding of the chemokines to their respective receptors activates cell signal transduction and actin reorganization leading to cellular locomotion (Luster, 1998; Miekus *et al.*; Monteagudo *et al.*, 2007), a criterion for cancer growth. SCC and AK tissues demonstrated upregulation of expression for all chemokines tested whereas BD, nodular BCC and SK exhibited downregulation of some genes. This is consistent with the relatively benign and less invasive characteristics of these lesions.

Previous studies have found IL8 is an autocrine growth factor and potent angiogenesis promoter in many tumors such as bronchogenic carcinoma and melanoma (Huang *et al.*, 2002; Smith *et al.*, 1994). In our study, *IL8* was most upregulated in SCC, consistent with the angiogenic and metastatic behaviour of SCC. For other chemokines, CXCR4 and CXCL12 have been shown to be involved in migration and metastasis in various cancers, including head and neck SCC (Basile *et al.*, 2008; Katayama *et al.*, 2005; Ueda *et al.*, 2010). Our qPCR results confirmed that these two genes were significantly upregulated in SCC. Our data also revealed that AK had significant upregulation of *CXCR4* as well as its ligand *CXCL12*, which implied that AK had a potential aggressive capability and may be more likely to transform to SCC as compared to the other non-melanoma skin lesions.

3.2.3.2 Malignant keratinocytes, especially in SCC tumors, synthesized CXCR3

In a direct comparison between non-melanoma skin lesions, our results demonstrated that SCC had the strongest upregulation in *CXCR3* and its ligands followed by AK, BD, nodular BCC and SK. From our previous study indicating CXCR3 ligands enhance BCC cell growth in a dose-dependent manner (Lo *et al.*, 2010), CXCR3 ligands may be active in promoting keratinocyte skin lesion formation and growth, but they may be relatively more important for SCC, AK, and BD as compared to SK.

CXCR3 signalling has been shown to be involved in the progression or metastasis of melanoma, colon cancer, and ovarian carcinoma (Furuya *et al.*, 2007; Kawada *et al.*, 2007; Kawada *et al.*, 2004). K13 is normally expressed in the internal epithelia but not in the normal epidermis of the skin (Gimenez-Conti *et al.*, 1990). In cutaneous human SCC, however, K13 is expressed by the tumor keratinocytes (Commandeur *et al.*, 2009; Hudson *et al.*, 2010). K13 localization has also been shown to be a specific SCC keratinocyte marker in mouse skin cancer models (Aoyagi *et al.*, 2008; Commandeur *et al.*, 2009; Nischt *et al.*, 1988; Rundhaug *et al.*, 1997; Slaga *et al.*, 1995). In the present study, immunohistology revealed that most $K13^+$ SCC keratinocytes expressed CXCR3. Potentially, CXCR3 ligands can promote SCC cell proliferation and motility similar to that observed for BCC (Chapter 2A) (Lo *et al.*, 2010).

In addition, our IHC showed that CXCR3 was detected in the cornified layer of the epidermis of SCC biopsies, which might be due to non-specific labeling. Previous publications have shown that besides its consistent expression in cutaneous SCC, K13 localization present in the suprabasal layer has been shown to be a marker of malignant conversion (Aoyagi *et al.*, 2008; Commandeur *et al.*, 2009; Nischt *et al.*, 1988). These

observations are further supported by our data that K13 was expressed by all SCC keratinocytes and was also detected in the suprabasal layer of the epidermis in the tumor biopsies.

3.2.3.3 HaCaT cells as an *in vitro* model of epithelial keratinocyte tumors

To study the impact of CXCR3 on neoplastic keratinocytes, *in vitro* functional experiments were conducted. The spontaneously immortalized human keratinocyte HaCaT cell line (Boukamp, 2005; Boukamp *et al.*, 1988) has been used as a model of neoplastic keratinocytes to study NMSC *in vitro* (Boukamp, 2005). HaCaT cells exhibit UV-specific mutation of both alleles of the *p53* gene (Boukamp *et al.*, 1988). Also, several chromosomal aberrations in HaCaT cells, such as loss of 3p and 9p, where senescence genes resided (Mueller *et al.*, 2001), as well as gain of 3q, are characteristically found in SCCs (Boukamp, 2005; Boukamp *et al.*, 1997). As such, this cell line has been utilized as a model to study the functions and effects of over-expression or suppression of certain genes in skin cancer *in vitro* (Boukamp, 2005). In addition, transfection of the *Harvey*-ras oncogene in HaCaT cells followed by subcutaneous injection into mouse models resulted in *in vivo* metastatic SCC conversion (Mueller *et al.*, 2001). We have previously shown that CXCR3 enhanced proliferation of both primary BCC cells and HaCaT cells with the latter responded faster (Lo *et al.*, 2010). Here, we investigated the impact of CXCR3 on the neoplastic migration and invasion characteristics of HaCaT cells. Also, we studied the impact of the loss of CXCR3 signaling on HaCaT cells.

3.2.3.4 CXCR3/CXCL11 induced migration and invasion of HaCaT cells

Satish L *et al.* used scratch assays and showed that HaCaT cells at the edges of the wound migrated when culturing with CXCL11 peptide (Satish *et al.*, 2005). However, such experimental setup might be limited by several drawbacks. For instance, the shape and size of the scratches might be varied among different wells of the multi-well plate within the same experiment and the induction of wounds by scratching might damage cells at the edges (Hulkower and Herber, 2011). In our study, we used Transwell culture chambers and Boyden chambers to conduct migration and invasion assays respectively in a three dimensional basis, which allowed for more accurate evaluation and prediction of cell motility *in vivo* (Hulkower and Herber, 2011). Furthermore, the filter membrane of Boyden chambers was coated with matrigel matrix, as a closer representation of physiological conditions (Hulkower and Herber, 2011). The immortalized keratinocytes showed significant increases in migration and invasion in a dose dependent manner in response to CXCL11 peptide. The results imply that CXCR3/CXCL11 may be involved in neoplastic keratinocyte migration and invasion, which may contribute to the aggressive characteristics of SCC.

As mentioned earlier, CXCR3 signaling has been shown to be associated with cancer cell migration and invasion through the regulation of MMP expression, for example, in osteosarcoma and breast cancer (Pradelli *et al.*, 2009; Shin *et al.*, 2010). In this study, the effects of CXCL11 on the expression of *MMPs* in neoplastic keratinocytes, HaCaT cells, were examined. Similar to BCC keratinocytes (Sections 3.1.2.10 and 3.1.3.9), CXCR3/CXCL11 signaling did not cause any substantial impact on *MMP* expression in HaCaT cells even though the invasion rate of HaCaT cells was much higher than that of BCC cells under CXCL11 stimuli. The data provide further evidence that MMP1, 2, 3 and 9 might

not be involved in CXCR3-induced cell motility of keratinocyte tumors, such as BCC (Chapter 3A) and SCC. Further studies will be required to investigate the mechanism of CXCR3/CXCL11-induced migration and invasion of HaCaT cells.

3.2.3.5 CXCR3 signaling was important for supporting cell survival and preventing cell death of HaCaT cells

Our results revealed that HaCaT cells treated with CXCR3 neutralizing antibody had lower cell growth rates and higher death rates compared to untreated controls. In the recovery study when the chemokine receptor inhibition was removed, those cells previously exposed to anti-CXCR3 antibody were not able to recover their full proliferative capacity and survival. Further studies were conducted to determine whether exogenous CXCL11 supplementation would be required to support cell recovery. Treating HaCaT cells with recombinant CXCL11 plus anti-CXCR3 yielded similar effects on cell growth and death rates as treatment with CXCR3 neutralizing antibody alone, but to a lesser extent. Such observations suggest that enhancement of CXCR3 signaling with exogenous CXCL11 supplementation may partially counter the effects of CXCR3 blockade. However, in the subsequent recovery studies, cells previously exposed to antibody treatment could not fully restore their cell growth rate and survival to the pre-treatment levels even when they were stimulated with CXCL11 peptide. One of the possibilities is that since HaCaT cells express CXCR3 and ligands (Lo *et al.*, 2010), in addition to CXCL11, signaling from CXCL9 and/or CXCL10 binding to CXCR3, or other modulator proteins, may be required to augment the effects of CXCR3 during neoplastic keratinocyte growth. Another possible reason is that the

impact of CXCR3 neutralization may be so severe that prolonged suppression of the signaling pathway (> 72 hours) may lead to irreversible damage to the keratinocytes *in vitro*.

3.2.4 Conclusion

Taken together, CXCR3/ligand signaling may be essential for cell proliferation, survival, and invasion of neoplastic keratinocytes. Development of treatments for the blockade of CXCR3 or its chemokine ligands may be effective for non-melanoma skin diseases including cutaneous SCC.

Chapter 4. Basal cell carcinoma expresses immune privilege-associated genes partly due to CXCR3 signaling

4.1 Introduction

4.1.1 Background

Since basal cell carcinoma (BCC) is the most prevalent form of cancer worldwide (Kyrgidis *et al.*, 2010), using BCC as a model to study the mechanism of immunosuppression utilized by tumor cells could potentially be of great significance in understanding the pathogenesis of carcinomas. Many cancer cells may express factors that confer resistance to inflammatory cell mediated activity and may actively suppress immune targeting mechanisms. Local immunoprotective mechanisms have been associated with BCC initiation and progression (Kaur *et al.*, 2006; Walling *et al.*, 2004). However, genetic associations and signaling pathways that confer potential immune privilege in BCC are still not known.

4.1.2 Immune privilege

Immune privilege (IP) is a mechanism that protects specific sites from host immune responses to foreign antigen via releasable cytokines and other factors from immunoregulation-associated cells (Meyer *et al.*, 2008; Wahl *et al.*, 2006). Classical IP sites of the body include the anterior eye chamber, brain, testicles, placenta, the fetus and anagen stage hair follicles (Arck *et al.*, 2008; Fijak *et al.*, 2011; Niederkorn, 2003; Weetman, 1999). IP can be characterized by very low expression of major histocompatibility complex class I (MHC-I) molecules, downregulation of MHC-II-dependent antigen presentation, production

of immunoregulatory agents such as indoleamine 2,3-dioxygeanse and cluster of differentiation 200, and absence of lymphatics (Meyer *et al.*, 2008).

4.1.3 Indoleamine 2,3-dioxygenase

Indoleamine 2,3-dioxygenase (IDO) is a cytosolic heme-containing enzyme that catalyzes the catabolism of molecules consisting of an indole ring, such as tryptophan (Taylor and Feng, 1991). IDO catalyzes the initial rate-limiting step of the catabolism of tryptophan, which is a rare essential amino acid, and results in the production of L-kynurenine (Fallarino *et al.*, 2002). It was initially identified as an inhibitor of tryptophan-dependent microorganism growth, such as streptococci and staphylococci (MacKenzie *et al.*, 1999).

Expression of IDO can be induced by inflammation, wound healing, and tumor growth (Forouzandeh *et al.*, 2008; Li *et al.*, 2006; Sun *et al.*, 2010). The most potent inducer of IDO is interferon-γ (Lob *et al.*, 2009), which elicits the gene expression in immune cells, including activated dendritic cells, as well as epithelial cells and fibroblasts (Terness *et al.*, 2002). Other mediators of the protein expression include lipopolysaccharide, tumor-necrosis factor-α and toll-like receptor ligands (Braun *et al.*, 2005; Fujigaki *et al.*, 2001; von Bubnoff *et al.*, 2003; Wingender *et al.*, 2006). In addition, regulatory T cells (Tregs) have been shown to induce IDO expression in dendritic cells (DCs) upon binding of cytotoxic T lymphocyte-associated antigen 4 (CTLA4) expressed on Tregs and CD80/CD86 on DCs (Beissert *et al.*, 2006). Also, Sharma and colleagues demonstrated that plasmacytoid DCs from mouse tumor-draining lymph nodes expressed IDO, which activated resting $CD4^+/CD25^+/Foxp3^+$ Tregs and led to inhibition of antigen-specific T cells (Sharma *et al.*, 2007). IDO is expressed by

many cell types, such as fibroblasts, macrophages, and DCs, to suppress cytotoxic activities, enhance immune suppression and maintain peripheral tolerance in healthy organisms (Carlin *et al.*, 1989; Dai and Gupta, 1990; Hwu *et al.*, 2000; Mahnke *et al.*, 2007; Pradier *et al.*, 2010).

Furthermore, IDO has been shown to have immunosuppressive activity in cancers (Huang *et al.*, 2010). Uttenhov and colleagues detected IDO at both mRNA and protein levels in many tumor tissues, for example; colorectal carcinomas, pancreatic carcinomas and endometrical carcinomas (Uyttenhove *et al.*, 2003). The data suggest that IDO might play a role in enhancing tumor development (Uyttenhove *et al.*, 2003). The local depletion of tryptophan in the tumor microenvironments could suppress DNA synthesis and division of T cells. IDO may also reduce inflammation, and enhance Fas-mediated T-cell apoptosis via tryptophan degradation products (Fallarino *et al.*, 2002).

4.1.4 Cluster of differentiation 200

Cluster of differentiation 200 (CD200) and its receptor, CD200R are transmembrane glycoproteins and belong to the immunoglobulin superfamily (Cherwinski *et al.*, 2005). CD200, formerly known as OX-2, is expressed by cells from both hemopoietic and non-hemopoietic origins such as some T cells and B cells, dendritic cells, and Langerhans cells. In addition, keratinocytes that mainly comprise the hair follicle outer root sheath and bulge, neurons of central nervous system and retina, cells of degenerating ovarian follicles, cells of glomeruli and cells of the syncytiotrophoblast are all known producers of CD200 (Abid *et al.*, 2010; Cherwinski *et al.*, 2005; Fallarino *et al.*, 2004; Meyer *et al.*, 2008). The expression of CD200R, on the other hand, is restricted to leukocytes including some T cells and B cells,

dendritic cells, macrophages, mast cells, neutrophils and basophils (Berger *et al.*, 1998). In the epidermis, CD200R is detected in Langerhans cells and dendritic epidermal T cells in mice (Schatton and Frank, 2009). It has been shown that binding of CD200 with CD200R causes immunoregulation of $CD200R^+$ cells, in which inflammatory and cell-mediated immune responses are attenuated (Cherwinski *et al.*, 2005). For instance, CD200R has been shown to be an inhibitory receptor on mast cells that suppresses degranulation upon CD200 binding (Cherwinski *et al.*, 2005). Also, CD200/CD200R ligation has been shown to prevent proliferation and cytokine secretion of dendritic epidermal T cells (Rosenblum *et al.*, 2005). In fact, it has been demonstrated that ligation of CD200 to CD200R on murine plasmacytoid DCs causes the expression of IDO and subsequently inhibits T cells; these IDO^+ DC may also stimulate activation of Tregs as mentioned above (Fallarino *et al.*, 2004; Sharma *et al.*, 2007).

4.1.5 Rationale

Based on our previous microarray results (Yu *et al.*, 2008) and qPCR screening of 27 immunoregulatory genes (Figure 1.4) (unpublished), *IDO* was significantly upregulated in human BCC tissues as compared to non-lesional skin epithelium samples. However, whether IP is functionally involved in BCC tumorigenesis is not known and the impact of IDO on BCC development has yet to be established.

Evidence has shown that certain cytokines and chemokines are involved in tumor growth and immunosuppression (Furuya *et al.*, 2007; Lo *et al.*, 2010). The chemokines CXCR3 and its ligands CXCL9, CXCL10 and CXCL11 are significantly upregulated in BCC

tissues (Lo *et al.*, 2010). Addition of CXCL11 to primary human BCC cell cultures results in increased numbers and enhanced homogeneity of BCC keratinocytes.

Here we hypothesized that expression of immunoregulation molecules was associated with BCC growth. We performed screening of a set of immune privilege-related genes in BCC and studied the protein localization for selected genes of interest in the tumor tissues. The data suggested that the immunoregulatory molecules, CD200 and CD200R might be involved in immunosuppression in BCC. Furthermore, we hypothesized that IDO was involved in the immunoprotection of BCCs and that CXCR3 signaling may facilitate this immunoprotection. We investigated the expression and function of IDO in human BCC tissues and cell culture systems. Our findings suggest that BCCs synthesize functional IDO stimulated in part by CXCR3 ligands. The local expression of IDO may be important for BCC development.

4.2 Results

4.2.1 Immunosuppressive gene profile in human BCC tissues

The expression of 36 immunosuppression-related genes in ten human nodular BCC tissues as compared to ten non-lesional skin epithelium samples was analyzed by qPCR. Among those, expression of 26 genes was significantly upregulated in BCC samples (Figure 4.1). The genes code for secretory factors, antigen presenting molecules, complement regulatory proteins and cell surface markers.

IDO2 was upregulated at the highest level (21.2-fold change) in BCC tissues followed by *IDO1* (9.5-fold change) (Figure 4.1A). Other secretory genes that had increased

expression included decoy receptor 3 (*DCR3* at 8.8-fold change), transforming growth factor β II (*TGFβII* at 5.5-fold change) and interleukin 10 (*IL10* at 3.3-fold change). Interestingly, the immunosuppressive agent, alpha-melanocyte stimulating hormone (*α-MSH*), was downregulated in the BCC tissues (0.5-fold change) (Figure 4.1A).

Almost all of the MHC-I- (e.g. *HLA-A*, also known as *MHC-IA*, at 3.9-fold change) and MHC-II-related genes (e.g. *HLA-DRβ1*, also known as *MHC-II DR beta 1*, at 3.4-fold change) were significantly upregulated in BCC (Figure 4.1C). Similarly, immunoregulatory associated MHC genes, such as MHC-I polypeptide-related sequence A (*MICA* at 3.4-fold change), *MICB* (10.1-fold change) and *HLA-E* (1.8-fold change) were upregulated (Figure 4.1C). Also, beta-2 microglobulin (β_2M), which is a component of MHC-I, demonstrated a substantially increased expression in BCC at 2.4-fold change (Figure 4.1C).

Among the cell surface markers, *CD80* was expressed at the highest level at 5.8-fold change in BCC followed by *CD200* and *CD200R* (5.0- and 2.1-fold change respectively) (Figure 4.1D). Also, *Fas* was significantly downregulated in BCC (0.3 fold-change). For complement regulatory proteins, only *CD46* was significantly upregulated at 1.9-fold change (Figure 4.1B).

Figure 4.1 Expression of immunoregulation-associated genes in BCC

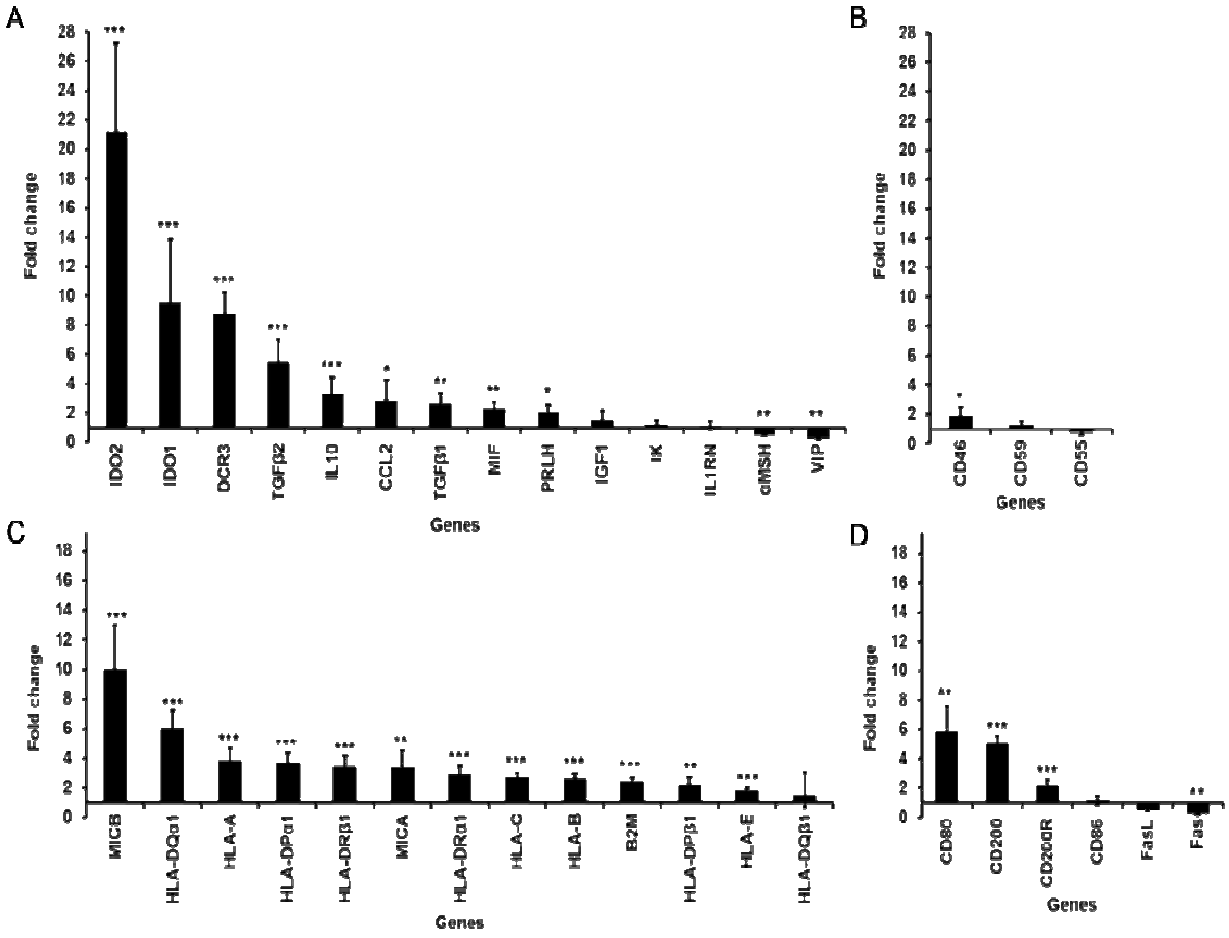

Tissue samples of nodular BCC (n = 10) were analyzed by qPCR. The expression level for each gene was compared to NL tissues (n = 10), and was presented as fold change using the equation $2^{-\Delta\Delta Ct}$. The gene profile was categorized as secretory factors (A), complement regulatory proteins (B), antigen presenting and/or processing molecules (C) and cell surface markers (D). Error bar represents the range difference of fold change ($2^{-\Delta\Delta Ct - \Delta Ct\ SE}$ and $2^{-\Delta\Delta Ct + \Delta Ct\ SE}$). Statistical significance was measured by Student's t-test; p-value <0.05 was indicated as *, <0.005 as **, <0.0005 as ***.

4.2.2 CD200 was mainly expressed by BCC keratinocytes while CD200R was expressed by $CD3^+$ or other stromal cell types

Dual labeling IHC was conducted to determine the cell types expressing CD200 and its receptor in three human nodular BCC biopsies. The data suggested that most of the CD200 expression was localized in $K17^+$ BCC keratinocytes in the tumor biopsies (Figure 4.2A). Interestingly, the expression level of K17 and CD200 was not consistent within the tumor masses; some regions of the tumors showed stronger labeling intensity of CD200 and lower expression of K17 (top right hand corner of the tumor) as compared to the others (left hand side of the tumor) (Figure 4.2A). CD200R, on the other hand, was not coexpressed with K17 (Figure 4.2B). Some CD200R labeling resided along the boundary of the tumor nests, which was probably due to non-specific binding to the basement membrane of the tumors (Figure 4.2B). Also, the majority of CD200R expression was localized in the stroma in the BCC biopsies (Figure 4.2B). A small set of $CD200R^+$ cells coexpressed CD3 (Figure 4.2C), but other $CD200R^+$ cells were $CD3^-$.

Figure 4.2 Dual labeling immunohistochemistry of CD200 and CD200R with K17 as well as CD200R with CD3 in human BCC tissues

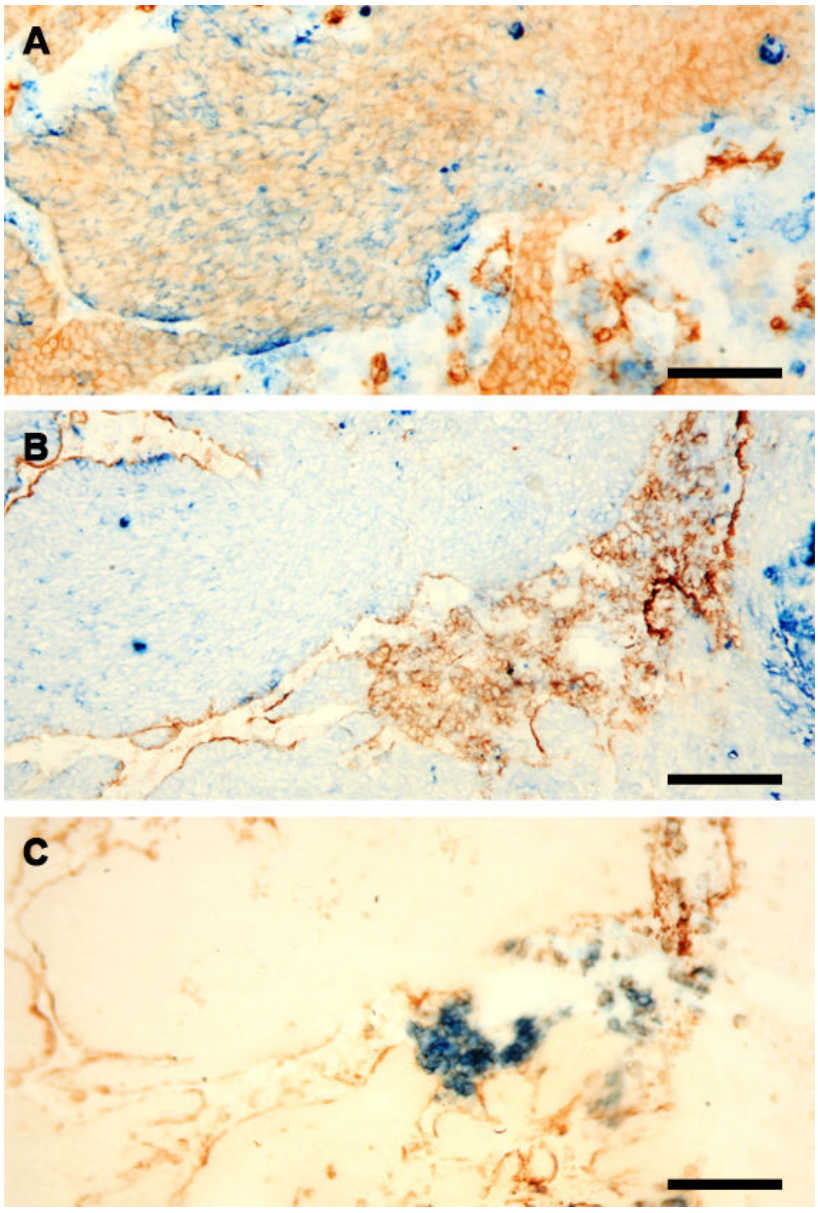

Human nodular BCC biopsies were analyzed for coexpression of K17 (blue) with CD200 (red) (A) and CD200R (red) (B) by dual labeling immunohistochemistry. The tumor tissues were also examined for the coexpression of CD200R (red) and CD3 (blue) (C). Scale bars = 80 μm (A – C).

4.2.3 *IDO1* and *2* expression levels were upregulated in human BCC tissues

In this qPCR analysis, hair follicle shaft and bulb tissues from 5 patient samples as well as 10 human nodular BCC and 10 non-lesional skin epithelium tissues, which were the same patient samples used in Section 4.2.1, were studied. The results revealed that the mRNA for *IDO1* and *2* were significantly increased in human nodular BCC tissues (9.5- and 21.2-fold change respectively) as compared to NL interfollicular tissues (Figure 4.3). In contrast, HF bulb tissues had substantially less expression of *IDO1* and *2* mRNA (0.29- and 0.28-fold change respectively) than normal interfollicular skin samples. In addition, HF shaft tissues had insignificant differential expression of these 2 genes.

Figure 4.3 Gene expression of *IDO1* and *2* in BCC, hair follicle bulb and shaft tissues

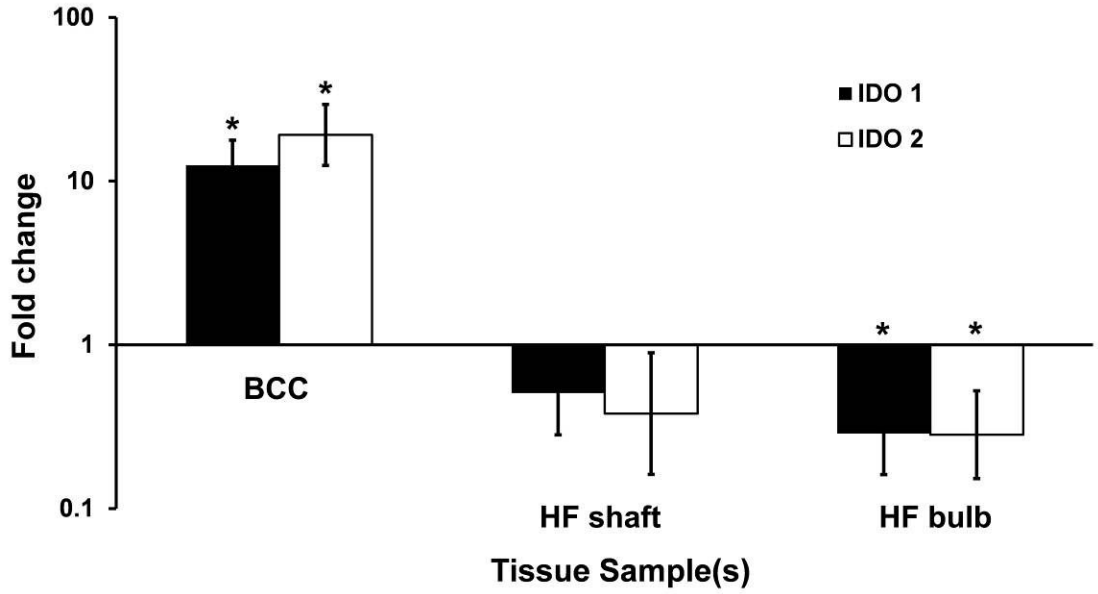

Human nodular BCC (n = 10), and normal hair follicles (HFs) (n = 5; 30 follicular bulb and shaft tissues from each sample) were studied. Non-lesional interfollicular skin epithelium tissues were used as controls. The expression levels were measured in terms of fold change using the $2^{-\Delta\Delta Ct}$ equation. Error bars represent the range factor difference ($2^{-\Delta\Delta Ct - \Delta Ct\ SE}$ and $2^{-\Delta\Delta Ct + \Delta Ct\ SE}$). Statistical significance was calculated by Student's t-test, and * indicates p-value < 0.05.

4.2.4 IDO was present in human BCC tumor masses and colocalized with K17

In three nodular BCC biopsies, IHC showed that positive staining of IDO was detected in tumor masses (Figure 4.4). To further verify the results, double label IHC of five nodular BCC tissues and five NL samples was conducted. The data indicated that IDO was co-expressed with K17 within the tumor nests. K17 was solely expressed by BCC cells with the tumor surface, especially the protruding peripheral regions, exhibiting higher staining intensity than the central tumor areas (Figures 4.5F - J). For IDO, the central areas of the tumor mass had higher labeling intensity than the peripheral regions (Figures 4.5F, H, I). Some weak staining of IDO was present in the stromal cells. For the NL biopsies, IDO was found in the HFs (Figures 4.5A – C), sebaceous glands (Figures 4.5A, D) and eccrine glands (Figures 4.5A, E); the localization of K17 was only found in or close to the stem cell bulge regions of HFs (Figures 4.5A, B, C). No specific co-expression of these 2 proteins was observed in the stroma of the biopsies.

Figure 4.4 Immunohistochemistry of IDO in human nodular BCC tissues

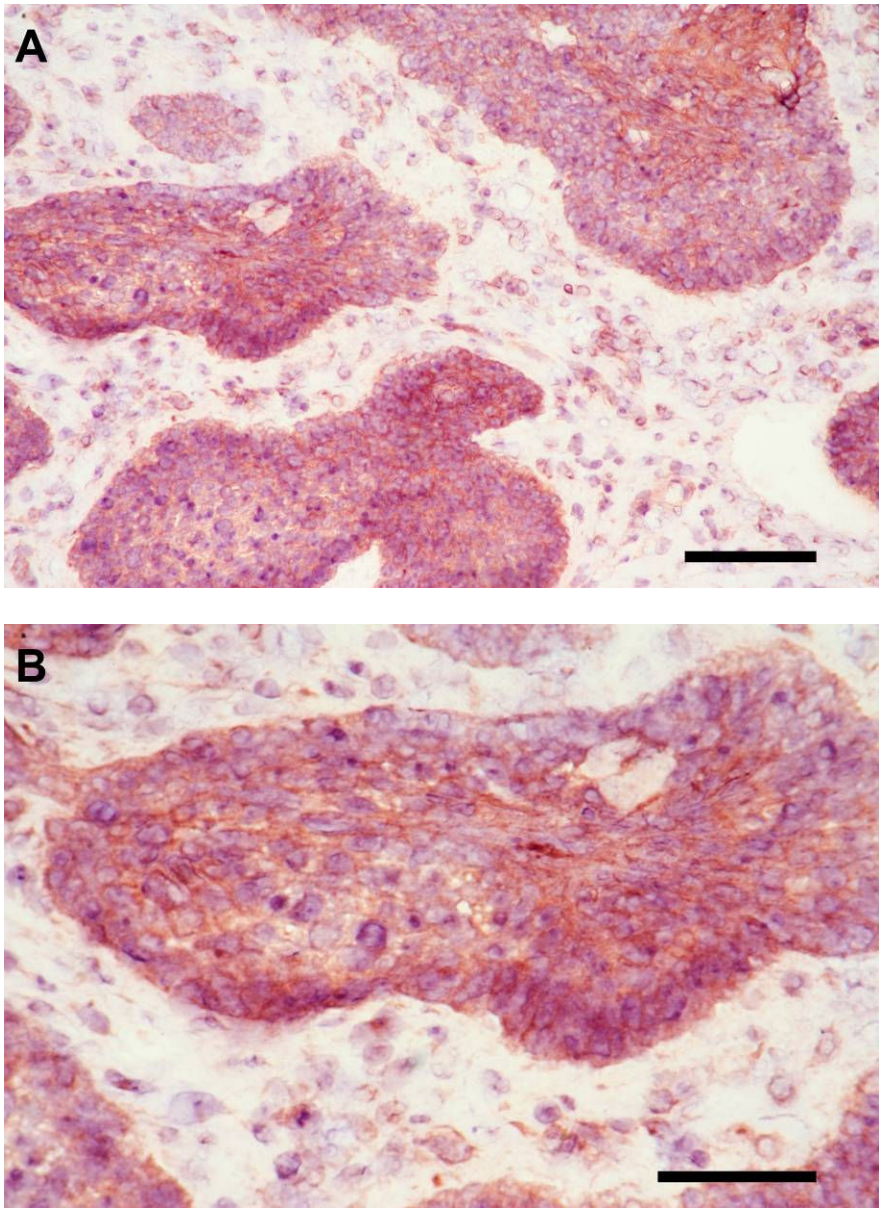

Cryosections of frozen nodular BCC biopsies were prepared (n = 3). The positive labeling of IDO is indicated as red. Hematoxylin was used for counterstaining. Representative photographic IHC images are shown. Expression of IDO was observed in the tumor nests. Scale bar equals 100 μm (A) and 60 μm (B).

Figure 4.5 Dual immunohistochemistry of K17 and IDO in nodular BCC and non-lesional skin epithelium tissues

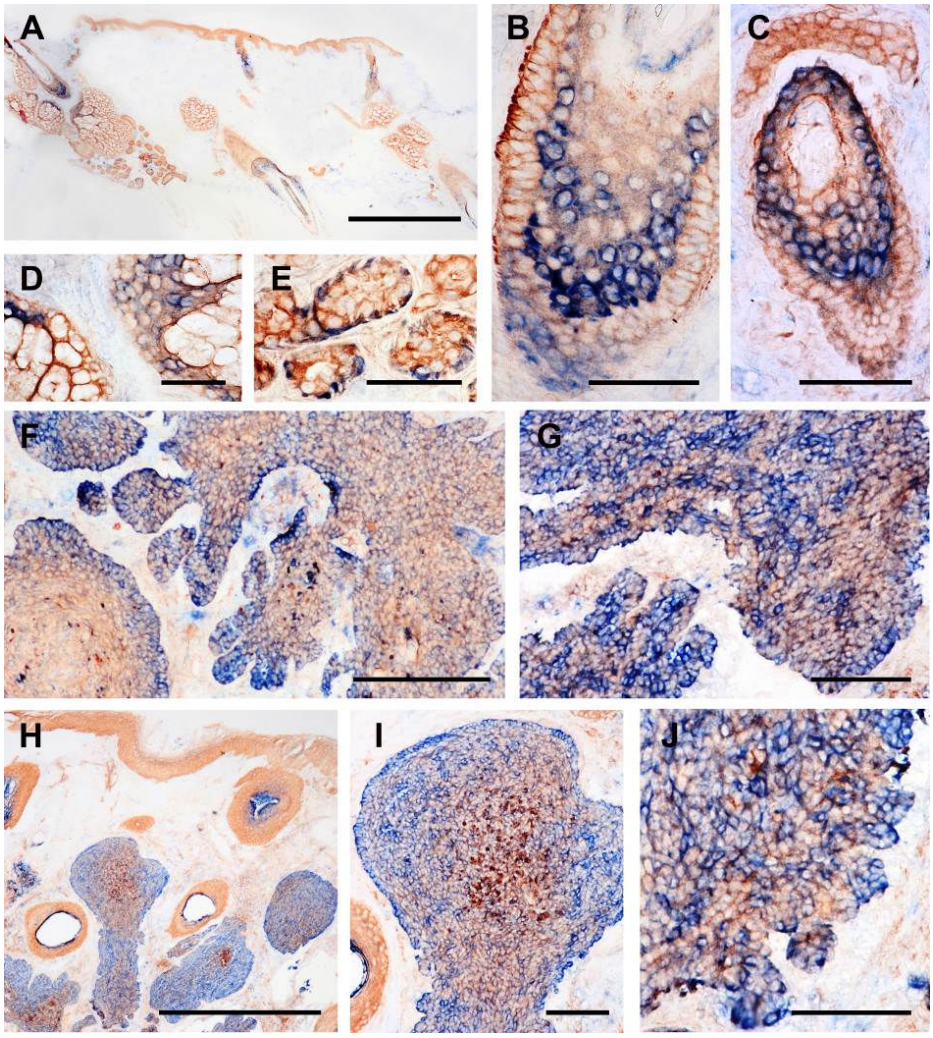

Cryosections of frozen non-lesional skin epithelium (NL) (A - E) and nodular BCC (F – J) biopsies were prepared (n = 5 for each tissue type). The co-expression of K17, which is indicated as blue, and IDO, which is indicated as red, was analyzed. Representative photographic IHC images are shown. Coexpression of K17 and IDO was observed in the tumor biopsies while no such specific labeling pattern was found in the NL tissues. Scale bar = 800 µm (A, H); scale bar = 200 µm (F); scale bar = 100 µm (G, I); scale bar = 80 µm (J); scale bar = 60 µm (B – E).

4.2.5 IDO and its splice variant were detected in human BCCs

Western blot analysis of IDO expression indicated that full-length IDO (42 kDa) was expressed in five nodular BCC and five morpheiform BCC, which is a more invasive subtype (Vargo, 2003; Wong *et al.*, 2003), whereas the five NL control samples had no or very weak expression of the protein (Figures 4.6). Notably, an IDO splice variant with protein size about 30 kDa was detected in both tumor and NL tissues with expression in morpheiform BCC at the highest level. This protein was generally expressed at a higher level than the 42 kDa band in the same respective tissue samples. The labeling of β-actin protein was used as an internal standardization to confirm equal amount of protein sample loading. The same results were obtained by replacing the polyclonal rabbit anti-human IDO antibody with the commercial monoclonal rabbit anti-human IDO antibody (data not shown).

Figure 4.6 Immunoblotting of IDO in BCC and non-lesional skin epithelium tissues

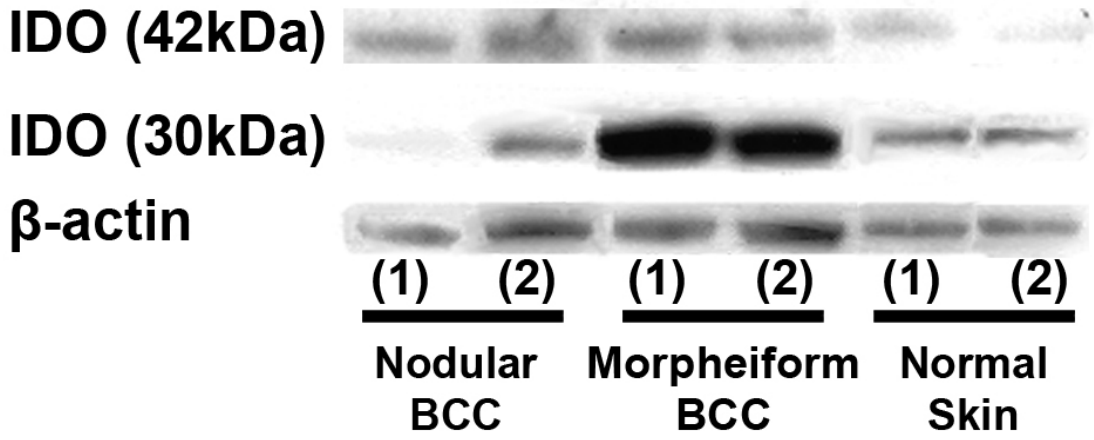

Protein extraction and Western blot analysis of IDO using nodular and morpheiform BCCs as well as non-lesional skin epithelium (NL) tissues were performed (n = 5 for each tissue type). The protein expression of IDO in the 2 random representative samples of each tissue type was shown. Immunolabeling of β-actin was used as loading control. The full-length IDO protein (42 kDa) was detected in BCC tissues as well as in NL samples with less labeling intensity. A splice variant form of IDO (~30 kDa) was found in all tissues, in which morpheiform BCCs showed the highest labeling level.

4.2.6 CXCL11 treatment did not enhance cell proliferation of normal human skin keratinocytes

Three BCC and three normal KC cell cultures were treated with different concentrations of CXCL11 peptide and were evaluated for their cell growth responses. As expected, BCC cell growth rates significantly increased under 10 nM and 20 nM CXCL11 dosage treatments (2.63- and 2.50-fold increase respectively) as compared to the untreated control (Figure 4.7A). Normal skin keratinocytes, on the other hand, did not have significantly increase in cell proliferation under the chemokine supplementation (Figure 4.7B).

Figure 4.7 Proliferation of primary human BCC cells and normal keratinocytes under CXCL11 treatment

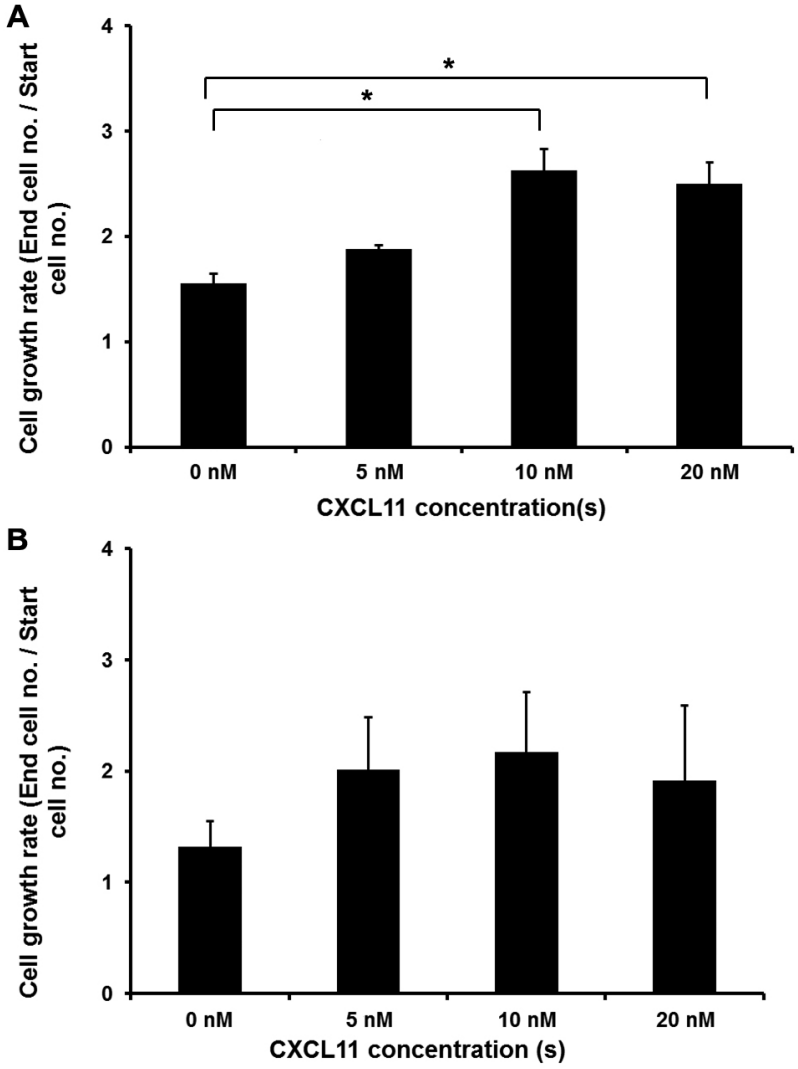

Human BCC-derived cells (n = 3) (A) and normal keratinocytes (n = 3) (B) were treated with CXCL11 peptide at various concentrations for 1 month. The cells were evaluated for cell growth rates by cell counting using the Trypan blue exclusion test. The y-axis represents the mean cell growth rate ± SE. The cells without any peptide treatment were used as control. Statistical analysis was done by Student's t-test. * indicates p-value < 0.05.

4.2.7 L-kynurenine was generated by human BCC cells under CXCL11 treatment but was not detected in normal primary human keratinocyte cell cultures

Primary cell cultures were obtained from three nodular BCC samples and three non-lesional skin tissues. When 5 nM CXCL11 peptide was added to the hBCC cell cultures, statistically insignificant reduction of kynurenine was observed compared to the untreated hBCC cell culture (Figures 4.8A). However, hBCCs exposed to 10 nM and 20 nM CXCL11 exhibited statistically significant increases in kynurenine synthesis (0.14 µg and 0.15 µg per 10,000 cells respectively). This confirmed the functionality of human BCC-synthesized IDO and the data indicates that increased IDO activity in BCC cells *in vitro* was obtained in response to CXCL11 supplementation in a dose-dependent manner.

Normal primary human KCs were also treated with CXCL11 peptide and assayed for tryptophan catabolism. Kynurenine assay data revealed that there was no significant induction of tryptophan degradation by normal KCs (Figure 4.8B).

Figure 4.8 Kynurenine assay of primary human BCC and normal keratinocyte cell cultures

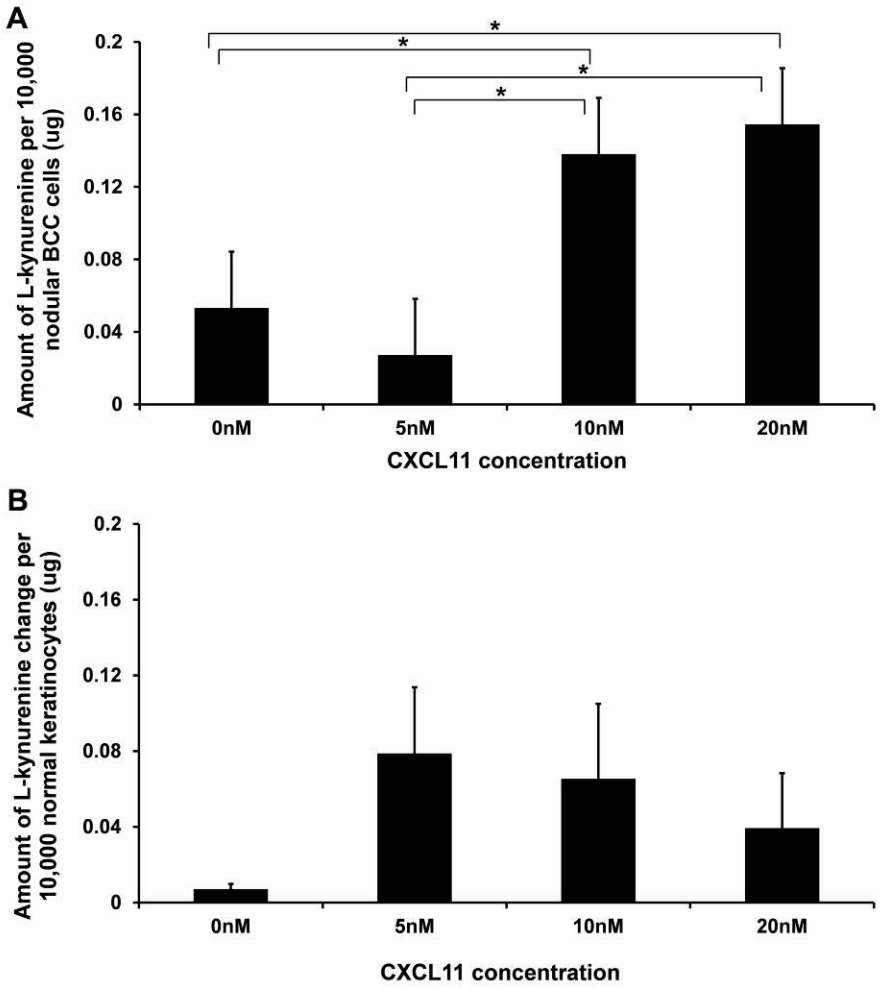

Primary human BCC cells (n = 3) (A) and normal keratinocytes (n = 3) (B) were treated with CXCL11 peptide at various concentrations for 1 month. The enzymatic activity of IDO in the cell cultures was tested by measuring the amount of kynurenine being produced from tryptophan catabolism. The y-intercept represents values of kynurenine increased in each treatment as compared to that in fresh media. Statistical analysis was done by ANOVA. * indicates p-value < 0.05.

4.2.8 CXCL11 treatment led to significant upregulation of *IDO2* expression in BCC cells but not in normal keratinocyte cell cultures

The CXCL11-treated hBCC and normal KC cells in the kynurenine assay were further evaluated for *IDO1* and *IDO2* expression by qPCR. For hBCC cell culture, *IDO1* expression was statistically insignificantly reduced in 5 nM, 10 nM and 20 nM treatments (0.51-, 0.53- and 0.26-fold change respectively) as compared to the untreated control (Figures 4.9A). On the other hand, *IDO2* expression was upregulated substantially at 9.85-, 28.15- and 35.81-fold under 5 nM, 10 nM and 20 nM CXCL11 treatments respectively in the hBCC cells compared to the 0 nM CXCL11 control (Figure 4.9A). For normal KC cell culture, no significant change of *IDO1* was observed with all CXCL11 treatments as compared to the untreated control (5 nM: 0.85-fold change; 10 nM: 0.84-fold change; 20 nM: 0.96-fold change) (Figure 4.9B). Normal KC cells expressed *IDO2* with a slight reduction after 5 nM CXCL11 exposure (0.78-fold change), and insignificant upregulation with 10nM and 20 nM peptide treatments (1.21- and 1.06-fold change) (Figure 4.9B).

Figure 4.9 Expression of mRNA for *IDO1* and *2* in CXCL11-treated human BCC and normal keratinocyte cell cultures

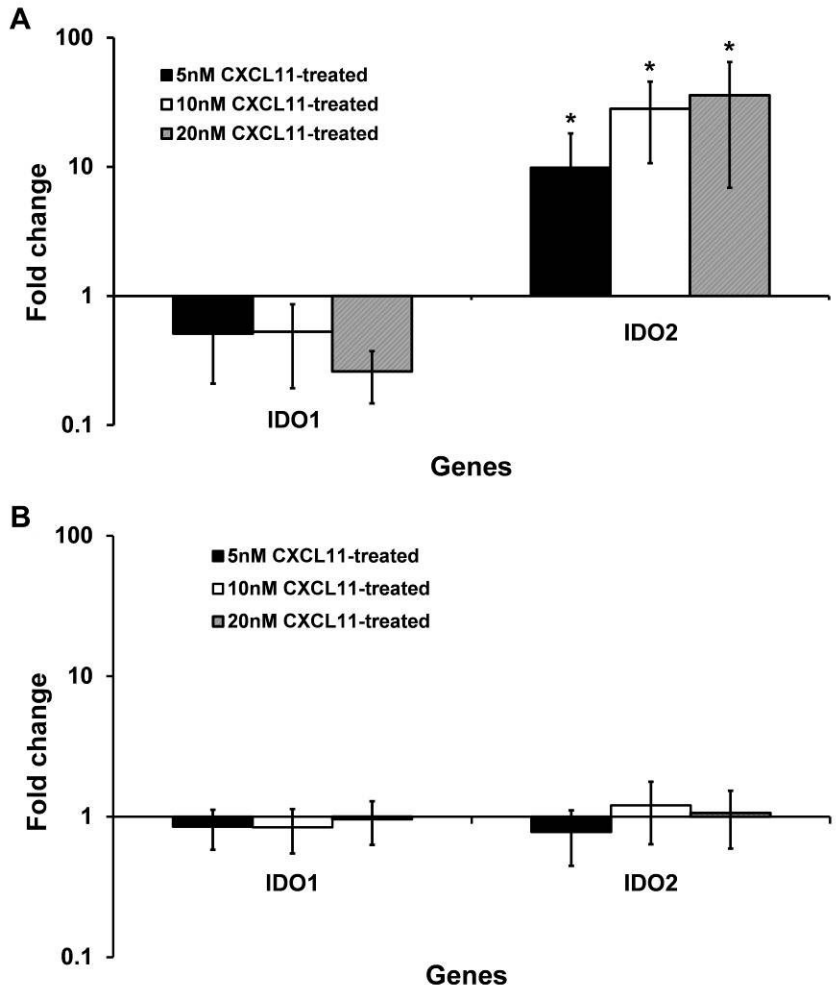

Primary human BCC cells (n = 3) (A) and normal keratinocytes (n = 3) (B) were supplemented with various concentrations of CXCL11 peptide for 1 month. Quantitative real-time RT-PCR was conducted to evaluate the gene expression of *IDO1* and *2* in the treated cells. The expression levels were measured in terms of fold change by using the $2^{-\Delta\Delta Ct}$ equation. Error bars represent the range factor difference ($2^{-\Delta\Delta Ct - \Delta Ct\ SE}$ and $2^{-\Delta\Delta Ct + \Delta Ct\ SE}$). Statistical significance was calculated by Student's t-test, and * indicates p-value < 0.05.

4.3 Discussion

4.3.1 Immune privilege gene profile in human nodular BCCs

IP has been indicated to be involved in the development of various cancers, such as malignant melanoma and colon adenocarcinoma (Berger *et al.*, 1998; Schatton and Frank, 2009). In BCC, an impaired host immune system is one of the major predisposing factors of the tumor growth (Madan *et al.*, 2010). Also, reduced expression of anti-apoptotic genes in T-cells of xeroderma pigmentosum patients is associated with the development of BCC (Abid *et al.*, 2010). As such, immunosuppression may be involved in BCC tumorigenesis as well.

Our gene screening data demonstrated that some immunosuppressive molecules might be associated with nodular BCC growth. For instance, expression of *DCR3* was upregulated and *Fas* was reduced in nodular BCC tissues as compared to non-lesional skin epithelium samples. DCR3 belongs to tumor necrosis factor receptor family. It competes with the death receptor, Fas, for its ligand, FasL, and in so doing helps prevent apoptosis of Fas^+ cells (Xiong *et al.*, 2011). Overexpression of DCR3 has been shown to be associated with the progression and metastasis of esophageal squamous cell carcinoma (Xiong *et al.*, 2011). The expression of *DCR3* and downregulation of *Fas* expression in BCC may increase resistance to inflammatory cell mediated pro-apoptotic signals. Further, *IL10*, an immunosuppressant which reduces T cell responses (Kim *et al.*, 1995; Meyer *et al.*, 2008), had substantially increased expression in BCCs in our study. Our data was consistent with a study done by Kim and colleagues, who showed that *IL10* was upregulated in BCC by RT-PCR and that IL10 was detected in the medium of cultured tumor tissue (Kim *et al.*, 1995).

Interestingly, our data revealed an overall upregulation of *MHC-I* and *MHC-II* genes in BCC tissues. Such observation is different from other IP sites, such as the hair follicle bulb, where MHC expression is curtailed. Also, Meyer and colleagues found that reduced protein expression of MHC-Ia, β_2M and MHC-II was present in the hair follicle bulge region (Meyer *et al.*, 2008). The data suggests that manipulation of the antigen processing and presenting molecules may not be an IP mechanism adopted by BCCs. Potentially, there may be increased antigen presentation on the surface of BCC cells.

Both *MICA* and *MICB* were also found to be upregulated in BCC. MICA and MICB are ligands of the natural killer group 2-receptor type D (NKG2D) expressed by natural killer cells, $CD8^+\alpha\beta$T cell and γδT (Bauer *et al.*, 1999; Kennedy *et al.*, 2002). Such ligation causes activation of the cytolytic response of the immune cells (Groh *et al.*, 1999). MICA and MICB are stress-inducible antigens which are closely related and functionally indistinguishable. Their expressions are restricted to intestinal epithelium in normal tissues (Bahram *et al.*, 1994; Bahram and Spies, 1996; Bauer *et al.*, 1999; Groh *et al.*, 1999). However, increased expression of these two molecules has been detected in various carcinomas such as lung, breast, ovary, prostate, kidney, and colon cancers (Groh *et al.*, 1999). The data suggest that MICA and MICB might act as tumor-associated antigens, where interaction with γδT cells might be involved in immune surveillance of those cancers (Groh *et al.*, 1999), which might happen in BCC as well.

HLA-E, on the other hand, is an immunosuppressor; it is a non-classical MHC-Ib molecule (Meyer *et al.*, 2008; Wei and Orr, 1990). In our study, expression of *HLA-E* was substantially increased in human nodular BCC tissues. Similarly, over-expression of HLA-E was detected in other malignancies such as melanoma and colon cancers (Bianchini *et al.*,

2006; Derre *et al.*, 2006) It has been shown that HLA-E binds with the inhibitory receptor, NKG2A on natural killer (NK) cells, $CD8^+$ αβT cells, and $CD8^+$ γδT cells; the interaction inhibits the immune response of NK cells and cytotoxic T cells (Braud *et al.*, 1998; Li *et al.*, 1996; Wischhusen *et al.*, 2007).

CD80 (B7-1) and CD86 (B7-2) are B lymphocyte activation antigens. They are known as B7 molecules and are under the immunoglobulin superfamily. They provide costimulatory or coinhibitory signals for T cells by binding with CD28 or cytotoxic T lymphocyte antigen 4 (CTLA4) respectively (Peach *et al.*, 1995; Seliger *et al.*, 2008). Nengwen and colleagues revealed that murine keratinocytes, which were isolated from neonatal skin tissues, had increased expression of CD80 in proportion to the time of culturing (Nengwen *et al.*, 2009). Also, they observed that only autologous keratinocytes were able to suppress T cell responses in an *in vitro* lymphocyte challenge assay while allogeneic keratinocytes stimulated T cell proliferation. They further demonstrated that the autologous keratinocyte-induced inhibition of T cells was due to the ligation of CD80 with CTLA4 expressed on T cells (Nengwen *et al.*, 2009). In my study, *CD80* was upregulated in nodular BCC tissues while *CD86* was not differentially expressed in the tumors. The results were consistent to a study conducted by Lei and colleagues, in which, CD80 was expressed by murine keratinocyte stem cells while CD86 was not detected in the cells (Lei *et al.*, 2005). Potentially, the *CD80* expression in the present study may contribute to immune suppression during the tumor growth by binding with CTLA4 expressed on T cells, by which cell proliferation may be inhibited.

4.3.2 BCC tumors expressed CD200 whereas the surrounding area contained CD200R$^+$ cells

Upregulation of *CD200* and *CD200R* in BCC tissues suggests that immune regulation may be involved in the tumor growth. However, since only cells bearing CD200R are affected by the signaling of CD200 ligation, defining the localization of CD200 and CD200R may allow for a better understanding of their roles in BCC. To accomplish that, dual immunohistochemistry labeling was used to determine the cell types expressing these two proteins. CD200 was found expressed in K17$^+$ BCC tumor masses. In addition, certain regions within the tumor masses showed stronger labeling intensity of CD200 than in other areas, which might mean CD200 expression masked the K17 marker on BCC cells at those sites. In contrast, the dual labeling results indicated that CD200R was not expressed by BCC cells but was mainly detected in stromal cells. As CD200R is expressed by various types of leukocytes (Rosenblum *et al.*, 2006), dual staining of CD200R and CD3 was conducted. Some CD200R$^+$ cells were positively labeled with CD3 as well, which suggested that those CD200R$^+$ T cells might be targets of immune suppression upon ligation of CD200 expressed by BCC cells. Those CD200R$^+$/CD3$^-$ cells in the stroma could be leukocytes such as dendritic cells and mast cells (Berger *et al.*, 1998). Their expression of CD200R may also result in alteration of their immune functions (Cherwinski *et al.*, 2005; Fallarino *et al.*, 2004). Overexpression of CD200 has been shown as a tumor promoting signal in various cancers, such as multiple myeloma, melanoma, and breast cancer (Gorczynski *et al.*, 2010; Moreaux *et al.*, 2006; Petermann *et al.*, 2007). Gorczynski and colleagues revealed that increased expression of CD200 in a mouse breast cancer cell line enhanced the tumor cell growth rate and metastasis (Gorczynski *et al.*, 2010). As such, CD200/CD200R may confer similar tumor

progression effects on BCC as on other cancers. However, further investigations will be needed to determine the functional impact of CD200 and its receptor for BCC IP.

4.3.3 Human nodular BCC tissues expressed *IDO1* and *IDO2*

Due to the fact that T cells are sensitive to tryptophan depletion, expression of IDO is also associated with immunosuppression and tumorigenesis (Munn *et al.*, 1999; Sun *et al.*, 2010; Uyttenhove *et al.*, 2003). In the current study, the mRNAs for *IDO1* and *IDO2* were both significantly upregulated in human nodular BCC tissues as compared to NL interfollicular skin tissues. The data suggests that BCC tumors may exhibit certain immunosuppression mechanisms via IDO activity for tumor progression. In contrast, the significantly lower mRNA expression for *IDO* in HF tissues as compared to NL interfollicular skin tissues implies that IDO may not be as essential in supporting the growth of HF as that of BCC.

4.3.4 Human nodular BCC keratinocytes synthesized IDO

IDO1 and IDO2 have been shown to promote immune tolerance to various types of tumors (Uyttenhove *et al.*, 2003; Witkiewicz *et al.*, 2009). Besides being involved in promoting T cell homeostasis and self-tolerance, IDO expression is detected in the placenta during pregnancy, possibly to prevent rejection of the allogenic fetus by maternal T cells (Fallarino *et al.*, 2002; Hwu *et al.*, 2000; Mellor and Munn, 1999; Munn *et al.*, 1999; Munn *et al.*, 1998). The detection of IDO protein in BCC biopsies as well as the co-expression of IDO with K17 in BCC tumor masses suggested that IDO was synthesized by BCC keratinocytes and might exert an immunosuppressive activity to support the tumor growth. In

addition, IDO expression was more prevalent in the tumors than in the stroma, suggesting the tumor cells produced and utilized IDO more efficiently than the infiltrating cells, and might suppress the immune system via IDO signaling. Consistent with a previous study (Meyer *et al.*, 2008), IDO protein localized in the HF outer root sheath in the normal skin biopsies by immunohistochemistry, however our qPCR data suggested hair follicles express relatively little *IDO* as compared to non-lesional interfollicular skin tissues.

4.3.5 CXCL11 induced functional IDO and its splice variants by human BCC cells

Human IDO1 and IDO2 share significant structural homology (43 %) (Ball *et al.*, 2009). Both genes are localized on the chromosome 8p arm where *IDO2* resides downstream of *IDO1* (Ball *et al.*, 2009; Metz *et al.*, 2007). Human IDO1 and IDO2 proteins are 403 and 420 amino acids respectively and genetic polymorphisms have been determined in both (Metz *et al.*, 2007). They have multiple promoter regions for their gene sequences and more than 1 splice variant has been identified (Ball *et al.*, 2009; Metz *et al.*, 2007). For instance, two of the IDO2 functional polymorphisms have been identified; R248W contains an altered essential amino acid and results in > 90 % reduction in the catalytic activity whereas Y359 STOP polymorphism expresses a premature stop codon and completely shuts down IDO2 activity (Hou *et al.*, 2007; Metz *et al.*, 2007; Witkiewicz *et al.*, 2009).

Here, Western blot suggested that an IDO splice variant was more abundant than the full-length IDO protein in most of the BCC tissues as well as in NL tissues. Notably, IDO was more highly expressed in morpheiform BCCs compared to nodular BCCs, possibly consistent with the more invasive/aggressive nature of the morpheiform subtype. The data elicited the question whether the IDO isoform was functional. In order to verify the

enzymatic activity of IDO, we measured the amount of L-kynurenine in the conditioned medium of cell cultures by colorimetric analysis. While there is the potential for IDO expression from non-tumor cells, such as inflammatory cells and fibroblasts, our previous studies indicated that culturing BCC-tissue derived cells with CXCL11 promoted a progressive population homogeneity such that by 21 days over 98 % of cells are $K17^+$ (Lo *et al.*, 2010). In this study, we cultured both BCCs and normal KCs for one month prior to use.

In the current study, significantly increased kynurenine was produced with 10 nM and 20 nM CXCL11 supplementation in the BCC cell culture. The data suggests that CXCL11 induces the tumor cells to synthesize functional IDO whether as an isoform or otherwise. The qPCR analysis revealed an upregulation of *IDO2* only in CXCL11-treated BCC cells while no such gene expression change was seen in the treated normal KCs. This provides further support that the chemokine signaling may play a role in the IDO immunosuppression mechanism and such signal transduction is specific for tumor keratinocytes only.

The qPCR result of *IDO1* and *IDO2* using human BCC tissue samples differed from that using the primary BCC cell culture. This may be due to the fact that the base line controls in the 2 experiments were different; the human BCC tissue study used NL skin epithelium tissues as the control while the *in vitro* study of CXCL11-treated hBCC cells used untreated BCC cells as the control. Furthermore, total RNA fresh human BCC tissues was extracted from cells including BCC keratinocytes as well as inflammatory cells and fibroblasts, which could affect *IDO* expression levels of the biopsies. In contrast, the *in vitro* experiment only tested BCC keratinocytes and the RNA extraction was from a single cell type only.

4.3.6 CXCL11 did not significantly promote cell proliferation and IDO enzymatic activity in normal human skin keratinocytes

CXCL11 supplementation did not have significant impact on normal skin keratinocytes, in terms of cell proliferation, in contrast to observations for immortalized keratinocyte HaCaT cells and human BCC cells (Chapter 3A) (Lo *et al.*, 2010). As expected, during the same experiments, primary BCC cells exhibited a significantly enhanced cell growth, which was consistent with our previous study (Lo *et al.*, 2010).

It has been shown that normal human KCs were able to express a low level of IDO at both transcription and translation levels with IFN-γ (von Bubnoff *et al.*, 2004). However, the induced IDO in the stimulated KCs was not able to carry out enzymatic activity (von Bubnoff *et al.*, 2004). Our results were largely consistent with such findings. In this study, unlike BCC keratinocytes, exposure of normal KCs to CXCL11 did not result in induction of tryptophan catabolism which confirms that no functional IDO was expressed by normal human KCs. QPCR analysis further revealed no significant change in *IDO1* or *IDO2* expression in the treated normal KCs with CXCR3 ligand exposure. It has been suggested that expression of IDO may not be correlated with its enzymatic activity. In fact, expression of functional IDO in cells is rare under normal conditions (Huang *et al.*, 2010). Various post-translational requirements are needed for activation of IDO; for instance, presence of enzyme co-factors such as hemin, sufficient redox potentials, and modification of IDO protein structure (Huang *et al.*, 2010). The lack of *IDO1* or *IDO2* upregulation, and the unresponsiveness in enzymatic activity of any normal human KC-produced IDO, may be due to a lack of cytokine activation or other signaling pathway interaction, e.g. CD200 (Fallarino *et al.*, 2004).

4.4 Conclusion

By summarizing the results obtained in these studies and other groups, it is evident that CD200/CD200R signaling may be involved in developing immunosuppression during BCC growth. Also, IDO may be one of the essential mediators for BCC progression. This mechanism may also be of significance in understanding immunoprotection in other keratinocyte carcinomas. As such, abrogation of IDO-induced immune tolerance via interference in CXCR3 signaling might be a novel treatment for BCC patients and potentially for other forms of cancer.

Chapter 5. Conclusions

5.1 Rationale of the thesis projects

The rapidly increasing incidence rate and high treatment costs of non-melanoma skin cancers (NMSCs) have raised the awareness and urge from the scientific community to seek strategies to improve current treatments and develop novel drug medications. Although medications targeting sonic hedgehog (SHH) signaling have been shown to cause regression of basal cell carcinoma (BCC) and prevent new tumor growth (Epstein, 2008; Iwasaki *et al.*, 2010), various side-effects have been observed in patients under the treatments as the SHH signaling pathway is important for tissue development and maintenance in healthy individuals (Amin *et al.*, 2010; Iwasaki *et al.*, 2010). The present studies tried to elucidate novel genes and the potential impacts of their activity on BCC and other NMSC growth. Such observations may shed light on novel targets for the development of new approaches to treat NMSCs.

5.2 Summary of findings

5.2.1 Role of CXCR3 signaling in cell growth and motility in BCC and other NMSCs

With the preliminary data from a microarray analysis and immunoregulatory related-gene profile screening by quantitative real-time RT-PCR (qPCR), the expression of the chemokine *CXCL11* was upregulated at the highest level followed by *CXCL9*, *CXCL10* and their receptor *CXCR3* in human BCC tissues using non-lesional skin epithelium samples as the control (Chapter 3A). By using dual staining immunohistochemistry (IHC) of cytokeratin

17 (K17), together with CXCR3 or its ligands in human BCC biopsies, CXCR3, CXCL10 and CXCL11 were shown to be mainly expressed by $K17^+$ BCC cells while CXCL9 was expressed by the stromal cells.

To pursue the study of CXCR3 functions in BCC, *in vitro* experiments were needed; however, there is no human BCC cell line commercially available and culturing primary human BCC cells has been previously reported as difficult (Brysk *et al.*, 1992). As CXCR3 and its ligands, especially CXCL11, seemed to be primarily expressed by BCC cells, we anticipated that supplementation of CXCL11 in human BCC-derived cell cultures would be a reasonable approach to try to overcome the cell propagation hurdle. The data suggested that CXCL11 peptide induced proliferation of the tumor tissue-isolated cells. To further determine the cell types that survived and proliferated in the cultures, dual staining IHC of K17 and CXCR3 of those cells was conducted. The results revealed three major cell populations in the cultures: $K17^+/CXCR3^-$, $K17^+/CXCR3^+$ and $K17^-/CXCR3^+$. By day 21, the two $K17^+$ cell groups formed the majority of the cell population and accounted for > 98 % of the culture. The data indicated that CXCR3/CXCL11 signaling may be involved in enhancing the homogeneity of $K17^+$ primary human BCC cells.

To pursue the functional assay further, loss of function of CXCR3 *in vitro* may provide more evidence about the significant role of the chemokine signaling in BCC. CXCR3 neutralizing antibody was applied to BCC cells, which resulted in reduced cell growth rate and enhanced cell death as compared to those cells without any treatment. The *in vitro* analyses indicated that CXCR3 signaling may be important for cell proliferation as well as survival of BCC cells. To determine if the chemokine signaling has an impact on other BCC tumorigenic properties, migration and invasion assays using Transwell culture and Boyden

chambers were performed. CXCL11 peptide was able to induce a significant chemoattractive effect on BCC cell migration, but it had very little impact on cell invasion, which is consistent with the very low metastatic rate of BCC in general (Wong *et al.*, 2003). Interestingly, CXCL11 was not able to enhance *MMP1*, *2*, *3* and *9* expressions in BCC cells despite the migration effects the chemokines exerted on the tumor cells. Taken together, the proliferation, survival and motility effects mediated by CXCR3 and its ligands provide more insight into the pathogenesis of BCC (Chapter 3A).

Compared to BCC, cutaneous squamous cell carcinoma (SCC) is a less common type of NMSC, but with higher metastatic and patient mortality rates (Clayman *et al.*, 2005; Epstein *et al.*, 1968; Madan *et al.*, 2010). Chemokines such as CXCR4/CXCL12 signaling have been shown to be involved in head and neck SCC cell proliferation and migration (Katayama *et al.*, 2005; Ueda *et al.*, 2010). As such, study of the role of CXCR3 and its ligands in cutaneous SCC and its precancerous forms would enhance the understanding of neoplastic keratinocyte tumorigenesis.

My first approach was a gene screening analysis of chemokines in cutaneous SCC, actinic keratosis (AK), Bowen's disease (BD), BCC, and seborrheic keratosis (SK), as compared to non-lesional skin epithelium tissues (Chapter 3B). The data revealed that *CXCR3*, as well as *CXCL9*, *10* and *11*, were upregulated at the highest level in SCC samples. Also, dual staining IHC further indicated that CXCR3 was mainly expressed by cytokeratin 13^+ SCC keratinocytes. By using HaCaT cells as neoplastic keratinocyte model, it was deduced that inhibition of CXCR3 signaling, with or without CXCL11 supplementation, led to substantial decrease in the cell growth rate and elevation of cell death rate. More importantly, those previously treated HaCaT cells were not able to recover their growth

capacity and survival even after the CXCR3 neutralizing antibody treatment was removed and propagated with additional CXCL11 peptide. Similar to BCC cells, CXCR3 signaling may support proliferation and prevent cell death of HaCaT cells while temporary inhibition of CXCR3 signaling resulted in irreversible damage to HaCaT cells.

After that, the effect of CXCR3 and its ligands was examined for their potential contribution to other neoplastic characteristics of HaCaT cells. Unlike what was observed in BCC cells, both the migration and invasion rates of HaCaT cells increased significantly in response to CXCL11 peptide in a dose-dependent manner. However, the CXCL11 treatment was still not able to enhance the expression of *MMPs* in HaCaT cells. These findings suggested that CXCR3 and its ligands may be tumorigenic promoters of other NMSCs in addition to BCC (Chapter 3B).

5.2.2 Potential net immune privilege in BCC partly induced by CXCR3 signaling

In addition to gaining the ability to undergo uncontrollable proliferation and metastasis, cancer cells facilitate progression and initiation of new tumor growth by acquiring other tumorigenic properties such as immunosuppression. Since CXCR3 was shown to be involved in tumor cell growth and motility in BCC, its role in inducing immune suppression in the tumor was investigated as well.

According to our preliminary microarray data, the immunosuppressive enzyme, indoleamine 2,3-dioxygenase (*IDO*) was significantly upregulated in human BCC samples as compared to non-lesional skin epithelium tissues (Section 1.10). Such outcome triggered our interest in determining the gene profile of immunosuppression of BCC. In fact, subsequent qPCR analysis revealed that the expression of a set of immune privilege (IP)-associated

genes was significantly upregulated in human BCC tumors using non-lesional skin epithelium tissues as the control (Chapter 4). Those genes included *IDO1*, *IDO2*, *CD200*, *CD200R*, *IL10*, *DCR3*, *HLA-E*, etc. All these genes have been shown to attenuate the immune response of various inflammatory cells, such as natural killer cells and T cells (Braud *et al.*, 1998; Cherwinski *et al.*, 2005; Fallarino *et al.*, 2002; Kim *et al.*, 1995; Xiong *et al.*, 2011).

As both *CD200* and *CD200R* were upregulated in BCC tissues, it was critical to examine if they were expressed specifically by BCC cells. The dual labeling IHC data suggested that CD200 was mainly expressed by BCC cells whereas CD200R was expressed by stromal cells including T cells. Such outcome implied that BCC expressed CD200, in ligation with CD00R on T cells, might cause alteration of the immune response of T cells (Cherwinski *et al.*, 2005; Rosenblum *et al.*, 2005). More studies should be conducted to provide further support of inhibition of host immune response by CD200 signaling in BCCs (described below).

IDO1 and IDO2 share significant structural homology and are involved in immune suppression in a wide range of cancers (Ball *et al.*, 2009; Uyttenhove *et al.*, 2003; Witkiewicz *et al.*, 2009). Both of the genes are localized on chromosome 8 with *IDO2* downstream of *IDO1* (Ball *et al.*, 2009; Metz *et al.*, 2007). As *IDO2* and *IDO1* were expressed at the highest level in BCC tissues in the qPCR screen, I decided to pursue the study of their impact on BCC further. Dual labeling IHC and Western blot revealed that IDO was expressed by BCC cells. Morpheiform BCC, which is a more aggressive subtype, had stronger expression than the nodular form, which is a relatively less aggressive subtype. Also, treatment with CXCL11 peptide led to increased enzymatic activity of IDO in BCC cells *in*

vitro. Expression of *IDO2*, but not *IDO1*, was significantly upregulated as the concentration of the peptide increased. The data implied that CXCR3/CXCL11 signaling in BCC may enhance the activity of IDO, which may in turn lead to tryptophan deficiency and T cell apoptosis in the tumor microenvironment.

5.3 Potential role of CXCR3 in the pathogenesis of BCC and other non-melanoma skin malignancies

Guanine nucleotide-binding proteins (G proteins) are in heterotrimeric structure; the G_{α} subunit is tightly bound with $G_{\beta\gamma}$ subunit during the inactive state (Thelen, 2001). A G protein is activated by G protein-coupled receptor (GPCR); such signaling effect is designated by the subtype of G_{α}, which mainly includes $G_{\alpha s}$ and $G_{\alpha i}$ that respectively simulates or inhibits the production of cyclic adenosine monophosphate from adenosine triphosphate (Birnbaumer, 2007; Thelen, 2001). The GPCR, CXCR3 has been shown to have three major subtypes: CXCR3A, CXCR3B and CXCR3 alt (Ehlert *et al.*, 2004; Lasagni *et al.*, 2003). They exert different signaling effects via different G-protein coupling mechanisms and are expressed by different cell types (Ehlert *et al.*, 2004; Lasagni *et al.*, 2003; Vandercappellen *et al.*, 2008). CXCR3A couples with $G_{\alpha i}$ and induces DNA synthesis, cell differentiation and chemotaxis; the subtype has been detected on activated T cells and natural killer cells (Aksoy *et al.*, 2006; Ji *et al.*, 2008; Vandercappellen *et al.*, 2008). CXCR3B couples with $G_{\alpha s}$ and has been implicated in angiostatic activity and inhibition of endothelial cell proliferation (Kim *et al.*, 2002; Lasagni *et al.*, 2003; Vandercappellen *et al.*, 2008). CXCR3 alt is co-expressed with CXCR3A, but with fewer functional effects; it induces chemotaxis upon CXCL11 ligation (Aksoy *et al.*, 2006; Ehlert *et al.*, 2004).

BCC, cutaneous SCC and its pre-malignant forms are solid tumors that, in addition to tumor cells, consist of stromal cells such as fibroblasts and endothelial cells as well as inflammatory infiltrates including T cells, B cells, neutrophils, dendritic cells (DCs) and macrophages. The chemokines *CXCL9*, *10*, *11*, receptor *CXCR3* and its subtypes were highly expressed in all the tumor tissues mentioned, which were composed of both tumor and stromal cells. Thus, opposing forces between tumor suppression (by inflammatory cells producing chemokines) and progression (by tumor cells expressing chemokines) are probably exerted in the lesion microenvironment. Based on the results of the present studies, there may be a net tumor promoting effect mediated by CXCR3 and its ligands in BCC and other non-melanoma skin malignancies.

Melanoma and colon cancer cells have been shown to exploit CXCR3 signaling for cell survival and metastasis (Kawada *et al.*, 2007; Kawada *et al.*, 2004). Also, it has been shown that CXCR3 is associated with increased cell proliferation as its expression is triggered when human bronchial epithelial cells are activated and proliferate (Aksoy *et al.*, 2006). In fact, elevated expression of CXCR3 in the airway epithelial cells is tightly linked to the late S phase and G_2-M phase of the cell cycle (Aksoy *et al.*, 2006). My results revealed that CXCR3 was highly detected on BCC and SCC cells as compared to the stromal cells. As increased expression of the chemokine receptor has been shown to be correlated with enhanced cell growth rate (Aksoy *et al.*, 2006), our data indicate that BCC or SCC cells may proliferate at a faster rate than other cell types in the lesions, which may in turn lead to more CXCR3 production by the tumor cells. Subsequently, the upregulation of CXCR3 may apply positive feedback effects on the tumor cells to further promote cell proliferation and survival

as seen in epithelial cells and other cancer cells such as colon cancer (Aksoy *et al.*, 2006; Kawada *et al.*, 2007).

The effect of chemokines on leukocyte trafficking has been shown to be a multistep process (Vandercappellen *et al.*, 2008). Leukocytes initially roll along endothelium, and attach to the endothelial layer when locally expressed chemokines bind to their specific receptors on the leukocytes. The cells transmigrate through the endothelium towards the underlying tissues that produce the chemokines. Leukocytes migrate and approach the tissues along the chemokine gradient (Vandercappellen *et al.*, 2008). As both BCC and HaCaT cells migrated in response to CXCL11 peptide, CXCR3 ligands produced by tumor cells from other tumor nests or stromal cells in the surrounding area of the tumor may induce the cancerous cells to move outward away from the tumor nests and may ultimately result in tumor spreading.

Immune privilege has been revealed as a mechanism adopted by various cancer types to enhance tumorigenesis (Lo *et al.*, 2011; Uyttenhove *et al.*, 2003). My data suggested that expression and enzymatic activity of IDO was induced by CXCR3 signaling in BCC. As such, IP, partly via inhibition of T cells, would be expected at the BCC tumor sites. Also, CD200 was shown to be upregulated in BCC tumors, which may further accentuate the tumor immunosuppression; for instance, ligation of CD200 with CD200R expressing on T cells leading to alteration of T cell response, or binding of CD200 with $CD200R^{+}$ dendritic cells in the stroma to elevate the expression of IDO (Fallarino *et al.*, 2004; Rosenblum *et al.*, 2005).

In addition, Durr and colleagues demonstrated that CXCL12 was upregulated in B-cell lymphoma patients and that T regulatory cells (Tregs) expressing CXCR4, which is a

receptor of CXCL12, were chemoattracted to the lesional sites, induced immunosuppression and promoted tumor growth (Durr *et al.*, 2010). Also, it has been demonstrated that naive Tregs increased the expression of CXCR3 under the treatment of interleukin 12 (McClymont *et al.*, 2011). Based on my data, CXCR3 ligands were detected in the tumor microenvironment. As such, any Tregs expressing CXCR3 may be attracted to the lesions, which may promote immune tolerance at the tumor sites.

More studies will be needed to investigate how CXCR3 and its ligands interact with other signaling pathways to confer other neoplastic properties to BCC and other NMSCs. For example, CXCR3 signaling could modify neoplastic properties that increase the frequency of tumor reoccurrence or resistance to treatments. The results summarized here may serve as a foundation for the development of new drug medications or for the improvement of current treatment. CXCR3 signaling could be directly targeted to inhibit tumor cell proliferation. Alternatively, strategies to disrupt CXCR3 signaling pathway mediation of IDO production may lead to collapse of the immune privilege in the tumor sites. Such outcome may enhance the efficacy of current medical treatments such as imiquimod or PEP005 gel, which promotes host immune responses as well as tumor cell death (Madan *et al.*, 2010; Patel *et al.*, 2011), to cause regression of tumors.

5.4 Future directions

My results suggest that activation of CXCR3 signaling may be one of the key events in the pathogenesis of BCCs and other NMSCs. Further studies are needed to bring this postulation forward and provide more evidence for better knowledge translation and development of treatments.

5.4.1 BCC tumor regression upon suppression of CXCR3 *in vivo*

The impacts of CXCR3 signaling stimulation and suppression from the *in vitro* studies can be verified and pursued further by *in vivo* experiments using BCC xenograft models. The inhibition of CXCR3/ligand interaction can be induced via injection of a CXCR3 drug antagonist, such as AMG487, or human CXCR3 (hCXCR3) small hairpin RNA (shRNA), and the effects on tumor growth can be monitored.

5.4.1.1 BCC xenograft model

Primary human BCC cells can be prepared and cultured for 1 month with 10 nM CXCL11 peptide (Peprotech) as in Sections 2.3 and 2.4 to obtain homogeneity of $K17^+$ BCC cell culture (Lo *et al.*, 2010). Approximately 5 x 10^5 BCC cells can be orthotopically injected into the backs of the C3SnSmn.CB17-*Prkdc*^{scid}/J severe combined immunodeficient mice (The Jackson Laboratory, Sacramento, CA) (Carlson *et al.*, 2002; Chen *et al.*, 2006; Nonoyama *et al.*, 1993). When the tumors become palpable, the mice can be administered with shRNA or AMG487, which has been used in a study of murine breast cancer (Walser *et al.*, 2006).

5.4.1.2 CXCR3 inhibition via shRNA transfection

To knockdown CXCR3, a validated single hCXCR3 shRNA, TRCN0000011318, from the MISSION Lentiviral Transduction Particles shRNA set SHCLNV-NM_001504 (Sigma-Aldrich) and a non-target control shRNA, SHC002 (Sigma-Aldrich) can be used. Viral transduction and infection of BCC cells can be conducted according to the Lentiviral

Transduction Protocol developed by the Sigma MISSION RNAi Team (Laner-Plamberger *et al.*, 2009). Infected BCC cell colonies can be selected for puromycin-resistance, and can be expanded after being re-plated in the complete growth medium. Total RNA isolation and cDNA synthesis of each candidate cell line can be carried out, and their extent of CXCR3 silencing can be assayed by qPCR.

The BCC xenograft mouse model can be treated under three settings: untreated controls, mice receiving intratumoral injections of control-shRNA and mice receiving CXCR3 shRNA. After 60 days of the injection, tumors from each mouse group can be analyzed.

5.4.1.3 Treatment with a CXCR3 antagonist, AMG487

AMG487 is an orally bioavailable CXCR3 antagonist (Tonn *et al.*, 2009). It has been used to inhibit CXCR3-induced metastasis of murine breast cancer (Walser *et al.*, 2006). For the BCC xenograft mice, 0 mg/kg or 5 mg/kg AMG487 (Amgen, South San Francisco, CA) can be injected subcutaneously twice a day every seven days. On day 21, tumors from each AMG487 dosage group can be analyzed.

5.4.1.4 Evaluation of tumor growth and regression

To evaluate the growth of tumors, tumor numbers from the mice can be counted visually, and the tumor size can be measured with calipers. To assess the degree of regression, tumor tissues from the transgenic mouse models under different CXCR3 inhibition treatments can be excised, and examined for tumor composition and cell proliferating signals. First of all, in order to verify the success of CXCR3 inhibition in the mouse model upon the

shRNA CXCR3 and AMG487 treatments, the expression of *CXCR3* and its ligands in the tumor tissues can be evaluated by qPCR and *in situ* hybridization. Secondly, any alteration or regression of tumor cellular structure due to CXCR3 suppression can be assessed by using routine histology tests such as hematoxylin/eosin staining. In addition, to determine the reduction of tumor proliferating signals in the mouse models under those treatments, the expression of a cell proliferation marker, Ki67 can be measured by IHC and Western blot. Finally, to elucidate what CXCR3-associated signaling pathway is involved in BCC regression under blockade of CXCR3, Western blot can be used to test the protein expression of CXCR3 downstream targets, such as phosphorylation of ERK1/ERK2 and Akt, which is also involved in cell proliferation and tumor cell growth like colon cancer (Franke, 2008; Kawada *et al.*, 2007; Willox *et al.*, 2010).

Reduced expression of CXCR3 and its ligands, Ki67, as well as CXCR3 downstream targets in the tumor biopsies and alteration of tumor structures from CXCR3-knockout mouse models as compared to the control models will be indicators of suppression of tumor growth via CXCR3 signaling inhibition. As such, induction of local CXCR3 signaling abrogation in tumor sites may be a novel strategy to cause BCC regression. More importantly, if the degree of tumor growth inhibition is comparable between the shRNA CXCR3 and AMG487 treatments, modality involving AMG487 application may be a novel study of clinical trials for the cure of BCC.

5.4.2 CXCR3 induced BCC and HaCaT cell motility and signaling pathway involved

CXCR3/CXCL11 signaling was shown to induce migration of both BCC and HaCaT cells (Sections 3.1.2.9 and 3.2.2.5 respectively). Interestingly, qPCR analysis revealed a lack

of significant impact on matrix metalloproteinase (*MMP*) expression under CXCL11 supplementation in both BCC and HaCaT cells (Sections 3.1.2.10 and 3.2.2.6). MMPs degrade components of the extracellular matrix and basement membrane, and are involved in invasion and metastasis in aggressive cancers (Egeblad and Werb, 2002; Shiomi *et al.*, 2010; Woessner, 1991). As such, the role of MMPs in migration and local spreading of BCC and HaCaT cells may not be as significant as in other invasive malignancies. More studies on the signaling pathway of CXCR3-induced BCC and HaCaT cell motility may shed light on the mechanism of local invasion and progression of the cancers.

5.4.2.1 Verification of CXCR3 signaling effects on BCC and HaCaT cell migration

To ensure CXCR3 and its ligands exert chemoattractive effects on BCC and HaCaT cells, inhibition of CXCR3 in both cell types and the impacts on tumor cell migration can be conducted. BCC cells can be isolated and cultured in complete growth medium supplemented with cyclic-adenosine monophosphate for 10 days as stated in Sections 2.3 and 2.6. The BCC and HaCaT cells can be transferred to Transwell culture chamber (BD Biosciences) for migration assays. Approximately 2 x 10^4 cells per well can be seeded in the upper compartment of the chamber, in which, 0 µg/mL, 50 µg/mL and 100 µg/mL monoclonal mouse neutralizing anti-human CXCR3 antibody (Cat. No. mab160) (R&D Systems) can be applied. In the lower compartment of the chamber, 10 nM CXCL11 peptide (Peprotech) can be added. After 72 hours, the rate of migration of BCC and HaCaT cells can be determined as stated in Section 2.1.2.9. In addition, a separate set of BCC and HaCaT cells can be seeded at 2 x 10^4 cells per well in a multi-well plate and treated with the same concentrations of CXCR3 neutralizing antibody. By 72 hours, those cells can be harvested and counted; the

cell number of each antibody dosage treatment can be used as baseline to calculate the percentage of migration.

Any reduction in cell migration of the culture treated with the neutralizing anti-CXCR3 antibody as compared to the untreated cells will provide more support for CXCR3 involvement in BCC and HaCaT cell migration.

5.4.2.2 Profile of cell motility-associated genes during CXCR3-induced BCC and HaCaT cell migration

To determine any downstream target contribution to cell migration upon CXCR3 activation, gene screening analysis of the CXCL11-treated BCC and HaCaT cells can be conducted by qPCR. The BCC cells can be isolated as stated in Section 2.3 and cultured with 10 nM CXCL11 peptide (Peprotech) for 1 month to obtain homogeneity of $K17^+$ BCC cell culture (Lo *et al.*, 2010). For each BCC and HaCaT cell assay, around 8 x 10^4 cells per well can be seeded in a 12-well plate, and can be treated with 0 nM , 5 nM, 10 nM and 20 nM CXCL11 peptide (Peprotech) for 72 hours; the peptide dosage setup can be conducted in triplicate. After that, the cells can be processed by total RNA isolation as in Section 2.11. For cDNA synthesis, the SABiosciences's RT^2 First Strand Kit (Cat. No. C-03/330401) (Qiagen) can be used as suggested by the manufacturer. By using the RT^2 Profiler PCR Array (Qiagen), a panel of 84 genes involved in cell motility pathway can be analyzed for their expression in those CXCL11-treated cells. The genes that can be analyzed are those associated with chemotaxis (e.g. *MAPK1*), adhesion (e.g. *ACTN1*), Rho signaling (e.g. *RHO*), growth signaling (e.g. *EGFR*), integrin-mediated signaling (e.g. *ITGB2*), cell polarity (e.g. *CDC42*) and proteolysis (e.g. *AKT1*). The expression level of each gene can be presented as fold

change and calculated as per Section 2.12. Genes with significantly differential expression in the CXCL11-treated cells as compared to the untreated controls can be further analyzed for the protein expression by Western blot. The BCC cells can be prepared and propagated for 1 month as stated above. After that, both BCC and HaCaT cells can be treated with or without 10 nM CXCL11 for 72 hours and protein extracted from the cells can be analyzed by Western blot as stated in Section 2.15.

Proteins with increased expression in the peptide-treated BCC and HaCaT cells can be potentially downstream targets of the CXCR3 pathway and may be involved in the chemokine signaling-induced migration of both of the cell types. Abrogation of those downstream molecules may be able to reduce or inhibit spreading of the tumors.

5.4.3 Role of CXCR3 signaling in primary cell culture of cutaneous SCC

The human immortalized keratinocyte cell line, HaCaT cells contain UV-specific mutations of the *p53* gene, and have chromosomal aberrations that are characteristically detected in SCC (Boukamp, 2005; Boukamp *et al.*, 1988; Boukamp *et al.*, 1997). As such, this cell line has been used as *in vitro* model for skin carcinogenesis investigation (Boukamp, 2005). Since there was no other commercial human cutaneous SCC cell line available at the time of study, HaCaT cells were used in my projects in order to elucidate the CXCR3 signaling effects on neoplastic keratinocytes. However, to obtain better prediction of CXCR3 impact on SCC, a more accurate *in vitro* model will be needed.

5.4.3.1 Isolation and propagation of primary human cutaneous SCC-derived cells

How can the *in vitro* model be obtained? As suggested in Chapter 2A, primary human BCC-isolated cells were successfully cultured and could even sustain various subsequent analyses. The critical part is to define the correct growth medium and supplementation. Single cell suspensions from human cutaneous SCC tissues can be isolated according to Section 2.3. As the complete growth medium consisting of the base medium M154 (Invitrogen), the Human Keratinocyte Growth Supplement (Invitrogen) and 10 nM CXCL11 peptide (Peprotech) has been shown to be optimal for primary human BCC cells (Sections 3.1.2.5 and 3.1.2.6) (Lo *et al.*, 2010), such medium can be used to culture SCC-derived cells. Cell growth will be monitored on day 0, 7, 14 and 21. For the control setup, the isolated cells can be cultured in the same medium without CXC11 supplementation. Also, after each time-point incubation, the cells can be further analyzed for the expression of a cutaneous SCC keratinocyte marker, cytokeratin 13 (K13) (Commandeur *et al.*, 2009), by immunohistochemistry.

At each time-point treatment, increased cell proliferation of the CXCL11-treated cells as compared to the untreated cell cultures can suggest that CXCR3 signaling may support the growth of the primary isolated cells from SCC tumors. Moreover, since the cells will be isolated directly from the tumor tissues, the cultures will be heterogeneous and contain both tumor and stromal cells. Expression of K13 in the cell culture will differentiate SCC keratinocytes from other cell types such as inflammatory cells and fibroblasts.

5.4.3.2 Functional assays of CXCR3 in the primary SCC-derived cell cultures

For the SCC-derived cells, when the cultures reach homogeneity of $K13^+$ cells, they can be utilized in the loss of function study of CXCR3 and its effects on cell survival and recovery (Sections 2.7 – 2.9) as well as migration and invasion assays in response to CXCL11 (Section 2.10) according to the experiments done in Chapter 3B.

Results similar to those obtained in HaCaT cells in Chapter 3B and Section 5.4.2 can further support the postulation that CXCR3 signaling may be involved in the cell proliferation, survival, migration and invasion of SCC. Suppression of CXCR3 is not only a potential cure for BCC and SCC, but may be a strategy for other keratinocyte malignancies.

5.4.4 Effects of CXCR3 on the CD200R signaling and IDO in BCC tumor and stromal cells

CXCR3/CXCL11 signaling was shown to induce the expression of functional IDO in BCC *in vitro* (Sections 4.2.5, 4.2.7 and 4.2.8) (Lo *et al.*, 2011). Also, gene screening analysis and IHC indicated that CD200 and CD200R were expressed by tumor and stromal cells respectively in the BCC tumor microenvironment (Section 4.2.2). It has been shown that binding of CD200 to CD200R expressed on DCs caused the cells to express IDO (Fallarino *et al.*, 2004). Additional experiments will be required to determine if CD200/CD200R is part of the CXCR3-IDO signaling pathway in BCCs.

5.4.4.1 Expression of CD200 in CXCL11-treated BCC cells

As stated in Section 2.3, BCC cells can be isolated and cultured in 10 nM CXCL11 (Peprotech) for 1 month. The cells can be further treated with or without 10 nM CXCL11,

and can be analyzed for the expression of *CD200* by qPCR and its protein by Western blot. Upregulation of *CD200* and increase of its protein expression under CXCL11 treatment as compared to the untreated control may suggest the induction of CD200 by CXCR3 signaling in BCC *in vitro*.

5.4.4.2 Ionizing radiation induced-BCC transgenic mouse model

The transgenic Ptch+/- heterozygous mouse strain, STOCK *Ptch1*^{tm1Mps}/J (The Jackson Laboratory, Sacramento, CA) develop BCC tumors under ionizing radiation exposure (Aszterbaum *et al.*, 1999; So *et al.*, 2004). In brief, when the mice reach three months of age, they can be exposed to five Gy of γ-radiation using the cesium-137 radiation device (Best Industries, Springfield, VA) (Aszterbaum *et al.*, 1999; So *et al.*, 2004).

5.4.4.3 Effects of blockade of CD200R on the expression and activity of IDO in BCC tissues

Tumors from the BCC transgenic mouse model can be excised and single cell suspension can be obtained. The cell population will be a mixture of tumor cells, stromal cells and inflammatory cells. The cells can be seeded at 8 x 10^4 cells per well of a 12-well plate, and can be treated with polyclonal goat anti-human CD200R neutralizing antibody (Cat. No. af3414) (R & D Systems) at concentrations 0 µg/mL, 10 µg/mL, 50 µg/mL and 100 µg/mL in addition to 10 nM CXCL11 peptide (Peprotech); each dosage setup can be conducted in triplicate. After that, the cells can be harvested and the supernatant can be collected.

The cell pellets can be processed by protein extraction and Western blot to determine the expression of IDO. As stated in Chapter 4, CD200R was expressed by stromal cells but not the tumor cells, and *IDO* was upregulated in BCC *in vitro* when CXCL11 peptide was applied. Also, the study of Section 4.4.4.1 may reveal that CD200 expression may be induced in BCC cells with CXCL11 supplementation. If that is the case, for the BCC cell cultures treated with CD200R neutralizing antibody plus CXCL11, any reduction or absence of IDO as compared to cells treated with CXCL11 peptide alone suggest that prevention of CD200 binding with CD200R expressed on stromal cells may reduce IDO production.

Moreover, the supernatant can be analyzed for IDO enzymatic activity by kynurenine assay as in Section 2.16. Again, decrease of kynurenine amount in the conditioned medium of cultures treated with CD200R neutralizing antibody plus CXCL11 as compared to those supplemented with CXCL11 only can provide more evidence that ligation of CD200 with CD200R on stromal cells may induce the expression of functional IDO.

The observation may suggest that $CD200R^+$ stromal cells may be a source of IDO in the tumor microenvironment upon ligation with CD200 expressed by BCC cells, which may be enhanced by CXCR3 signaling (as can be examined in Section 5.4.4.1). These findings may expand the understanding of the IDO-conferred IP in BCCs.

5.4.5 NFκB may be potential linkage between the signaling of CXCR3 and IDO in BCC tumor cells

As BCC tumorigenesis has been demonstrated to involve CXCR3 and IDO signaling effects (Chapters 3A and 4), these two mediators may be potentially linked in the same signaling pathway. Expression of CXCR3 ligands has been shown to be induced via nuclear

factor kappa B (NFκB) activity in breast cancer cells (Shin *et al.*, 2010). Interestingly, CXCR4/CXCL12 has been indicated to mediate NFκB activity in BCC (Chu *et al.*, 2008). However, the effect of CXCR3 signaling on NFκB in BCC has yet to be established. Moreover, non-canonical NFκB signaling is required for the induction of *IDO* (Puccetti and Grohmann, 2007). As such, future studies can be conducted to determine if NFκB activity is involved in the interaction between CXCR3 and IDO signaling pathways (stated below).

5.4.5.1 Expression and activity of non-canonical NFκB pathway in CXCL11-treated BCC cells

CXCL11 treatment of human BCC cells can be done as in Section 5.4.4.1. The cells can be evaluated for the mRNA (by qPCR) and protein expression (by Western blot) of the non-canonical NFκB pathway-related molecules including NFκB/p52, RelB, and inhibitor of NFκB kinase α (IKKα).

The DNA binding activity of NFκB of the CXCL11-treated BCC cells can be measured by using the TransAM NFκB Transcription Factor ELISA kit (Active Motif, Carlsbad, CA) (Zong *et al.*, 2011). The BCC cells can be lysed and processed to obtain nuclear extracts according to the manufacturer's protocol followed by the ELISA experiment (Active Motif).

Increased expression of these molecules and NFκB activity under CXCL11 treatment as compared to the untreated control may suggest the induction of non-canonical NFκB pathway by CXCR3 signaling in BCC *in vitro*.

5.4.5.2 Impact of inhibition of NFκB pathway on IDO enzymatic activity in BCC

Ionizing radiation induced-BCC transgenic mice can be prepared as in section 5.4.4.2. The tumor cells can be isolated as indicated in section 5.4.4.3. They can be treated with siRNA for IKKα or control scrambled RNA (Tas *et al.*, 2007) in addition to 10 nM CXCL11 peptide supplementation (Peprotech). The cells can be examined for the expression of IDO by Western blot and the conditioned medium can be tested by kynurenine assay.

The experiment of section 5.4.5.1 may reveal that non-canonical NFκB pathway may be induced by CXCR3 signaling in BCC cells. As such, for the treatments of CXCL11 peptide plus IKKα inhibition, reduction in IDO expression and enzymatic activity may indicate that CXCR3-induced NFκB signaling may be required for functional IDO expression in BCC cells. More importantly, the observation may shed light on the potential molecular pathway that CXCR3 signaling may mediate non-canonical NFκB activity, which may subsequently induce IDO in BCC.

5.4.6 Local suppression of *IDO* and stimulation of host immune response to induce BCC cell death

The IDO expressed by BCC may weaken the host immune response by causing T cell apoptosis via tryptophan degradation at the tumor sites, which may facilitate the tumor growth (Chapter 4) (Lo *et al.*, 2011). Besides engineering anti-proliferative signals in tumor cells, the enhancement of host immune response may induce the tumors to undergo regression. As such, disruption of IP in the tumors may be an appropriate approach.

5.4.6.1 IDO suppression in BCC *in vivo* via treatment with 1-methyl-tryptophan

1-methyl-tryptophan (1-MT) is a competitive inhibitor of IDO (Soliman *et al.*, 2010). It was used as treatment of murine adenocarcinoma models to induce reduction of tumor size (Li *et al.*, 2010). In this study, BCC transgenic mouse models can be prepared as stated in Section 5.4.4.2. When the tumors become palpable, 400 mg/kg 1-MT (Sigma-Aldrich) will be administered via intratumoral injection twice a day for 1 week (Li *et al.*, 2010). Any reduction of tumor sizes can be monitored and may be an indicator of increased T cell activity. However, complete eradication of tumors will not be expected as IDO-induced IP only facilitate tumor progression but is not required for the initiation process. As such, adjuvant medication can be followed (stated below).

5.4.6.2 Elevation of host immune response via PEP005 gel and imiquimod application

Topical PEP005 gel (ingenol mebutate) and imiquimod have been shown as anti-tumor treatments as stated in Section 1.8.2 (Madan *et al.*, 2010; Patel *et al.*, 2011). PEP005 gel induces necrosis and infiltration of leukocytes, mainly neutrophils (Challacombe *et al.*, 2006; Hampson *et al.*, 2008; Ogbourne *et al.*, 2004). A Phase II study showed that topical PEP005 gel 0.05 % led to promising histological clearance rate of superficial BCC on arms; however, adverse effects were reported (Siller *et al.*, 2010). Imiquimod cream acts as a toll-like receptor-7 agonist and enhances the host immune response (Madan *et al.*, 2010). Topical 5 % imiquimod cream has been used as treatment for superficial BCC with high cure rates; however, the efficacy reduces dramatically when applied to more aggressive subtypes, such as nodular BCC (Madan *et al.*, 2010). Such inefficacy of PEP005 gel and imiquimod cream

may be due to immunosuppression in the BCC microenvironment (Chapter 4) and the dosage of PEP005 gel was too high.

As IP of the BCC transgenic mouse model in section 5.4.6.1 may be reduced by interfering with IDO, anti-*IDO* treatment can be used in conjunction with drug medication that stimulates immune response to enhance efficacy of the treatment. Either topical PEP005 gel 0.0025 %, 0.005 % and 0.01 % or 5 % imiquimod cream can be applied to tumors that have previously undergone the 1-MT treatment. Changes of tumor morphology and numbers can be evaluated as stated in Section 5.4.1.4. The impacts of PEP005 gel and imiquimod cream on the tumors can be compared.

Any regression of tumors *in vivo* will suggest that destruction of immunosuppression and elevation of host immune response in the tumor microenvironment may be an efficient strategy to eliminate BCC tumors without causing systemic side-effects as seen in other drug medication and chemotherapies.

5.4.7 Cancer stem cells, potentially having CXCR3 as a biological marker, may be involved in BCC initiation

BCC has been shown to arise from the basal layer of the epidermis, where epithelial keratinocyte stem cells reside, and potentially from the hair follicle bulge region (Epstein, 2008; Sellheyer and Krahl, 2008). Thus, tumor-initiating cells with stem-like features have been suspected to be involved in BCC growth (Sellheyer, 2011). The “cancer stem cell” (CSC) hypothesis was first described in leukemia, and was later on applied to breast and brain cancers (Cleary, 2009; Dirks, 2010; Nguyen *et al.*, 2010). CSC is defined as a single cell within a tumor that acquires the ability to self-renew and give rise to heterogenous

lineages of cancer cells that contribute to tumor formation; CSC can arise from stem cells, progenitor cell or differentiated cells (Sellheyer, 2011). As such, it may be important to identify tumor cells exerting stem cell characteristics in BCC. Also, since CXCR3 signaling has been shown to be significantly involved in BCC growth (Lo *et al.*, 2011; Lo *et al.*, 2010), the chemokine expression will be examined.

5.4.7.1 Clonal expansion of BCC tumor initiating cells

BCC tumor will be isolated from patient tissues followed by single cell suspension. The cells will be labeled with markers CXCR3 and CD3, and will be analyzed and sorted by FACS. The cells will be separated into three groups: $CXCR3^+/CD3^-$ (BCC keratinocytes with CXCR3 expression), $CXCR3^+/CD3^+$ (inflammatory infiltrate cells) and $CXCR3^-/CD3^-$ (BCC keratinocytes without CXCR3 expression). The $CXCR3^+/CD3^-$ and $CXCR3^-/CD3^-$ (i.e. all BCC keratinocytes) will be collected as single cells. These single cells will be seeded and cultured as one cell per well in a multi-well plate and will be monitored for clonal expansion.

The capability of a single cell to give rise to colonies will be an indicator of exerting the stem cell characteristic of self-renewal. Any expanded cell population originated from the $CXCR3^+$ group may imply that tumor cells possessing stem-cell feature express CXCR3 as a marker. If clonal expansion (with or without CXCR3 expression) will be observed in this experiment, these cells will be examined for their ability to induce tumor growth.

5.4.7.2 Generation of BCC tumors by xenograft of clonal expanded tumor-initiating cells

The clones of $CXCR3^+$ cells will be transfected with green fluorescent protein TagGFP while the clones of $CXCR3^-$ cells will be transfected with red fluorescent protein

TurboRFP (Axxora LLC, San Diego, CA). Each C3SnSmn.CB17-*Prkdc*^{scid}/J severe combined immunodeficient mouse (The Jackson Laboratory, Sacramento, CA) (Carlson *et al.*, 2002; Chen *et al.*, 2006; Nonoyama *et al.*, 1993) will be orthotopically injected with a clone of CXCR3^{+} or CXCR3^{-} on each side of its back. The mice will be monitored for tumor formation. When the tumors become palpable, they will be examined for the expression of green protein, red protein or neither.

If any tumor expresses the green fluorescence, it implies that it is originated from the clones of CXCR3^{+} cells. More importantly, if higher numbers or all of the tumors consist of green fluorescence-expressing cells, it will be an indicator that stem-like BCC tumor-initiating cells express CXCR3. Such data may provide further support of CXCR3 being the potential biomarker and novel target for treatment of BCC.

Taken together, my projects have identified a novel marker, CXCR3 in BCC and other NMSC tumorigenesis, including SCC. Abrogation of the chemokine signaling pathway according to the proposed future studies may reveal intracellular impacts on BCC and SCC during CXCR3 activation, which may further delineate potential approach to minimize or even suppress the development of the tumors. More importantly, the observations may shed light on new modalities for the cure of NMSCs and other cancers.

Bibliography

Abid K, El Mezni F, Kamoun MR, Fazaa B, Zermani R, Hadouchi C*, et al.* (2010) Xeroderma pigmentosum skin: an immune privilege site for tumor development. *J Cutan Pathol* 37:452-9.

Aksoy MO, Yang Y, Ji R, Reddy PJ, Shahabuddin S, Litvin J*, et al.* (2006) CXCR3 surface expression in human airway epithelial cells: cell cycle dependence and effect on cell proliferation. *Am J Physiol Lung Cell Mol Physiol* 290:L909-18.

Alessi E, Venegoni L, Fanoni D, Berti E (2008) Cytokeratin profile in basal cell carcinoma. *Am J Dermatopathol* 30:249-55.

Amin SH, Tibes R, Kim JE, Hybarger CP (2010) Hedgehog antagonist GDC-0449 is effective in the treatment of advanced basal cell carcinoma. *The Laryngoscope* 120:2456-9.

Aoyagi H, Asami T, Yoshizawa H, Wanichanon C, Iwasaki S (2008) Newly developed technique for dual localization of keratins 13 and 14 by fluorescence immunohistochemistry. *Acta Histochem* 110:324-32.

Apaydin R, Gurbuz Y, Bayramgurler D, Bilen N (2005) Cytokeratin contents of basal cell carcinoma, epidermis overlying tumour, and associated stromal amyloidosis: an immunohistochemical study. *Amyloid* 12:41-7.

Arck PC, Gilhar A, Bienenstock J, Paus R (2008) The alchemy of immune privilege explored from a neuroimmunological perspective. *Current opinion in pharmacology* 8:480-9.

Armitage P, Doll R (1954) The age distribution of cancer and a multi-stage theory of carcinogenesis. *British journal of cancer* 8:1-12.

Arora A, Attwood J (2009) Common skin cancers and their precursors. *The Surgical clinics of North America* 89:703-12.

Asada M, Schaart FM, de Almeida HL, Jr., Korge B, Kurokawa I, Asada Y*, et al.* (1993) Solid basal cell epithelioma (BCE) possibly originates from the outer root sheath of the hair follicle. *Acta Derm Venereol* 73:286-92.

Aszterbaum M, Epstein J, Oro A, Douglas V, LeBoit PE, Scott MP*, et al.* (1999) Ultraviolet and ionizing radiation enhance the growth of BCCs and trichoblastomas in patched heterozygous knockout mice. *Nat Med* 5:1285-91.

Aszterbaum M, Rothman A, Johnson RL, Fisher M, Xie J, Bonifas JM*, et al.* (1998) Identification of mutations in the human PATCHED gene in sporadic basal cell carcinomas and in patients with the basal cell nevus syndrome. *J Invest Dermatol* 110:885-8.

Athar M, Tang X, Lee JL, Kopelovich L, Kim AL (2006) Hedgehog signalling in skin development and cancer. *Exp Dermatol* 15:667-77.

Baggiolini M (2001) Chemokines in pathology and medicine. *J Intern Med* 250:91-104.

Bahram S, Bresnahan M, Geraghty DE, Spies T (1994) A second lineage of mammalian major histocompatibility complex class I genes. *Proc Natl Acad Sci U S A* 91:6259-63.

Bahram S, Spies T (1996) Nucleotide sequence of a human MHC class I MICB cDNA. *Immunogenetics* 43:230-3.

Balkwill F, Mantovani A (2001) Inflammation and cancer: back to Virchow? *Lancet* 357:539-45.

Ball HJ, Yuasa HJ, Austin CJ, Weiser S, Hunt NH (2009) Indoleamine 2,3-dioxygenase-2; a new enzyme in the kynurenine pathway. *Int J Biochem Cell Biol* 41:467-71.

Basile J, Thiers B, Maize J, Sr., Lathers DM (2008) Chemokine receptor expression in non-melanoma skin cancer. *J Cutan Pathol* 35:623-9.

Bastiaens MT, ter Huurne JA, Kielich C, Gruis NA, Westendorp RG, Vermeer BJ*, et al.* (2001) Melanocortin-1 receptor gene variants determine the risk of nonmelanoma skin cancer independently of fair skin and red hair. *American journal of human genetics* 68:884-94.

Bauer S, Groh V, Wu J, Steinle A, Phillips JH, Lanier LL*, et al.* (1999) Activation of NK cells and T cells by NKG2D, a receptor for stress-inducible MICA. *Science* 285:727-9.

Beissert S, Schwarz A, Schwarz T (2006) Regulatory T cells. *J Invest Dermatol* 126:15-24.

Benjamin CL, Ananthaswamy HN (2007) p53 and the pathogenesis of skin cancer. *Toxicol Appl Pharmacol* 224:241-8.

Berger A, Piqueras B, Pages F, Tartour E, Cugnenc PH, Fridman WH (1998) [Fas, fas ligand, immune tolerance, and cancer: implications in cancer of the colon]. *Bulletin du cancer* 85:129-33.

Bernstein SC, Lim KK, Brodland DG, Heidelberg KA (1996) The many faces of squamous cell carcinoma. *Dermatol Surg* 22:243-54.

Bianchini M, Levy E, Zucchini C, Pinski V, Macagno C, De Sanctis P*, et al.* (2006) Comparative study of gene expression by cDNA microarray in human colorectal cancer tissues and normal mucosa. *Int J Oncol* 29:83-94.

Billings SD, Southall MD, Li T, Cook PW, Baldridge L, Moores WB*, et al.* (2003) Amphiregulin overexpression results in rapidly growing keratinocytic tumors: an in vivo xenograft model of keratoacanthoma. *Am J Pathol* 163:2451-8.

Birnbaumer L (2007) Expansion of signal transduction by G proteins. The second 15 years or so: from 3 to 16 alpha subunits plus betagamma dimers. *Biochim Biophys Acta* 1768:772-93.

Booth V, Clark-Lewis I, Sykes BD (2004) NMR structure of CXCR3 binding chemokine CXCL11 (ITAC). *Protein Sci* 13:2022-8.

Booth V, Keizer DW, Kamphuis MB, Clark-Lewis I, Sykes BD (2002) The CXCR3 binding chemokine IP-10/CXCL10: structure and receptor interactions. *Biochemistry* 41:10418-25.

Boukamp P (2005) Non-melanoma skin cancer: what drives tumor development and progression? *Carcinogenesis* 26:1657-67.

Boukamp P, Peter W, Pascheberg U, Altmeier S, Fasching C, Stanbridge EJ*, et al.* (1995) Step-wise progression in human skin carcinogenesis in vitro involves mutational inactivation of p53, rasH oncogene activation and additional chromosome loss. *Oncogene* 11:961-9.

Boukamp P, Petrussevska RT, Breitkreutz D, Hornung J, Markham A, Fusenig NE (1988) Normal keratinization in a spontaneously immortalized aneuploid human keratinocyte cell line. *J Cell Biol* 106:761-71.

Boukamp P, Popp S, Altmeyer S, Hulsen A, Fasching C, Cremer T*, et al.* (1997) Sustained nontumorigenic phenotype correlates with a largely stable chromosome content during long-term culture of the human keratinocyte line HaCaT. *Genes Chromosomes Cancer* 19:201-14.

Bowden GT (2004) Prevention of non-melanoma skin cancer by targeting ultraviolet-B-light signalling. *Nat Rev Cancer* 4:23-35.

Boyce ST, Ham RG (1983) Calcium-regulated differentiation of normal human epidermal keratinocytes in chemically defined clonal culture and serum-free serial culture. *J Invest Dermatol* 81:33s-40s.

Braud VM, Allan DS, O'Callaghan CA, Soderstrom K, D'Andrea A, Ogg GS*, et al.* (1998) HLA-E binds to natural killer cell receptors CD94/NKG2A, B and C. *Nature* 391:795-9.

Braun D, Longman RS, Albert ML (2005) A two-step induction of indoleamine 2,3 dioxygenase (IDO) activity during dendritic-cell maturation. *Blood* 106:2375-81.

Brysk MM, Santschi CH, Bell T, Wagner RF, Jr., Tyring SK, Rajaraman S (1992) Culture of basal cell carcinoma. *J Invest Dermatol* 98:45-9.

Bumpous J (2009) Metastatic cutaneous squamous cell carcinoma to the parotid and cervical lymph nodes: treatment and outcomes. *Curr Opin Otolaryngol Head Neck Surg* 17:122-5.

Buzzell RA (1996) Carcinogenesis of cutaneous malignancies. *Dermatol Surg* 22:209-15.

CanadianCancerSociety (2011) Canadian Cancer Statistics 2011. *Canadian Cancer Statistics*:1-135.

Carlin JM, Borden EC, Sondel PM, Byrne GI (1989) Interferon-induced indoleamine 2,3-dioxygenase activity in human mononuclear phagocytes. *J Leukoc Biol* 45:29-34.

Carlson JA, Combates NJ, Stenn KS, Prouty SM (2002) Anaplastic neoplasms arising from basal cellcarcinoma xenotransplants into SCID-beige mice. *J Cutan Pathol* 29:268-78.

Challacombe JM, Suhrbier A, Parsons PG, Jones B, Hampson P, Kavanagh D*, et al.* (2006) Neutrophils are a key component of the antitumor efficacy of topical chemotherapy with ingenol-3-angelate. *J Immunol* 177:8123-32.

Chen GS, Yu HS, Lan CC, Chow KC, Lin TY, Kok LF*, et al.* (2006) CXC chemokine receptor CXCR4 expression enhances tumorigenesis and angiogenesis of basal cell carcinoma. *Br J Dermatol* 154:910-8.

Chen SC, de Groot M, Kinsley D, Laverty M, McClanahan T, Arreaza M*, et al.* (2009) Expression of chemokine receptor CXCR3 by lymphocytes and plasmacytoid dendritic cells in human psoriatic lesions. *Arch Dermatol Res*.

Cherwinski HM, Murphy CA, Joyce BL, Bigler ME, Song YS, Zurawski SM*, et al.* (2005) The CD200 receptor is a novel and potent regulator of murine and human mast cell function. *J Immunol* 174:1348-56.

Chinem VP, Miot HA (2011) Epidemiology of basal cell carcinoma. *An Bras Dermatol* 86:292-305.

Chu CY, Cha ST, Lin WC, Lu PH, Tan CT, Chang CC*, et al.* (2008) Stromal-cell-derived factor-1{alpha} (SDF-1{alpha}/CXCL12)-enhanced angiogenesis of human basal cell carcinoma cells involves ERK1/2-NF-{kappa} B/interleukin-6 pathway. *Carcinogenesis*.

Clark-Lewis I, Dewald B, Geiser T, Moser B, Baggiolini M (1993) Platelet factor 4 binds to interleukin 8 receptors and activates neutrophils when its N terminus is modified with Glu-Leu-Arg. *Proc Natl Acad Sci U S A* 90:3574-7.

Clayman GL, Lee JJ, Holsinger FC, Zhou X, Duvic M, El-Naggar AK*, et al.* (2005) Mortality risk from squamous cell skin cancer. *J Clin Oncol* 23:759-65.

Cleary ML (2009) Regulating the leukaemia stem cell. *Best Pract Res Clin Haematol* 22:483-7.

Collins K, Jacks T, Pavletich NP (1997) The cell cycle and cancer. *Proc Natl Acad Sci U S A* 94:2776-8.

Commandeur S, de Gruijl FR, Willemze R, Tensen CP, El Ghalbzouri A (2009) An in vitro three-dimensional model of primary human cutaneous squamous cell carcinoma. *Exp Dermatol* 18:849-56.

Cooper SJ, MacGowan J, Ranger-Moore J, Young MR, Colburn NH, Bowden GT (2003) Expression of dominant negative c-jun inhibits ultraviolet B-induced squamous cell carcinoma number and size in an SKH-1 hairless mouse model. *Mol Cancer Res* 1:848-54.

Cox NH, Eedy DJ, Morton CA (2007) Guidelines for management of Bowen's disease: 2006 update. *Br J Dermatol* 156:11-21.

Czarnecki D, Staples M, Mar A, Giles G, Meehan C (1994) Metastases from squamous cell carcinoma of the skin in southern Australia. *Dermatology* 189:52-4.

Dai W, Gupta SL (1990) Regulation of indoleamine 2,3-dioxygenase gene expression in human fibroblasts by interferon-gamma. Upstream control region discriminates between interferon-gamma and interferon-alpha. *J Biol Chem* 265:19871-7.

Datta D, Flaxenburg JA, Laxmanan S, Geehan C, Grimm M, Waaga-Gasser AM*, et al.* (2006) Ras-induced modulation of CXCL10 and its receptor splice variant CXCR3-B in MDA-MB-435 and MCF-7 cells: relevance for the development of human breast cancer. *Cancer Res* 66:9509-18.

Delecluse C, Fukuyama K, Epstein WL (1976) Dibutyryl cyclic AMP-induced differentiation of epidermal cells in tissue culture. *J Invest Dermatol* 66:8-13.

Derre L, Corvaisier M, Charreau B, Moreau A, Godefroy E, Moreau-Aubry A*, et al.* (2006) Expression and release of HLA-E by melanoma cells and melanocytes: potential impact on the response of cytotoxic effector cells. *J Immunol* 177:3100-7.

Devesa SS, Grauman DG, Blot WJ, Pennello GA, Hoover RN, Fraumeni JF (1999) Atlas of cancer mortality in the United States 1950-94. *NIH Publication No 99-4564*:1 - 35.

Dirks PB (2010) Brain tumor stem cells: the cancer stem cell hypothesis writ large. *Mol Oncol* 4:420-30.

Dunn JE, Jr., Levin EA, Linden G, Harzfeld L (1965) Skin Cancer as a Cause of Death. *Calif Med* 102:361-3.

Durr C, Pfeifer D, Claus R, Schmitt-Graeff A, Gerlach UV, Graeser R*, et al.* (2010) CXCL12 mediates immunosuppression in the lymphoma microenvironment after allogeneic transplantation of hematopoietic cells. *Cancer Res* 70:10170-81.

Egeblad M, Werb Z (2002) New functions for the matrix metalloproteinases in cancer progression. *Nat Rev Cancer* 2:161-74.

Ehlert JE, Addison CA, Burdick MD, Kunkel SL, Strieter RM (2004) Identification and partial characterization of a variant of human CXCR3 generated by posttranscriptional exon skipping. *J Immunol* 173:6234-40.

Epstein E, Epstein NN, Bragg K, Linden G (1968) Metastases from squamous cell carcinomas of the skin. *Arch Dermatol* 97:245-51.

Epstein EH (2008) Basal cell carcinomas: attack of the hedgehog. *Nat Rev Cancer* 8:743-54.

Fallarino F, Asselin-Paturel C, Vacca C, Bianchi R, Gizzi S, Fioretti MC*, et al.* (2004) Murine plasmacytoid dendritic cells initiate the immunosuppressive pathway of tryptophan catabolism in response to CD200 receptor engagement. *J Immunol* 173:3748-54.

Fallarino F, Grohmann U, Vacca C, Bianchi R, Orabona C, Spreca A*, et al.* (2002) T cell apoptosis by tryptophan catabolism. *Cell Death Differ* 9:1069-77.

Fan H, Khavari PA (1999) Sonic hedgehog opposes epithelial cell cycle arrest. *J Cell Biol* 147:71-6.

Fernandez EJ, Lolis E (2002) Structure, function, and inhibition of chemokines. *Annu Rev Pharmacol Toxicol* 42:469-99.

Fijak M, Bhushan S, Meinhardt A (2011) Immunoprivileged sites: the testis. *Methods Mol Biol* 677:459-70.

Forouzandeh F, Jalili RB, Germain M, Duronio V, Ghahary A (2008) Skin cells, but not T cells, are resistant to indoleamine 2, 3-dioxygenase (IDO) expressed by allogeneic fibroblasts. *Wound Repair Regen* 16:379-87.

Franke TF (2008) PI3K/Akt: getting it right matters. *Oncogene* 27:6473-88.

Fujigaki S, Saito K, Sekikawa K, Tone S, Takikawa O, Fujii H*, et al.* (2001) Lipopolysaccharide induction of indoleamine 2,3-dioxygenase is mediated dominantly by an IFN-gamma-independent mechanism. *Eur J Immunol* 31:2313-8.

Furuya M, Suyama T, Usui H, Kasuya Y, Nishiyama M, Tanaka N*, et al.* (2007) Up-regulation of CXC chemokines and their receptors: implications for proinflammatory microenvironments of ovarian carcinomas and endometriosis. *Hum Pathol* 38:1676-87.

Gailani MR, Stahle-Backdahl M, Leffell DJ, Glynn M, Zaphiropoulos PG, Pressman C*, et al.* (1996) The role of the human homologue of Drosophila patched in sporadic basal cell carcinomas. *Nat Genet* 14:78-81.

Gallagher RP, Ma B, McLean DI, Yang CP, Ho V, Carruthers JA*, et al.* (1990) Trends in basal cell carcinoma, squamous cell carcinoma, and melanoma of the skin from 1973 through 1987. *J Am Acad Dermatol* 23:413-21.

Garrett MD (2001) Cell cycle control and cancer. *Current Science* 81:515 - 22.

Garssen J, Norval M, el-Ghorr A, Gibbs NK, Jones CD, Cerimele D*, et al.* (1998) Estimation of the effect of increasing UVB exposure on the human immune system and related resistance to infectious diseases and tumours. *J Photochem Photobiol B* 42:167-79.

Gimenez-Conti I, Aldaz CM, Bianchi AB, Roop DR, Slaga TJ, Conti CJ (1990) Early expression of type I K13 keratin in the progression of mouse skin papillomas. *Carcinogenesis* 11:1995-9.

Giuliani N, Bonomini S, Romagnani P, Lazzaretti M, Morandi F, Colla S*, et al.* (2006) CXCR3 and its binding chemokines in myeloma cells: expression of isoforms and potential relationships with myeloma cell proliferation and survival. *Haematologica* 91:1489-97.

Glogau RG (2000) The risk of progression to invasive disease. *J Am Acad Dermatol* 42:23-4.

Gloster HM, Jr., Brodland DG (1996) The epidemiology of skin cancer. *Dermatol Surg* 22:217-26.

Gorczynski RM, Clark DA, Erin N, Khatri I (2010) Role of CD200 expression in regulation of metastasis of EMT6 tumor cells in mice. *Breast cancer research and treatment*.

Grachtchouk M, Mo R, Yu S, Zhang X, Sasaki H, Hui CC*, et al.* (2000) Basal cell carcinomas in mice overexpressing Gli2 in skin. *Nat Genet* 24:216-7.

Grachtchouk M, Pero J, Yang SH, Ermilov AN, Michael LE, Wang A*, et al.* (2011) Basal cell carcinomas in mice arise from hair follicle stem cells and multiple epithelial progenitor populations. *J Clin Invest* 121:1768-81.

Groh V, Rhinehart R, Secrist H, Bauer S, Grabstein KH, Spies T (1999) Broad tumor-associated expression and recognition by tumor-derived gamma delta T cells of MICA and MICB. *Proc Natl Acad Sci U S A* 96:6879-84.

Gudbjartsson DF, Sulem P, Stacey SN, Goldstein AM, Rafnar T, Sigurgeirsson B*, et al.* (2008) ASIP and TYR pigmentation variants associate with cutaneous melanoma and basal cell carcinoma. *Nat Genet* 40:886-91.

Guo HR, Yu HS, Hu H, Monson RR (2001) Arsenic in drinking water and skin cancers: cell-type specificity (Taiwan, ROC). *Cancer causes & control : CCC* 12:909-16.

Hafner C, Vogt T (2008) Seborrheic keratosis. *J Dtsch Dermatol Ges* 6:664-77.

Hahn H, Wicking C, Zaphiropoulous PG, Gailani MR, Shanley S, Chidambaram A*, et al.* (1996) Mutations of the human homolog of Drosophila patched in the nevoid basal cell carcinoma syndrome. *Cell* 85:841-51.

Hall RA, Premont RT, Lefkowitz RJ (1999) Heptahelical receptor signaling: beyond the G protein paradigm. *J Cell Biol* 145:927-32.

Hampson P, Kavanagh D, Smith E, Wang K, Lord JM, Ed Rainger G (2008) The anti-tumor agent, ingenol-3-angelate (PEP005), promotes the recruitment of cytotoxic neutrophils by activation of vascular endothelial cells in a PKC-delta dependent manner. *Cancer immunology, immunotherapy : CII* 57:1241-51.

Hanahan D, Weinberg RA (2011) Hallmarks of cancer: the next generation. *Cell* 144:646-74.

Harwood CA, Surentheran T, McGregor JM, Spink PJ, Leigh IM, Breuer J*, et al.* (2000) Human papillomavirus infection and non-melanoma skin cancer in immunosuppressed and immunocompetent individuals. *Journal of medical virology* 61:289-97.

Hou DY, Muller AJ, Sharma MD, DuHadaway J, Banerjee T, Johnson M*, et al.* (2007) Inhibition of indoleamine 2,3-dioxygenase in dendritic cells by stereoisomers of 1-methyl-tryptophan correlates with antitumor responses. *Cancer Res* 67:792-801.

Huang L, Baban B, Johnson BA, 3rd, Mellor AL (2010) Dendritic cells, indoleamine 2,3 dioxygenase and acquired immune privilege. *Int Rev Immunol* 29:133-55.

Huang S, Mills L, Mian B, Tellez C, McCarty M, Yang XD*, et al.* (2002) Fully humanized neutralizing antibodies to interleukin-8 (ABX-IL8) inhibit angiogenesis, tumor growth, and metastasis of human melanoma. *Am J Pathol* 161:125-34.

Hudson LG, Gale JM, Padilla RS, Pickett G, Alexander BE, Wang J*, et al.* (2010) Microarray analysis of cutaneous squamous cell carcinomas reveals enhanced expression of epidermal differentiation complex genes. *Mol Carcinog* 49:619-29.

Hulkower KI, Herber RL (2011) Cell migration and invasion assays as tools for drug discovery. *Pharmaceutics* 3:107-24.

Hwu P, Du MX, Lapointe R, Do M, Taylor MW, Young HA (2000) Indoleamine 2,3-dioxygenase production by human dendritic cells results in the inhibition of T cell proliferation. *J Immunol* 164:3596-9.

Iwasaki JK, Srivastava D, Moy RL, Lin HJ, Kouba DJ (2010) The molecular genetics underlying basal cell carcinoma pathogenesis and links to targeted therapeutics. *J Am Acad Dermatol*.

Ji J, Kump E, Wernli M, Erb P (2007) Gene silencing of transcription factor Gli2 inhibits basal cell carcinomalike tumor growth in vivo. *Int J Cancer* 122:50-6.

Ji R, Lee CM, Gonzales LW, Yang Y, Aksoy MO, Wang P*, et al.* (2008) Human type II pneumocyte chemotactic responses to CXCR3 activation are mediated by splice variant A. *Am J Physiol Lung Cell Mol Physiol* 294:L1187-96.

Jones D, Benjamin RJ, Shahsafaei A, Dorfman DM (2000) The chemokine receptor CXCR3 is expressed in a subset of B-cell lymphomas and is a marker of B-cell chronic lymphocytic leukemia. *Blood* 95:627-32.

Jones RR (1987) Ozone depletion and cancer risk. *Lancet* 2:443-6.

Joseph MG, Zulueta WP, Kennedy PJ (1992) Squamous cell carcinoma of the skin of the trunk and limbs: the incidence of metastases and their outcome. *Aust N Z J Surg* 62:697-701.

Karagas MR, Nelson HH, Sehr P, Waterboer T, Stukel TA, Andrew A*, et al.* (2006) Human papillomavirus infection and incidence of squamous cell and basal cell carcinomas of the skin. *J Natl Cancer Inst* 98:389-95.

Karagas MR, Stukel TA, Greenberg ER, Baron JA, Mott LA, Stern RS (1992) Risk of subsequent basal cell carcinoma and squamous cell carcinoma of the skin among patients with prior skin cancer. Skin Cancer Prevention Study Group. *JAMA : the journal of the American Medical Association* 267:3305-10.

Karagas MR, Stukel TA, Morris JS, Tosteson TD, Weiss JE, Spencer SK*, et al.* (2001) Skin cancer risk in relation to toenail arsenic concentrations in a US population-based case-control study. *American journal of epidemiology* 153:559-65.

Karagas MR, Stukel TA, Tosteson TD (2002) Assessment of cancer risk and environmental levels of arsenic in New Hampshire. *International journal of hygiene and environmental health* 205:85-94.

Katayama A, Ogino T, Bandoh N, Nonaka S, Harabuchi Y (2005) Expression of CXCR4 and its down-regulation by IFN-gamma in head and neck squamous cell carcinoma. *Clin Cancer Res* 11:2937-46.

Kaur P, Mulvaney M, Carlson JA (2006) Basal cell carcinoma progression correlates with host immune response and stromal alterations: a histologic analysis. *Am J Dermatopathol* 28:293-307.

Kawada K, Hosogi H, Sonoshita M, Sakashita H, Manabe T, Shimahara Y*, et al.* (2007) Chemokine receptor CXCR3 promotes colon cancer metastasis to lymph nodes. *Oncogene* 26:4679-88.

Kawada K, Sonoshita M, Sakashita H, Takabayashi A, Yamaoka Y, Manabe T*, et al.* (2004) Pivotal role of CXCR3 in melanoma cell metastasis to lymph nodes. *Cancer Res* 64:4010-7.

Kennedy C, Naipal A, Gruis NA, Struijk L, ter Schegget J, Willemze R*, et al.* (2002) MICA gene polymorphism is not associated with an increased risk for skin cancer. *J Invest Dermatol* 118:686-91.

Kerkela E, Ala-aho R, Lohi J, Grenman R, V MK, Saarialho-Kere U (2001) Differential patterns of stromelysin-2 (MMP-10) and MT1-MMP (MMP-14) expression in epithelial skin cancers. *British journal of cancer* 84:659-69.

Kim J, Modlin RL, Moy RL, Dubinett SM, McHugh T, Nickoloff BJ*, et al.* (1995) IL-10 production in cutaneous basal and squamous cell carcinomas. A mechanism for evading the local T cell immune response. *J Immunol* 155:2240-7.

Kim S, Bakre M, Yin H, Varner JA (2002) Inhibition of endothelial cell survival and angiogenesis by protein kinase A. *J Clin Invest* 110:933-41.

Kokolakis G, Panagis L, Stathopoulos E, Giannikaki E, Tosca A, Kruger-Krasagakis S (2008) From the protein to the graph: how to quantify immunohistochemistry staining of the skin using digital imaging. *J Immunol Methods* 331:140-6.

Kricker A, Armstrong BK, English DR, Heenan PJ (1995) Does intermittent sun exposure cause basal cell carcinoma? a case-control study in Western Australia. *Int J Cancer* 60:489-94.

Kripke ML (1988) Impact of ozone depletion on skin cancers. *The Journal of dermatologic surgery and oncology* 14:853-7.

Kunkel SL, Strieter RM, Lindley IJ, Westwick J (1995) Chemokines: new ligands, receptors and activities. *Immunol Today* 16:559-61.

Kurzen H, Esposito L, Langbein L, Hartschuh W (2001) Cytokeratins as markers of follicular differentiation: an immunohistochemical study of trichoblastoma and basal cell carcinoma. *Am J Dermatopathol* 23:501-9.

Kyrgidis A, Tzellos TG, Vahtsevanos K, Triaridis S (2010) New concepts for basal cell carcinoma. Demographic, clinical, histological risk factors, and biomarkers. A systematic review of evidence regarding risk for tumor development, susceptibility for second primary and recurrence. *J Surg Res* 159:545-56.

Laner-Plamberger S, Kaser A, Paulischta M, Hauser-Kronberger C, Eichberger T, Frischauf AM (2009) Cooperation between GLI and JUN enhances transcription of JUN and selected GLI target genes. *Oncogene* 28:1639-51.

Lasagni L, Francalanci M, Annunziato F, Lazzeri E, Giannini S, Cosmi L*, et al.* (2003) An alternatively spliced variant of CXCR3 mediates the inhibition of endothelial cell growth induced by IP-10, Mig, and I-TAC, and acts as functional receptor for platelet factor 4. *J Exp Med* 197:1537-49.

Lehman TA, Modali R, Boukamp P, Stanek J, Bennett WP, Welsh JA*, et al.* (1993) p53 mutations in human immortalized epithelial cell lines. *Carcinogenesis* 14:833-9.

Lei J, Cheng J, Li Y, Li S, Zhang L (2005) CD80, but not CD86, express on cultured murine keratinocyte stem cells. *Transplantation proceedings* 37:289-91.

Leigh IM, Navsaria H, Purkis PE, McKay IA, Bowden PE, Riddle PN (1995) Keratins (K16 and K17) as markers of keratinocyte hyperproliferation in psoriasis in vivo and in vitro. *Br J Dermatol* 133:501-11.

Levin E, Premkumar A, Veenman L, Kugler W, Leschiner S, Spanier I*, et al.* (2005) The peripheral-type benzodiazepine receptor and tumorigenicity: isoquinoline binding protein (IBP) antisense knockdown in the C6 glioma cell line. *Biochemistry* 44:9924-35.

Li J, Yang Y, Inoue H, Mori M, Akiyoshi T (1996) The expression of costimulatory molecules CD80 and CD86 in human carcinoma cell lines: its regulation by interferon gamma and interleukin-10. *Cancer immunology, immunotherapy : CII* 43:213-9.

Li Y, Tredget EE, Ghaffari A, Lin X, Kilani RT, Ghahary A (2006) Local expression of indoleamine 2,3-dioxygenase protects engraftment of xenogeneic skin substitute. *J Invest Dermatol* 126:128-36.

Li Y, Xu J, Zou H, Wang C (2010) 1-MT enhances potency of tumor cell lysate-pulsed dendritic cells against pancreatic adenocarcinoma by downregulating the percentage of Tregs. *J Huazhong Univ Sci Technolog Med Sci* 30:344-8.

Livak KJ, Schmittgen TD (2001) Analysis of relative gene expression data using real-time quantitative PCR and the 2(-Delta Delta C(T)) Method. *Methods* 25:402-8.

Lo BK, Jalili RB, Zloty D, Ghahary A, Cowan B, Dutz JP*, et al.* (2011) CXCR3 ligands promote expression of functional indoleamine 2,3-dioxygenase (IDO) in basal cell carcinoma keratinocytes. *Br J Dermatol* 165:1030-6.

Lo BK, Yu M, Zloty D, Cowan B, Shapiro J, McElwee KJ (2010) CXCR3/ligands are significantly involved in the tumorigenesis of basal cell carcinomas. *Am J Pathol* 176:2435-46.

Lob S, Konigsrainer A, Rammensee HG, Opelz G, Terness P (2009) Inhibitors of indoleamine-2,3-dioxygenase for cancer therapy: can we see the wood for the trees? *Nat Rev Cancer* 9:445-52.

Loetscher M, Loetscher P, Brass N, Meese E, Moser B (1998) Lymphocyte-specific chemokine receptor CXCR3: regulation, chemokine binding and gene localization. *Eur J Immunol* 28:3696-705.

Loetscher P, Clark-Lewis I (2001) Agonistic and antagonistic activities of chemokines. *J Leukoc Biol* 69:881-4.

Lohmann CM, Solomon AR (2001) Clinicopathologic variants of cutaneous squamous cell carcinoma. *Adv Anat Pathol* 8:27-36.

Luster AD (1998) Chemokines--chemotactic cytokines that mediate inflammation. *N Engl J Med* 338:436-45.

Macdonald F, Ford CHJ, Casson AG (2004) In: *Molecular biology of cancer (second edition)* (Bushell G, Milles H, eds), New York: Garland Science/BIOS Scientific Publishers.

MacKenzie CR, Langen R, Takikawa O, Daubener W (1999) Inhibition of indoleamine 2,3-dioxygenase in human macrophages inhibits interferon-gamma-induced bacteriostasis but does not abrogate toxoplasmastasis. *Eur J Immunol* 29:3254-61.

Madan V, Lear JT, Szeimies RM (2010) Non-melanoma skin cancer. *Lancet* 375:673-85.

Mahnke K, Bedke T, Enk AH (2007) Regulatory conversation between antigen presenting cells and regulatory T cells enhance immune suppression. *Cellular immunology* 250:1-13.

Makishima H, Ito T, Asano N, Nakazawa H, Shimodaira S, Kamijo Y*, et al.* (2005) Significance of chemokine receptor expression in aggressive NK cell leukemia. *Leukemia* 19:1169-74.

Malumbres M (2011) Physiological relevance of cell cycle kinases. *Physiological reviews* 91:973-1007.

Malumbres M, Barbacid M (2005) Mammalian cyclin-dependent kinases. *Trends in biochemical sciences* 30:630-41.

Malumbres M, Barbacid M (2009) Cell cycle, CDKs and cancer: a changing paradigm. *Nat Rev Cancer* 9:153-66.

Malumbres M, Sotillo R, Santamaria D, Galan J, Cerezo A, Ortega S*, et al.* (2004) Mammalian cells cycle without the D-type cyclin-dependent kinases Cdk4 and Cdk6. *Cell* 118:493-504.

Marcelo CL, Duell EA, Stawiski MA, Anderson TF, Voorhees JJ (1979) Cyclic nucleotide levels in psoriatic and normal keratomed epidermis. *J Invest Dermatol* 72:20-4.

Marcelo CL, Tomich J (1983) Cyclic AMP, glucocorticoid, and retinoid modulation of in vitro keratinocyte growth. *J Invest Dermatol* 81:64s-8s.

Marks R, Staples M, Giles GG (1993) Trends in non-melanocytic skin cancer treated in Australia: the second national survey. *Int J Cancer* 53:585-90.

Maru SV, Holloway KA, Flynn G, Lancashire CL, Loughlin AJ, Male DK*, et al.* (2008) Chemokine production and chemokine receptor expression by human glioma cells: role of CXCL10 in tumour cell proliferation. *J Neuroimmunol* 199:35-45.

McClymont SA, Putnam AL, Lee MR, Esensten JH, Liu W, Hulme MA*, et al.* (2011) Plasticity of human regulatory T cells in healthy subjects and patients with type 1 diabetes. *J Immunol* 186:3918-26.

Mellor AL, Munn DH (1999) Tryptophan catabolism and T-cell tolerance: immunosuppression by starvation? *Immunol Today* 20:469-73.

Mellor AL, Munn DH (2008) Creating immune privilege: active local suppression that benefits friends, but protects foes. *Nat Rev Immunol* 8:74-80.

Metz R, Duhadaway JB, Kamasani U, Laury-Kleintop L, Muller AJ, Prendergast GC (2007) Novel tryptophan catabolic enzyme IDO2 is the preferred biochemical target of the antitumor indoleamine 2,3-dioxygenase inhibitory compound D-1-methyl-tryptophan. *Cancer Res* 67:7082-7.

Meyer KC, Klatte JE, Dinh HV, Harries MJ, Reithmayer K, Meyer W*, et al.* (2008) Evidence that the bulge region is a site of relative immune privilege in human hair follicles. *Br J Dermatol* 159:1077-85.

Miekus K, Jarocha D, Trzyna E, Majka M Role of I-TAC-binding receptors CXCR3 and CXCR7 in proliferation, activation of intracellular signaling pathways and migration of various tumor cell lines. *Folia Histochem Cytobiol* 48:104-11.

Miller DL, Weinstock MA (1994) Nonmelanoma skin cancer in the United States: incidence. *J Am Acad Dermatol* 30:774-8.

Moll R, Franke WW, Volc-Platzer B, Krepler R (1982) Different keratin polypeptides in epidermis and other epithelia of human skin: a specific cytokeratin of molecular weight 46,000 in epithelia of the pilosebaceous tract and basal cell epitheliomas. *J Cell Biol* 95:285-95.

Moller C, Stromberg T, Juremalm M, Nilsson K, Nilsson G (2003) Expression and function of chemokine receptors in human multiple myeloma. *Leukemia* 17:203-10.

Monteagudo C, Martin JM, Jorda E, Llombart-Bosch A (2007) CXCR3 chemokine receptor immunoreactivity in primary cutaneous malignant melanoma: correlation with clinicopathological prognostic factors. *J Clin Pathol* 60:596-9.

Moreaux J, Hose D, Reme T, Jourdan E, Hundemer M, Legouffe E*, et al.* (2006) CD200 is a new prognostic factor in multiple myeloma. *Blood* 108:4194-7.

Mudgil AV, Segal N, Andriani F, Wang Y, Fusenig NE, Garlick JA (2003) Ultraviolet B irradiation induces expansion of intraepithelial tumor cells in a tissue model of early cancer progression. *J Invest Dermatol* 121:191-7.

Mueller MM, Fusenig NE (1999) Constitutive expression of G-CSF and GM-CSF in human skin carcinoma cells with functional consequence for tumor progression. *Int J Cancer* 83:780-9.

Mueller MM, Peter W, Mappes M, Huelsen A, Steinbauer H, Boukamp P*, et al.* (2001) Tumor progression of skin carcinoma cells in vivo promoted by clonal selection, mutagenesis, and autocrine growth regulation by granulocyte colony-stimulating factor and granulocyte-macrophage colony-stimulating factor. *Am J Pathol* 159:1567-79.

Muller A, Homey B, Soto H, Ge N, Catron D, Buchanan ME*, et al.* (2001) Involvement of chemokine receptors in breast cancer metastasis. *Nature* 410:50-6.

Munn DH, Shafizadeh E, Attwood JT, Bondarev I, Pashine A, Mellor AL (1999) Inhibition of T cell proliferation by macrophage tryptophan catabolism. *J Exp Med* 189:1363-72.

Munn DH, Zhou M, Attwood JT, Bondarev I, Conway SJ, Marshall B*, et al.* (1998) Prevention of allogeneic fetal rejection by tryptophan catabolism. *Science* 281:1191-3.

Murakami T, Maki W, Cardones AR, Fang H, Tun Kyi A, Nestle FO*, et al.* (2002) Expression of CXC chemokine receptor-4 enhances the pulmonary metastatic potential of murine B16 melanoma cells. *Cancer Res* 62:7328-34.

Nakayama K (2010) Growth and progression of melanoma and non-melanoma skin cancers regulated by ubiquitination. *Pigment Cell Melanoma Res* 23:338-51.

Narod S (1999) Genetic epidemiology of prostate cancer. *Biochim Biophys Acta* 1423:F1-13.

Nengwen K, Li F, Li X, Juan S, Jianjun L, Chuntao Z*, et al.* (2009) B7-1 induces immunosuppression when expressed in cultured neonatal mice keratinocytes. *Immunobiology* 214:653-63.

Nguyen NP, Almeida FS, Chi A, Nguyen LM, Cohen D, Karlsson U*, et al.* (2010) Molecular biology of breast cancer stem cells: potential clinical applications. *Cancer Treat Rev* 36:485-91.

Niederkorn JY (2003) Mechanisms of immune privilege in the eye and hair follicle. *J Investig Dermatol Symp Proc* 8:168-72.

Nilsson M, Unden AB, Krause D, Malmqwist U, Raza K, Zaphiropoulos PG*, et al.* (2000) Induction of basal cell carcinomas and trichoepitheliomas in mice overexpressing GLI-1. *Proc Natl Acad Sci U S A* 97:3438-43.

Nischt R, Roop DR, Mehrel T, Yuspa SH, Rentrop M, Winter H*, et al.* (1988) Aberrant expression during two-stage mouse skin carcinogenesis of a type I 47-kDa keratin, K13, normally associated with terminal differentiation of internal stratified epithelia. *Mol Carcinog* 1:96-108.

Nonoyama S, Smith FO, Bernstein ID, Ochs HD (1993) Strain-dependent leakiness of mice with severe combined immune deficiency. *J Immunol* 150:3817-24.

Ogbourne SM, Suhrbier A, Jones B, Cozzi SJ, Boyle GM, Morris M*, et al.* (2004) Antitumor activity of 3-ingenyl angelate: plasma membrane and mitochondrial disruption and necrotic cell death. *Cancer Res* 64:2833-9.

Okuyama N, Matsumine A, Kosugi R, Wakabayashi H, Uchida A (2008) Matrix metalloproteinase-1 is a crucial bone metastasis factor in a human breast cancer-derived highly invasive cell line. *Oncol Rep* 20:1497-504.

Oppenheim JJ, Murphy WJ, Chertox O, Schirrmacher V, Wang JM (1997) Prospects for cytokine and chemokine biotherapy. *Clin Cancer Res* 3:2682-6.

Oro AE, Higgins KM, Hu Z, Bonifas JM, Epstein EH, Jr., Scott MP (1997) Basal cell carcinomas in mice overexpressing sonic hedgehog. *Science* 276:817-21.

Patel RV, Frankel A, Goldenberg G (2011) An update on nonmelanoma skin cancer. *The Journal of clinical and aesthetic dermatology* 4:20-7.

Peach RJ, Bajorath J, Naemura J, Leytze G, Greene J, Aruffo A*, et al.* (1995) Both extracellular immunoglobin-like domains of CD80 contain residues critical for binding T cell surface receptors CTLA-4 and CD28. *J Biol Chem* 270:21181-7.

Pellegrino A, Antonaci F, Russo F, Merchionne F, Ribatti D, Vacca A*, et al.* (2004) CXCR3-binding chemokines in multiple myeloma. *Cancer Lett* 207:221-7.

Petermann KB, Rozenberg GI, Zedek D, Groben P, McKinnon K, Buehler C*, et al.* (2007) CD200 is induced by ERK and is a potential therapeutic target in melanoma. *J Clin Invest* 117:3922-9.

Ponten F, Lundeberg J, Asplund A (2008) Principles of tumor biology and pathogenesis of BCCs and SCCs. In: *Dermatology (Second edition)* (Bolognia JL, Jorizzo J, Rapini R, eds) Vol. 2, Spain: Elsevier Limited, 1627-39.

Post PN, Stockton D, Davies TW, Coebergh JW (1999) Striking increase in incidence of prostate cancer in men aged < 60 years without improvement in prognosis. *British journal of cancer* 79:13-7.

Pradelli E, Karimdjee-Soilihi B, Michiels JF, Ricci JE, Millet MA, Vandenbos F*, et al.* (2009) Antagonism of chemokine receptor CXCR3 inhibits osteosarcoma metastasis to lungs. *Int J Cancer* 125:2586-94.

Pradier A, Passweg J, Villard J, Kindler V (2010) Human bone marrow stromal cells and skin fibroblasts inhibit natural killer cell proliferation and cytotoxic activity. *Cell transplantation*.

Preston DS, Stern RS (1992) Nonmelanoma cancers of the skin. *N Engl J Med* 327:1649-62.

Puccetti P, Grohmann U (2007) IDO and regulatory T cells: a role for reverse signalling and non-canonical NF-kappaB activation. *Nat Rev Immunol* 7:817-23.

Randle HW (1996) Basal cell carcinoma. Identification and treatment of the high-risk patient. *Dermatol Surg* 22:255-61.

Rane SG, Dubus P, Mettus RV, Galbreath EJ, Boden G, Reddy EP*, et al.* (1999) Loss of Cdk4 expression causes insulin-deficient diabetes and Cdk4 activation results in beta-islet cell hyperplasia. *Nat Genet* 22:44-52.

Reifenberger J, Wolter M, Knobbe CB, Kohler B, Schonicke A, Scharwachter C*, et al.* (2005) Somatic mutations in the PTCH, SMOH, SUFUH and TP53 genes in sporadic basal cell carcinomas. *Br J Dermatol* 152:43-51.

Robinson D, Hasharoni A, Evron Z, Segal M, Nevo Z (2000) Synovial chondromatosis: the possible role of FGF 9 and FGF receptor 3 in its pathology. *Int J Exp Pathol* 81:183-9.

Robledo MM, Bartolome RA, Longo N, Rodriguez-Frade JM, Mellado M, Longo I*, et al.* (2001) Expression of functional chemokine receptors CXCR3 and CXCR4 on human melanoma cells. *J Biol Chem* 276:45098-105.

Roewert-Huber J, Lange-Asschenfeldt B, Stockfleth E, Kerl H (2007) Epidemiology and aetiology of basal cell carcinoma. *Br J Dermatol* 157 Suppl 2:47-51.

Rosenblum MD, Woodliff JE, Madsen NA, McOlash LJ, Keller MR, Truitt RL (2005) Characterization of CD 200-receptor expression in the murine epidermis. *J Invest Dermatol* 125:1130-8.

Rosenblum MD, Yancey KB, Olasz EB, Truitt RL (2006) CD200, a "no danger" signal for hair follicles. *Journal of dermatological science* 41:165-74.

Rosso S, Zanetti R, Martinez C, Tormo MJ, Schraub S, Sancho-Garnier H*, et al.* (1996) The multicentre south European study 'Helios'. II: Different sun exposure patterns in the aetiology of basal cell and squamous cell carcinomas of the skin. *British journal of cancer* 73:1447-54.

Rowe DE, Carroll RJ, Day CL, Jr. (1992) Prognostic factors for local recurrence, metastasis, and survival rates in squamous cell carcinoma of the skin, ear, and lip. Implications for treatment modality selection. *J Am Acad Dermatol* 26:976-90.

Ruddon RW (2007) In: *Cancer Biology (Fourth edition)* (Oxford University Press I, ed), New York: Oxford University Press, Inc.

Rundhaug JE, Gimenez-Conti I, Stern MC, Budunova IV, Kiguchi K, Bol DK*, et al.* (1997) Changes in protein expression during multistage mouse skin carcinogenesis. *Mol Carcinog* 20:125-36.

Santamaria D, Barriere C, Cerqueira A, Hunt S, Tardy C, Newton K*, et al.* (2007) Cdk1 is sufficient to drive the mammalian cell cycle. *Nature* 448:811-5.

Sarkhosh K, Tredget EE, Uludag H, Kilani RT, Karami A, Li Y*, et al.* (2004) Temperature-sensitive polymer-conjugated IFN-gamma induces the expression of IDO mRNA and activity by fibroblasts populated in collagen gel (FPCG). *J Cell Physiol* 201:146-54.

Satish L, Blair HC, Glading A, Wells A (2005) Interferon-inducible protein 9 (CXCL11)-induced cell motility in keratinocytes requires calcium flux-dependent activation of mu-calpain. *Mol Cell Biol* 25:1922-41.

Scala S, Giuliano P, Ascierto PA, Ierano C, Franco R, Napolitano M*, et al.* (2006) Human melanoma metastases express functional CXCR4. *Clin Cancer Res* 12:2427-33.

Schatton T, Frank MH (2009) Antitumor immunity and cancer stem cells. *Annals of the New York Academy of Sciences* 1176:154-69.

Schirren CG, Rutten A, Kaudewitz P, Diaz C, McClain S, Burgdorf WH (1997) Trichoblastoma and basal cell carcinoma are neoplasms with follicular differentiation sharing the same profile of cytokeratin intermediate filaments. *Am J Dermatopathol* 19:341-50.

Seliger B, Marincola FM, Ferrone S, Abken H (2008) The complex role of B7 molecules in tumor immunology. *Trends in molecular medicine* 14:550-9.

Sellheyer K (2011) Basal cell carcinoma: cell of origin, cancer stem cell hypothesis and stem cell markers. *Br J Dermatol* 164:696-711.

Sellheyer K, Krahl D (2008) Basal cell (trichoblastic) carcinoma common expression pattern for epithelial cell adhesion molecule links basal cell carcinoma to early follicular embryogenesis, secondary hair germ, and outer root sheath of the vellus hair follicle: A clue to the adnexal nature of basal cell carcinoma? *J Am Acad Dermatol* 58:158-67.

Sharma MD, Baban B, Chandler P, Hou DY, Singh N, Yagita H*, et al.* (2007) Plasmacytoid dendritic cells from mouse tumor-draining lymph nodes directly activate mature Tregs via indoleamine 2,3-dioxygenase. *J Clin Invest* 117:2570-82.

Shin SY, Nam JS, Lim Y, Lee YH (2010) TNF{alpha}-exposed bone marrow-derived mesenchymal stem cells promote locomotion of MDA-MB-231 breast cancer cells through transcriptional activation of CXCR3 ligand chemokines. *J Biol Chem*.

Shiomi T, Lemaitre V, D'Armiento J, Okada Y (2010) Matrix metalloproteinases, a disintegrin and metalloproteinases, and a disintegrin and metalloproteinases with thrombospondin motifs in non-neoplastic diseases. *Pathology international* 60:477-96.

Shiomi T, Okada Y (2003) MT1-MMP and MMP-7 in invasion and metastasis of human cancers. *Cancer Metastasis Rev* 22:145-52.

Sica A, Saccani A, Bottazzi B, Bernasconi S, Allavena P, Gaetano B*, et al.* (2000) Defective expression of the monocyte chemotactic protein-1 receptor CCR2 in macrophages associated with human ovarian carcinoma. *J Immunol* 164:733-8.

Siller G, Rosen R, Freeman M, Welburn P, Katsamas J, Ogbourne SM (2010) PEP005 (ingenol mebutate) gel for the topical treatment of superficial basal cell carcinoma: results of a randomized phase IIa trial. *Australas J Dermatol* 51:99-105.

Skobe M, Fusenig NE (1998) Tumorigenic conversion of immortal human keratinocytes through stromal cell activation. *Proc Natl Acad Sci U S A* 95:1050-5.

Slaga TJ, DiGiovanni J, Winberg LD, Budunova IV (1995) Skin carcinogenesis: characteristics, mechanisms, and prevention. *Prog Clin Biol Res* 391:1-20.

Smith DR, Polverini PJ, Kunkel SL, Orringer MB, Whyte RI, Burdick MD*, et al.* (1994) Inhibition of interleukin 8 attenuates angiogenesis in bronchogenic carcinoma. *J Exp Med* 179:1409-15.

Sneddon JB, Zhen HH, Montgomery K, van de Rijn M, Tward AD, West R*, et al.* (2006) Bone morphogenetic protein antagonist gremlin 1 is widely expressed by cancer-associated stromal cells and can promote tumor cell proliferation. *Proc Natl Acad Sci U S A* 103:14842-7.

So P-L (2008) In: *The biology of cancer: Skin cancer* (Bozzone DM, ed), New York: Infobase Publishing, Inc.

So PL, Lee K, Hebert J, Walker P, Lu Y, Hwang J*, et al.* (2004) Topical tazarotene chemoprevention reduces Basal cell carcinoma number and size in Ptch1+/- mice exposed to ultraviolet or ionizing radiation. *Cancer Res* 64:4385-9.

Soliman H, Mediavilla-Varela M, Antonia S (2010) Indoleamine 2,3-dioxygenase: is it an immune suppressor? *Cancer J* 16:354-9.

Sompuram SR, Kodela V, Zhang K, Ramanathan H, Radcliffe G, Falb P*, et al.* (2002) A novel quality control slide for quantitative immunohistochemistry testing. *J Histochem Cytochem* 50:1425-34.

Son KD, Kim TJ, Lee YS, Park GS, Han KT, Lim JS*, et al.* (2008) Comparative analysis of immunohistochemical markers with invasiveness and histologic differentiation in squamous cell carcinoma and basal cell carcinoma of the skin. *Journal of surgical oncology* 97:615-20.

Struyf S, Salogni L, Burdick MD, Vandercappellen J, Gouwy M, Noppen S*, et al.* (2011) Angiostatic and chemotactic activities of the CXC chemokine CXCL4L1 (platelet factor-4 variant) are mediated by CXCR3. *Blood* 117:480-8.

Sun T, Chen XH, Tang ZD, Cai J, Wang XY, Wang SC*, et al.* (2010) Novel 1-alkyl-tryptophan derivatives downregulate IDO1 and IDO2 mRNA expression induced by interferon-gamma in dendritic cells. *Mol Cell Biochem*.

Svard J, Heby-Henricson K, Persson-Lek M, Rozell B, Lauth M, Bergstrom A*, et al.* (2006) Genetic elimination of Suppressor of fused reveals an essential repressor function in the mammalian Hedgehog signaling pathway. *Developmental cell* 10:187-97.

Tas SW, Vervoordeldonk MJ, Hajji N, Schuitemaker JH, van der Sluijs KF, May MJ*, et al.* (2007) Noncanonical NF-kappaB signaling in dendritic cells is required for indoleamine 2,3-dioxygenase (IDO) induction and immune regulation. *Blood* 110:1540-9.

Taylor MW, Feng GS (1991) Relationship between interferon-gamma, indoleamine 2,3-dioxygenase, and tryptophan catabolism. *Faseb J* 5:2516-22.

Terness P, Bauer TM, Rose L, Dufter C, Watzlik A, Simon H*, et al.* (2002) Inhibition of allogeneic T cell proliferation by indoleamine 2,3-dioxygenase-expressing dendritic cells: mediation of suppression by tryptophan metabolites. *J Exp Med* 196:447-57.

Thelen M (2001) Dancing to the tune of chemokines. *Nature immunology* 2:129-34.

Tonn GR, Wong SG, Wong SC, Johnson MG, Ma J, Cho R*, et al.* (2009) An inhibitory metabolite leads to dose- and time-dependent pharmacokinetics of (R)-N-{1-[3-(4-ethoxy-phenyl)-4-oxo-3,4-dihydro-pyrido[2,3-d]pyrimidin-2-y l]-ethyl}-N-pyridin-3-yl-methyl-2-(4-trifluoromethoxy-phenyl)-acetamide (AMG 487) in human subjects after multiple dosing. *Drug metabolism and disposition: the biological fate of chemicals* 37:502-13.

Ueda M, Shimada T, Goto Y, Tei K, Nakai S, Hisa Y*, et al.* (2010) Expression of CC-chemokine receptor 7 (CCR7) and CXC-chemokine receptor 4 (CXCR4) in head and neck squamous cell carcinoma. *Auris Nasus Larynx* 37:488-95.

Urbach F (1991) Incidence of nonmelanoma skin cancer. *Dermatol Clin* 9:751-5.

Uyttenhove C, Pilotte L, Theate I, Stroobant V, Colau D, Parmentier N*, et al.* (2003) Evidence for a tumoral immune resistance mechanism based on tryptophan degradation by indoleamine 2,3-dioxygenase. *Nat Med* 9:1269-74.

Vandercappellen J, Van Damme J, Struyf S (2008) The role of CXC chemokines and their receptors in cancer. *Cancer Lett* 267:226-44.

Varani J, Hattori Y, Chi Y, Schmidt T, Perone P, Zeigler ME*, et al.* (2000) Collagenolytic and gelatinolytic matrix metalloproteinases and their inhibitors in basal cell carcinoma of skin: comparison with normal skin. *British journal of cancer* 82:657-65.

Vargo N (2003) Basal cell and squamous cell carcinoma. *Semin Oncol Nurs* 19:12-21.

von Bubnoff D, Bausinger H, Matz H, Koch S, Hacker G, Takikawa O*, et al.* (2004) Human epidermal langerhans cells express the immunoregulatory enzyme indoleamine 2,3-dioxygenase. *J Invest Dermatol* 123:298-304.

von Bubnoff D, Bezold G, Matz H, Hanau D, De La Salle H, Bieber T (2003) Quantification of indoleamine 2,3-dioxygenase gene induction in atopic and non-atopic monocytes after ligation of the high-affinity receptor for IgE, Fc(epsilon)RI and interferon-gamma stimulation. *Clin Exp Immunol* 132:247-53.

Wahl SM, Wen J, Moutsopoulos N (2006) TGF-beta: a mobile purveyor of immune privilege. *Immunological reviews* 213:213-27.

Waldmann H (2010) Tolerance: an overview and perspectives. *Nat Rev Nephrol* 6:569-76.

Walling HW, Fosko SW, Geraminejad PA, Whitaker DC, Arpey CJ (2004) Aggressive basal cell carcinoma: presentation, pathogenesis, and management. *Cancer Metastasis Rev* 23:389-402.

Walser TC, Rifat S, Ma X, Kundu N, Ward C, Goloubeva O*, et al.* (2006) Antagonism of CXCR3 inhibits lung metastasis in a murine model of metastatic breast cancer. *Cancer Res* 66:7701-7.

Weetman AP (1999) The immunology of pregnancy. *Thyroid : official journal of the American Thyroid Association* 9:643-6.

Wei XH, Orr HT (1990) Differential expression of HLA-E, HLA-F, and HLA-G transcripts in human tissue. *Hum Immunol* 29:131-42.

Wenzel J, Tomiuk S, Zahn S, Kusters D, Vahsen A, Wiechert A*, et al.* (2008) Transcriptional profiling identifies an interferon-associated host immune response in invasive squamous cell carcinoma of the skin. *Int J Cancer* 123:2605-15.

Willox I, Mirkina I, Westwick J, Ward SG (2010) Evidence for PI3K-dependent CXCR3 agonist-induced degranulation of human cord blood-derived mast cells. *Molecular immunology* 47:2367-77.

Wingender G, Garbi N, Schumak B, Jungerkes F, Endl E, von Bubnoff D*, et al.* (2006) Systemic application of CpG-rich DNA suppresses adaptive T cell immunity via induction of IDO. *Eur J Immunol* 36:12-20.

Wischhusen J, Waschbisch A, Wiendl H (2007) Immune-refractory cancers and their little helpers--an extended role for immunetolerogenic MHC molecules HLA-G and HLA-E? *Semin Cancer Biol* 17:459-68.

Witkiewicz AK, Costantino CL, Metz R, Muller AJ, Prendergast GC, Yeo CJ*, et al.* (2009) Genotyping and expression analysis of IDO2 in human pancreatic cancer: a novel, active target. *J Am Coll Surg* 208:781-7; discussion 7-9.

Woessner JF, Jr. (1991) Matrix metalloproteinases and their inhibitors in connective tissue remodeling. *Faseb J* 5:2145-54.

Wong CS, Strange RC, Lear JT (2003) Basal cell carcinoma. *Bmj* 327:794-8.

Xanthou G, Williams TJ, Pease JE (2003) Molecular characterization of the chemokine receptor CXCR3: evidence for the involvement of distinct extracellular domains in a multi-step model of ligand binding and receptor activation. *Eur J Immunol* 33:2927-36.

Xie J, Murone M, Luoh SM, Ryan A, Gu Q, Zhang C*, et al.* (1998) Activating Smoothened mutations in sporadic basal-cell carcinoma. *Nature* 391:90-2.

Xiong G, Guo H, Ge X, Xu X, Yang X, Yang K*, et al.* (2011) Decoy receptor 3 expression in esophageal squamous cell carcinoma: correlation with tumour invasion and metastasis. *Biomarkers* 16:155-60.

Yang S, Zhu X, Cai L, Cheng H, Zhao R, Wang H*, et al.* (2010) Role of tumor-associated lymphatic endothelial cells in metastasis: a study of epithelial ovarian tumor in vitro. *Cancer Sci* 101:679-85.

Yoshikawa K, Katagata Y, Kondo S (1998) Biochemical and immunohistochemical analyses of keratin expression in basal cell carcinoma. *Journal of dermatological science* 17:15-23.

Yu M, Zloty D, Cowan B, Shapiro J, Haegert A, Bell RH*, et al.* (2008) Superficial, Nodular, and Morpheiform Basal-Cell Carcinomas Exhibit Distinct Gene Expression Profiles. *J Invest Dermatol* 128:1797-805.

Zafiropoulos A, Crikas N, Passam AM, Spandidos DA (2004) Significant involvement of CCR2-64I and CXCL12-3a in the development of sporadic breast cancer. *J Med Genet* 41:e59.

Zipin-Roitman A, Meshel T, Sagi-Assif O, Shalmon B, Avivi C, Pfeffer RM*, et al.* (2007) CXCL10 promotes invasion-related properties in human colorectal carcinoma cells. *Cancer Res* 67:3396-405.

Zong H, Wang F, Fan QX, Wang LX (2011) Curcumin inhibits metastatic progression of breast cancer cell through suppression of urokinase-type plasminogen activator by NF-kappa B signaling pathways. *Molecular biology reports*.